Biogeochemical Study of Trace Elements in Surface Sediment from the Marginal Sea (East China Sea) to the Open-Ocean (Northwestern Pacific)

By

ROY ANDREAS

ID number: 31178301

A Dissertation Submitted to
The Graduate School of Science and Engineering for Education, University of Toyama
in Partial Fulfillment of the Requirements for
the Degree of Doctor of Philosophy

UNIVERSITY OF TOYAMA

SEPTEMBER 2015

Biogeochemical Study of Trace Elements in Surface Sediment from the Marginal Sea (East China Sea) to the Open-Ocean (Northwestern Pacific)

By

ROY ANDREAS

ID number: 31178301

A Dissertation Submitted to
The Graduate School of Science and Engineering for Education, University of Toyama
in Partial Fulfillment of the Requirements for
the Degree of Doctor of Philosophy

UNIVERSITY OF TOYAMA

SEPTEMBER 2015

Thesis Approval Sheet

This thesis entitled

“Biogeochemical Study of Trace Elements in Surface Sediment from the Marginal Sea (East China Sea) to the Open-Ocean (Northwestern Pacific)” submitted by Roy Andreas is approved for degree of Doctor of Philosophy.

1. **Prof. JING ZHANG**	**Supervisor**
2. **Prof. AKIRA UEDA**	**Co- supervisor**
3. **Prof. TSUBAKI NORITATSU**	**Co- supervisor**
4. **Prof. KATSUMI MARUMO**	**Examiner**

This research was conducted at the Graduate School of Science and Engineering for Education, University of Toyama, Japan

The Information in this thesis is an original work of the author, and it is free of plagiarism. Where ever information was used from any other academic documents, reference are given appropriately

Acknowledgements

First and foremost I want to thank to my Supervisor Prof. Dr. Jing Zhang. I appreciate all her contribution of time, idea and funding to make my Ph.D course full of experience and knowledge that I has never had before. I also thank to the member of my thesis committees: Prof. Akira Ueda, Prof. Tsubaki Noritatsu, and Prof. Katsumi Marumo, whose have provided input and suggestions that may enhance this thesis. I want to express my gratitude to my laboratory member (Geochemistry laboratory) for supporting during my Ph.D course. I also thank to the Directorate General of Higher Education (DGHE), Ministry of Education and Culture, Republic of Indonesia for the scholarship to support my living cost and tuition fee during my Ph.D course.

Finally, I want to thank to my beloved wife (Euis Rahayu NA) and all my children for their support, encouragement and sacrifice. A special thank to my parents (ayah and mama) for a never ending support.

List of Publications in Peer Reviewed Journal

1. Andreas R and Zhang J (2014) Characteristics of Adsorption Interactions of Cadmium(II) onto Humin from Peat Soil in Freshwater and Seawater Media. Bulletin of Environmental Contamination and Toxicology. 92:352–357

Presentation at International Conference

1. Andreas R and Jing Zhang (2014) Concentration and Potential Mobility of Trace Metals in Surface Sediment of the North Pacific Ocean By BCR Sequential. Japan Geoscience Union Meeting (JpGU) 2014; Yokohama, Japan

2. Andreas R and Jing Zhang (2014) Bioavailability of Trace Metals in the Surface Sediment of the Northwestern North Pacific Ocean By BCR Sequential Methods with ICP-MS; Asia Oceania Geosciences Society (AOGS) 11th Annual Meeting; Sapporo, Japan

3. Andreas R and Jing Zhang (2014) Mobility and Environmental Risk of Trace Metals in Surface Sediment of the East China Sea (Outer Shelf Continent) By BCR Sequential Method; Asia Oceania Geosciences Society (AOGS) 11th Annual Meeting; Sapporo, Japan

Award and Honor

2011 – 2015: The Scholarship from Directorate General of Higher Education (DGHE), Ministry of Education and Culture, Republic of Indonesia

Oceanography Research Expeditions

1. Nagasaki-maru cruise (NN 337): Toyama bay, Japan; (8-12 October 2011)
2. Nagasaki-maru cruise (NN 354): East China Sea; (18-27 July 2012)
3. Geotraces research cruise by R/V Hakuho-maru (KH12-04)

   Leg1: Tokyo-Northwestern the North Pacific Ocean-Ducth Harbor (USA); (23 August-16 September 2012)

   Leg 2: Dutch Harbor-Northeastern the North Pacific Ocean-Vancouver (Canada); (17 September – 5 October 2012)
4. Paleoceanography research cruise by R/V Hakuho-maru (KH13-04)

   Leg 1: Tokyo-Japan Sea-Hakata Port; (28 June – 04 July 2013)

   Leg 2: Hakata Port-East China Sea-Singapore; (07 July – 16 July 2013)

   Leg 3: Singapore-Gulf of Thailand-Singapore; (21 – 26 July 2013)

   Leg 4: Singapore-Malaca Strait-Andaman Sea-Bay of Bengal-Singapore; (13 July–14 Augut 2013)

5. R/V Shinsei-Maru cruise (KS-14-11): East China Sea (08-17 June 2014)

Abstract

Surface sediment acts as the main repository and source of trace elements in the aquatic environment and plays an important role in the transport and storage. Understanding the source of trace elements and potential re-mineralization in the surface sediment can give us the integrated information of biogeochemical process compared with snapshot signal reflected by water column. The East China Sea (ECS), one of the largest marginal seas in the world, is an important terrestrial organic carbon sink with high productivity caused by large amounts of nutrients supplied from Changjiang River, coastal area of the Yellow Sea, and atmospheric input. Moreover, the outer shelf East China Sea (OSECS) is a bridge for water circulation and material transportation to other marginal sea (Yellow Sea and Japan Sea) and open ocean (Northwestern Pacific Ocean) through the Kuroshio Current (KC). Based on this information, three scientific questions were raised as follows 1) How the interaction of trace element with organic substances in the aquatic environment? 2) What is the source of trace elements in surface sediment in the OSECS and Northwestern Pacific Ocean (NwPO)? 3) How significant of potential re-mineralization of micronutrients in the surface sediment?

The surface sediment samples were carried out from the OSECS and NwPO in 2012 and 2013 by KT-12-25, KH-12-04, and KH-13-04 research cruises, respectively. A procedure proposed by the community Bureau of Reference (BCR) was used in this study to fractionate trace elements. It partitions, trace elements divided into four phases including carbonate, Fe/Mn oxides, organic matter and residual phase. Carbonate, oxide and organic matter are usually consider as indication of naturally marine biogenic, anthropogenic or authigenic source, while residual fraction represents the lithogenic source of trace elements. Trace elements concentration in each phases were measured by inductively coupled plasma-mass spectrometry (ICP-MS HP 4500, Agilent). Total organic carbon (TOC) and SiO_2 were observed by TOC analyzer (TOC-V_{CSH}, Shimadzu) and UV-Vis Spectrophotometer (UVmini-1240, Shimadzu), respectively.

In the freshwater and seawater, aquo complex ($Cd(H_2O)_6)^{2+}$) and chloro complex ($CdCl^+$ and $CdCl_2$) will be responsible for adsorption of Cd on organic

substances. At 2 < pH <7, cadmium was in Cd(II) and $(Cd(H_2O)_6)^{+2}$ which was soluble in water, at 7< pH <10, part of the soluble Cd was precipitated as $Cd(OH)_2$, while at pH >10, all of the Cd were precipitated as $Cd(OH)_2$. In freshwater media, adsorption process through a single phase indicated that aquo and chloro complexes were simultaneously adsorbed on organic substances, while in seawater media occurs in 2 different phases indicated that aquo and chloro complexes individually adsorbed on organic substances.

Spatial distribution of trace elements, TOC, carbonate and SiO_2 showed that generally the southern area has higher concentration compared with middle and northern area of OSECS, likely biogenic source controls the distribution of trace elements. Based on the chemical fractionation, the trace elements in surface sediment of OSECS come from various sources including lithogenic, ocean biogenic and authigenic sources. The northern and the middle part, Pb, Mn, Zn and Cd were dominated by ocean biogenic (carbonate and organic phase) while Fe and Co were dominated by lithogenic (residual phase). The proportion of oxides fraction in the southern was bigger than the middle and the northern of OSECS indicated another geochemical processes influenced the fractionation compositions. Since this area was close with Okinawa where submarine volcanoes have been found, hydrothermal plume likely influenced trace elements composition. Potential re-mineralization of Fe, and Zn from surface sediment to the pore water or bottom water as micronutrient was bigger compare with atmospheric input in the southern of OSECS, implying that sediment may be an important micronutrient source to the northwestern Pacific Ocean through the Kuroshio Current. The mean concentration of the trace elements in surface sediment of the NwPO were in the following order: Fe > Mn > Zn > Pb > Co > Cd. Cadmium in all stations was dominated by carbonate phase, indicating biogenic and authigenic sources. Manganese and cobalt at the station close with the land were strongly influenced by lithogenic source, while at the open-ocean by authigenic source. Lead and zinc distributed in all phases indicated various sources like biogenic, authigenic and lithogenic source. Iron in all stations dominated in residual phase suggesting lithogenic source.

In the aquatic environment, aquo and chloro complexes will be responsible for adsorption of trace elements on organic substances. The adsorption processes of aquo and chloro complexes functioned simultaneously in freshwater and individually in seawater media. By using chemical fractionation, trace elements in

surface sediment at the north and middle of OSECS are dominated by ocean biogenic and lithogenic, while southern area was largely influenced by hydrothermal plume source. Potential re-mineralization of Fe and Zn from surface sediment to the pore water or bottom water as micronutrient was higher than atmospheric input in the southern of OSECS, implying that surface sediment may be an important micronutrient source to the Japan Sea and the Northwestern Pacific Ocean.

Table of Contents

List of Figures

List of tables

PART I

General Introduction and Study Literature

Chapter I

General Introduction and Study Literature

1.1 Trace metals in aquatic system

1.1.1 Trace metal in marine water

The transport of trace metals from the terrestrial environment to the open ocean occurs through atmospheric deposition of metals, through transport in riverine discharge, as well as from inputs of trace metals from hydrothermal sources. Groundwater inputs are also likely important in some instances. For some metal/metalloids (e.g., Hg, Pb, Cd, and Se), the atmosphere is the dominant pathway for their addition to the ocean, while for the others, terrestrial inputs dominate (Chester 2003). Most metal or metalloids, there is substantial removal in the coastal zone in combination with particulate material removal that occurs during the mixing of river water and seawater in the estuary, and due to changes in the physical regime (Maybeck, 2004; Gaillardet et al., 2004). The estuarine zone is therefore an important location for the removal and trapping of metal in the sediment. Coastal and deep ocean sedimentation and burial is the long-term sink for most metals. In pre-industrial times, the extent of this deep ocean removal would have balanced the net surface erosion and volcanic inputs.

The extent that the trace metals and metalloids cycle through the various pathways in the biosphere to the ocean depends on their chemistry, their

abundance and their usefulness to humans. Metals are purposefully extracted from the Earth's interior and can be transported to the ocean after release in combination with human activity via rivers and the atmosphere. Once entering the ocean, it is the strength of metal complexation and the tendency to form complexes with dissolved natural organic matter (NOM), the solubility of the hydroxide, carbonate and other phases, the propensity of the metals to adsorb onto inorganic and organic solids, or be taken up by organisms, that determine the overall concentration and distribution of the metal in coastal and offshore ocean waters.

The export of material from rivers to the coastal zone is not evenly distributed globally because of the dominance of export from large rivers and because of spatial differences in terrain. Major inputs are the Amazon River region (~14% of the total input), southern Asia (34%) and eastern Asia (36%) (Maybeck, 2004). These regions all have large rivers and periods of high rainfall that drive the high particulate discharge (Gaillardet, 2004). Additionally, in these regions, inputs have been exacerbated in recent times due to enhanced erosion of the landscape as a result of biomass burning, forest removal and intensive agricultural development. In other regions, such activities are also leading to changes in the extent of particulate input to the coastal zone. This increased riverine particulate transport however is countered in many locations by the presence of reservoirs that act as particle traps and prevent the input of material to the estuarine and coastal waters. Such trapping is thought to have resulted in a decrease in silica inputs in some locations, with resultant impacts on the

abundance of diatoms, which are important phytoplankton in coastal waters (Conley et al., 1993; Billen and Garnier, 2007). There has also been some suggestion of coastal Fe limitation which could also be partially a result of decreased terrestrial material flux to the coastal zone. While it is most likely that many particle-reactive elements will be removed from the water column during estuarine mixing, it is possible for them to pass through without their concentration changing dramatically (so called *conservative* elements) or they may even be added to the water column as a result of estuarine processing.

1.1.2 Trace metal distribution in sediments

A main objective in terms of assessing the hazard or risk posed by metals in sediments is estimating the amount of metal that is potentially bio-available. The bioavailability of metals in sediments is a function of their distribution between the dissolved and solid phases, with dissolved metals in pore water generally considered to be the most bio-available fraction. Accordingly, several methods have been developed to estimate the distribution of metals among dissolved and solid phases in sediments. These methods have been thoroughly reviewed by Mudroch et al. (1999, 1997). Although bioavailability is also a function of aqueous phase speciation, limited research has been conducted to estimate metal speciation in pore waters. Generally, for the purpose of ecological risk assessments, the exposure of benthic organisms to sediment-associated metal is assumed to be proportional to the metal concentrations in interstitial water, although some studies indicate that uptake from overlying water (Hare et al., 2003; Roy and Hare, 1999) or ingested

sediment may be a significant source of body burdens of metals. Distribution of metals in sediment pore waters may be determined by field measurements, experimental methods, and mathematical modeling, with the latter also requiring some field measurements. Concentrations of metals in pore waters may be determined in the field by using pore water dialysis chambers or peepers and by methods that separate the solid phase from the pore water, although the latter have been shown to be less reliable (Mudroch et al., 1997). Several extraction schemes have been developed to determine the distribution of metal among operationally defined fractions (e.g., Forstner, 1995; Tessier et al., 1979). However, sequential extraction methods do not cleanly distinguish the occurrence and speciation of different forms of metals in sediments and soils (Tye et al., 2003; Tack and Verloo, 1999). Other experimental methods include leaching tests (e.g., Reuther, 1999). The results of any of these methods are concentrations of metals in pore water, which can be related to toxicity benchmarks.

Speciation/complexation models also may be used to estimate fractions of dissolved and bound metal species. These models rely on measurements of pH, dissolved oxygen, or Eh to establish redox conditions. The models assume that solid-phase binding is governed by sorption to iron and manganese oxides. Model estimates are less reliable when other solid-phase substrates are dominant (e.g., clay minerals) and are a function of the availability and accuracy of the stability constants for the metal-ligand reactions that are used in the calculations. Model estimates are less reliable when other solid-phase substrates are dominant

(e.g., clay minerals), and they are a function of the availability and accuracy of the stability constants for the metal-ligand reactions that are used in the calculations. For anoxic sediments, the availability of sulfide controls metal distribution and solubility. Operationally, AVSs (mainly iron mono-sulfide) have been considered as a measure of reactive sulfides (Forstner, 1995). Studies have demonstrated an inverse relationship between sediment acute toxicity and AVSs for marine and freshwater sediments (Di Toro et al., 1992, 1990; Ankley et al., 1991) as well as between pore water concentrations and AVSs (Brumbaugh et al., 1994; Casas and Crecelius, 1994). As a screening-level tool, the acute toxicity of anoxic sediments can be assessed by determining the ratio of AVSs to simultaneously extracted metal (SEM).

1.2 Rare Earth Elements

The rare earth elements consist of scandium, yttrium and the lanthanide elements with atomic numbers of 57 – 71, although promethium is not naturally occurring. Thus, this group comprises fourteen unique tracers in the lanthanide series. Each of these REEs is primarily trivalent due to the strong binding energy of the remaining electrons, however some REEs can occasionally also be found as quadrivalent or divalent forms in chemical compounds (Laufer et al., 1984; Tyler, 2004). Although the REEs can be divided into light (LREEs: lanthanum, cerium, praseodymium, neodymium, promethium, samarium and europium) and heavy REEs (HREEs: gadolinium, terbium, dysprosium, holmium, erbium, thulium, ytterbium, and lutetium), it is generally accepted that they form a geochemically coherent group and the natural abundances of individual REEs

are positively correlated (Markert, 1987; Tyler, 2004). However, the LREEs tend to be preferentially adsorbed over the HREEs in some cases (Koeppenkastrop and De Carlo, 1992). Previous work has shown that multiple REEs can be used in the same setting while maintaining the ability to differentiate the tracers (Matisoff et al., 2001; Liu et al., 2004; Polyakov et al., 2009), including the use of up to ten individual REEs to determine a sediment's source area (Michaelides et al., 2010). Although the REEs are called "rare" they are not actually that scarce, making up 0.015% of the earth's crust, and as a whole and are as abundant as copper, lead and zinc (Wang et al., 1989). The rarest REEs have abundances in the earth's crust that are greater than cadmium and selenium (Tyler, 2004). REEs also enter the soil environment in fertilizers, phosphogypsum, sewage sludge, incinerator bottom ashes and atmospheric deposition, which will alter the naturally occurring abundance (Hu et al., 2006). Most REEs are concentrated in the soil (avg. 165 ppm) or the soil parent material (avg. 178 ppm), with minimal contributions from groundwater (avg. 57.2 ppt), river water (avg. 78.3 ppt) and global rainwater inputs (avg. range: 9.8 – 690 ppt) (Laveuf and Cornu, 2009) and references therein. The total abundance of REEs in soils is less than 150 ppm, with no single REE having a concentration greater than 66 ppm (Hu et al., 2006). In the United States, individual REE concentrations in the soil were found to be less than 26 ppm (Wutscher and Perkins, 1993; Zhang et al., 2003; Kimoto et al., 2006a). Given the ability to label soil with an REE on the order of 10,000 ppm, there is minimal concern 18 of diluting the tracer, as long as the applied tracer is applied proportional to the enriched area (Polyakov et al., 2009). While REEs are not an

"ideal tracer" in every aspect of the definition provided previously, they satisfy many of the criteria. Since REEs are strongly bound to the soil particles via inner sphere surface complexation (Aja, 1998) and the physiochemical properties of the soil particles and aggregates are not significantly changed when REEs bind to them (Zhang et al., 2001), the labeled particles should behave identically to unlabeled soil particles. REEs can be used to label all particle size classes by mixing with the soil as a solution or powder, although some preferential adsorption to the silt and clay particles does occur (Kimoto et al., 2006a; Michaelides et al., 2010). The REE-labeled soil also persists in the environment for multiple years, providing a method to evaluate longer term erosion processes (Kimoto et al., 2006b). Further, there are three forms of REEs that can be applied to the soil, depending on the application: REE oxides are used primarily in terrestrial soil erosion detection (Zhang et al., 2003; Polyakov, 2004; Kimoto et al., 2006b; Stevens and Quinton, 2008; Polyakov et al., 2009; Michaelides et al., 2010), while the REE nitrate and REE chloride forms are most often used in studies where the soil remains inundated with water (Laufer et al., 1984; Chegrouche et al., 1997; Aja, 1998; Mahler et al., 1998a; Spencer et al., 2011b). The minimum detection limit for REEs can be as low as the parts per trillion level (ppt) for INAA (Loveland, 1989), less than 10 parts per billion for HPLC (Mahler et al., 1998a) and less than 10 ppt in a liquid solution for an ICP-MS (Hu et al., 1998; Coppin et al., 2002; Leybourne and Johannesson, 2008). These low detection limits allow for the REE-labeled soil to be recovered even after the sample is highly diluted, although high background concentrations may obscure the results. Further, the ICP-MS provides a quick and easy means

of analyzing a large quantity of samples (Jarvis, 1988). An ideal tracer should not be toxic to the environment that it is used in, so REEs, with their generally low toxicity, fit this criterion (Haley, 1979). In fact, the Chinese often use a spray fertilizer containing REEs at a rate up to 0.23 kg of REE /ha on more than 15 million hectares, with concentrations in plant tissue found to be relatively low (Tyler, 2004). The few plants known to bio-accumulate REEs include two subspecies of ferns (Dicranopteris dichotoma and 19 Athyrium yokoscence - up to 313 ppm of total REEs for dried leaves) and pokeweed (Phyrolacca americana - up to 280 ppm of total REEs for dried leaves) (Ichihashi et al., 1992), in addition to hickory trees (Carya sp. - up to 2,300 ppm of total REEs for dried leaves) (Robinson et al., 1958). These plants reflect the REE concentrations of the soil they are growing in, showing no preferential uptake of light or heavy REEs (Robinson et al., 1958; Ichihashi et al., 1992). The detection methods mentioned above can identify all of the REEs, such that a full spectrum of REEs can be analyzed with a single run of an INAA (Loveland, 1989), the ICP-MS (Jarvis, 1988) or HPLC (Mahler et al., 1998a). This reduces the number of times a sample will have to be run, as well as the time required to process samples in the lab. Further, given the low cost of producing REE-labeled soil, REEs have potential as sediment tracers (Stevens and Quinton, 2008). Despite the possibility of marginally high background levels and some plant bioaccumulation, rare earth elements appear to meet most of the criteria for an ideal sediment tracer.

1.3 Marine Sediment

1.3.1 Classification of Marine Sediment

Marine sediment originate from variety of source, including continental and oceanic crust, volcanoes, microbes, plants, and animals, chemical process, and outer space. However, identifying the source of particular deposit of marine sediments often proves difficult. Sediment may be altered from their original condition by any of number of physical, chemical, and biological transformations that take the place after the sediment is formed. Visual analysis of the texture and composition of the sediment samples, or descriptive classification, is often the first step in differentiating sediments. Size classification, base on the visual, mechanical, or laser-based sizing of sediment, aids in understanding physical and chemical changes in sediments that occur during transport and deposition.

Descriptive classifications prove highly useful for work at the sea and for describing the pattern of sediment distribution on the seafloor. Oceanographers employ a visual classification system called logging. In the system logging adopted by ocean drilling program, sediment are separated in to two broad categories:

1. Granular: resulting from the fragmentation of inorganic or organic parent material.

2. Chemical: forming directly from dissolved compounds in seawater.

Granular sediment may be formed by mechanical processes (weathering and

erosion), biological processes (secretion of shell or mineralized cell wall), or volcanic processes (above -or below-water ejection of ash and particles). Granular sediment may also be categorized as biogenous, originating from biological processes, or lithogenous, originating from rock.

Chemical sediment have a variety of pseudonyms and may be referred to collectively as hydrogenous (coming from water) or authigenic (forming in place). Chemical sediments include the fragments of limestone and limestone-like rock (dolomite, chert, chalk, etc.), which come from the compacted, buried and mineralized remains of marine organisms whose cell walls are composed of calcium carbonated and other chemical substances.

1.3.2 Sedimentary Processes

Collectively, processes that involve the production, transport, and deposition of sediments are called sedimentary processes or simply sedimentation. Sediments are produced through the erosion of rock, mostly continental, and through the activities of organisms, especially micro-organism that from skeletons or shells. The transport of sediment occurs by winds, rivers, ocean currents, ice flows, and a number of other geologic processes.

The hydrologic cycle plays a central role in the formation, transport, and deposition of sediments. Precipitation of water over landmasses leads to dissolution and fragmentation of rock through weathering. Surface runoff, rivers, and groundwater flow transport sediment and dissolved substances into the ocean. Ultimately, sediments are transported to continental basins, continental

margins, or the deep ocean floor, where they are deposited. The hydrologic cycle also plays a major role in continental weathering, the dissolution, fracturing, or chemical alteration of rock through physical, chemical, or biological processes. Physical weathering refer to the breaking apart or fragmentation of rock slides, debris flow, and other processes, such as earthquakes. Chemical weathering arises due to oxidation of minerals or elements within minerals, dissolution by natural acids, and dissolution of rock in water. Biological weathering stems from the activities of organisms that fracture, dissolved or chemically alter rock.

Sediments move when they interact with moving fluids, including air and water. Whether a given sediment grain moves as a result of fluid flow depends on a complex number of variable. In generally, three types of movement occur: 1) rolling, the tumbling of grain along surface; 2) saltation, the hopping of a grain along a surface; and 3) suspension, the floating of grain within the fluid. Small size grains, such as dust, are easier to move and suspend than larger sized grain such as cobble.

1.3.3 Deposition and Fate of Sediments

When sediments reach the seafloor, a number of processes may occur before their burial as sedimentary layers or rock. Immediately upon settling, sediments may be consumed or processed by organisms living on the sea floor. The reworking or processing by organisms is called bio-turbation. Bio-turbation disturbs the layering and chemistry of sediments because of activities of organisms. The degree of bio-turbation and the depth to which it occurs depend on the kinds of species present and their abundance.

Another important process on the sea floor is diagenesis, the physical, chemical or biological transformation of sediments or sedimentary rock that occurs once they are deposited. Microbial degradation, in particular, alters the chemical composition of sediments soon after they are deposited. The chemical environment of interstitial water-water in the spaces between sediment grain–determines the elements that may be released or retained by sediments. Diagenesis is a complex process that varies considerably over the broad expanse of the seafloor from the continental shelves to the deep basins.

One deposited, sediments and sedimentary rock form successive layers whose depth and properties reveal the history of their formation, transport, and deposition. In some case, tectonic processes may uplift and expose these sediments to the atmosphere.

1.4 East China Sea

1.4.1 Boundaries of the East China Sea Region

The East China Sea forms the largest shelf region in the Northwest Pacific Ocean. It is located at 24°-30° N and 118°-130° E, with a surface area of 770 000 km2 (Fig. 5). The East China Sea has a total water volume of 398 000 km3, with an average depth of 370 m. To the west, the East China Sea is bordered by China, with tremendous freshwater inputs and terrigenous sediment loads, notably from the Yangtze River. In the east the Kuroshio current, moves northward along the shelf edge with a water fl ow of 25-30 Sv (Su, 1998). The East China Sea borders the Pacific Ocean along the Ryukyu Archipelago. In the

north the East China Sea is separated from the Yellow Sea by a line from the northerly tip of the Yangtze River mouth to Cheju Island, and the East China Sea is connected with the Sea of Japan (i.e. the East Sea) through the Korean Strait. The East China Sea is connected with the South China Sea through the Taiwan Strait.

1.4.2 Physical Characteristics of the East China Sea

Geography

The East China Sea is bordered by China, the Korean peninsula, and the Japanese islands of Kyushu and Ryukyu. It is named the East China Sea because of its location to the east of mainland China. The length is from the northeast to southwest of the East China Sea is approximately 1 300 km. The width from the east to west is approximate 740 km (Qin and Zhao, 1987).

Circulation

In the East China Sea, the northeast flow of the Kuroshio Current limits the transport of East China Sea shelf waters to the Northwest Pacific Ocean. The Kuroshio enters the East China Sea from the northeast region of Taiwan and flows along the Okinawa Trough; it then turns to the east and leaves the East China Sea, joining the North Pacific Ocean at about 30^{o} N through the Tokara Strait (Figure 2). The Taiwan Warm Current is formed by water from the Taiwan Strait and the upwelling of the Kuroshio at the northeast corner of Taiwan (Su, 1998). The Taiwan Warm Current occupies the broad shelf of the East China Sea, and affects the region off the Yangtze River estuary at water depths of 50 m, inducing local

upwelling along the coast in the summer when the south monsoon prevails. Historically, the Yangtze River (Changjiang) carries 928.2 billion m3/year of freshwater and 486 million tonnes/year of total suspended matter (TSM) to the East China Sea. In the north, the Yellow Sea Coastal Current aff ects the northern part of the East China Sea in the winter. In the winter, the effl uent plumes from the Yangtze River, as limited by a salinity of 25-30‰, fl ow southward along the coast of China, forming part of the East China Sea Coastal Current (ECSCC), reaching the northern shelf of the South China Sea. In the summer when the Yangtze River floods, the freshwater effluent plumes disperse eastward over the broad shelf at the surface and can reach Cheju Island, affecting the southern part of the Korean coast, particularly when extreme flood events occur in the Yangtze River drainage basin.

1.4.3 Hydrology of the East China Sea

Rivers

The rivers have significant influence on the hydrologic conditions of the East China Sea, particularly the Yangtze River, Qiantangjiang, and Mingjiang

Yangtze River, the Yangtze River (Changjiang) is the longest river in China and one of the most famous rivers in the world. The Yangtze River is 6397 km long and drains an area of 1.81 million km2, of which 19% of is in China. The population in the Yangtze River catchment area is 40% of that of China and the Gross Domestic Product (GDP) of this area is more than 40% of entire country's GDP. Historically, the highest river sediment discharge has been 560 million

tons/year. The deposition of river sediments has formed the basis of the modern Yangtze River Delta. The Yangtze River flows across 9 provinces and 167 counties in China. There are many important cities in this drainage, such as Chongqing, Wuhan, Nanjin and Shanghai (Zhu, 1993), which form the most densely populated and economically developed areas in China. The landscape of the Yangtze River drainage basin is quite diverse. The area of alti plano, mountain, hill, and basin accounts for 84.7% of the total, with plains accounting for 11.3%, and rivers and lakes occupying 4% (Jiang and Peng, 1999). Storm-related fl oods occur frequently in the drainage basin, resulting in substantial annual economic losses. According to statistical data for 2002, 150 million people were affected by floods, 1 819 persons died in flood-related disasters and 120 000 km2 of farmland were damaged, with 1 460 000 houses destroyed; the direct economic losses combined to approximately 10 billion USD (84 billon Yuan) (MCA-DSD, 2003).

Qiantangjiang, the Qiantangjiang is the biggest river in Zhejiang Province and is 604 km long with a drainage basin of 4.88 million km2. The Qiantangjiang has its source in Anhui Province and empties into Hongzhou Bay. Qiantangjiang is rich in water resources. To date, four reservoirs and twelve water and electricity stations have been built (Zhu, 1993).

Mingjian, the Mingjiang fl ows across the middle of Fujian Province and is 223 km in length, with a total basin area of 61 000 km2. The basin is located in a subtropical area and the adjacent coastal area is well-vegetated, with a resulting high coverage ratio of forest over the watersheds. Mingjiang has a low sediment content, with the average sediment discharge at 5.70 million tonnes/year (Zhu,

1993)

Lakes

Lakes in the area are closely linked to rivers, but are more susceptible to anthropogenic effects. The plain in the middle of the Yangtze River has one of the densest areas of lakes in China.

Poyanghu, Poyanghu Lake is the largest freshwater lake in China and is located in Jiangxi Province. The hydrographic parameters of the lake change sharply during the year. In the flood season, the water level is 21.69 m above sea level, and the lake's average width is 17.3 km, with an acreage of 2 933 km2 and a maximum depth of 29.19 m. But years with the average lowest water level, the acreage is only 146 km2, or only 5% of the largest acreage (Wang and Dou 1998). Because of human activities such as land reclamation, sedimentation is affecting the fl ood storage capacity of the Poyanghu and its ecosystems have deteriorated. According to a national report, the acreage of Poyanghu decreased from 5 000 km2 in the 1950s to 2 933 km2 at present, and the loss of fl ood storage capacity is about 490.5 m3 (Wang and Dou, 1998).

Dongtinghu, Dongtinghu lake is the second largest freshwater lake in China and is located in Hunan Province. Dongtinghu is 143 km long, 17 km wide and 6.4 m deep, with an average acreage of 2 432 km2 and a storage capacity of 15.54 km3. The area of Dongtinghu has also decreased from 6 000 km2 in 1825 to 2 691 km2 at present because of human activities such as land reclamation (Wang and Dou, 1998).

Taihu, Taihu lake is the third biggest freshwater lake in China and is located in Jiangsu Province. The acreage of Taihu is 0.38% of China's area. The population of this area accounts for 3.08% of that of China. This area is highly developed and populated, and is called "the Golden Triangle", including Shanghai. Taihu is 68 km long, 35.7 km wide and 2.3 m deep, with an average acreage of 2 425 km2 and a storage capacity of 5.14 km3 (Wang and Dou, 1998).

Chaohu, Chaohu Lake is the fi fth biggest freshwater lake in China and is located in Anhui Province. Chaohu is 61.7 km long, 12.47 km wide and 2.7 m deep, with an average acreage of 770 km2 and a storage capacity of 2.07 km3 (Wang and Dou, 1998).

Qiandaoh,Qiandaohu Lake is located in Zhejiang Province. It covers 573 km2 and has an average depth of 34 m. The water transparency is 7-9 m, which is considered to be fi rstclass water quality by the local government (Qiandao Lake Online, 2004).

Dianshanhu, Dianshanhu Lake is located in Shanghai, and is Shanghai's freshwater fishing area. Dianshanhu is 12.8 km long, 4.98 km wide and 2.5 m deep, with an average acreage of 47.5 km2 and a storage capacity of 0.16 km3 (Wang and Dou, 1998).

1.4.4 River Input

The total riverine input to the East China Sea amounts to 1 200 billion m3/ year of freshwater and 500 million tons/year of suspended sediments, of which the Yangtze River accounts for 90-95% of both. Riverine inflow to the East

China Sea is highly variable with respect to water and sediment loads and water quality. The river drainage from the land and islands shows important seasonal patterns, under the influence of climate zones from sub-tropical in the south to temperate in the north, and anthropogenic perturbations, such as changes in land use, which may mean that nutrient concentrations from various rivers may differ by 5-10-fold (Zhang 2002). Concentrations of nutrients, particularly nitrogen, are higher in the catchments with extensive land development, particularly agriculture. Consequently, the nutrient species ratio can be up to 100-500 for N:P in the rivers emptying into the East China Sea, which is considerably higher than in European and North American river systems. Other water quality parameters, such as chemical oxygen demand (COD) and *Escherichia coli* counts have also been identified as problematic in coastal waters affected by land drainage.

1.3.5 Chemical Parameters

In the East China Sea, a high concentration of riverine nutrient species can be identified in the surface waters. The influence of land-source nutrients can be seen at the surface over a distance of up to 250-300 km away from the coast. High dissolved inorganic nitrogen/phosphorus (DIN/P) and dissolved inorganic nitrogen/silicon (DIN/Si) ratios resulting from land run-off aff ect a region that is more than about 400-450 km off the Yangtze River (Zhang, 2002). In off shore waters, the concentration of nutrients is relatively low, both for surface and near-bottom samples, and a gradient of nutrient species can be established from the coast to the broad shelf. The Kuroshio Current has a significant impact on the nutrient budget of the East China Sea. The concentration of nutrients (N, P and Si)

in deep waters can be one order of magnitude higher than at the surface in the region of the Kuroshio. Nutrient concentrations of the Kuroshio subsurface waters are 5 to 10-fold higher (N, P and Si) than those from the middle shelf area, which provides a signature of its upwelling across the entire continental slope. The Kuroshio sub-surface waters have relatively high P/N and Si/N ratios compared to land-sourced discharges. Thus the Kuroshio waters that intrude onto the shelf compensate for the nitrogen-rich and phosphorus-depleted freshwater effluent in coastal areas, such as off the Yangtze River delta, and consequently support high primary productivity in the water column. The change from phosphorus-limited environments on the coast to nitrogen-limited environments further off shore can be seen across the broad shelf.

1.5 Northwestern Pacific Ocean

Pacific Ocean currents follow the general pattern of those in the Atlantic. The North Equatorial Current flows westward in the general area of the northeast trades, and the South Equatorial Current follows a similar path in the region of the southeast trades. Between these two, the weaker North Equatorial Countercurrent sets toward the east, just north of the equator.

After passing the Mariana Islands, the major part of the North Equatorial Current curves somewhat toward the northwest, past the Philippines and Taiwan. Here it is deflected further toward the north, where it becomes known as the Kuroshio, and then toward the northeast past the Nansei Shoto and Japan, and on in a more easterly direction. Part of the Kuroshio, called the Tsushima Current, flows through Tsushima Strait, between Japan and Korea, and the Sea of Japan,

following generally the northwest coast of Japan. North of Japan it curves eastward and then southeastward to rejoin the main part of the Kuroshio. The limits and volume of the Kuroshio are influenced by the monsoons, being augmented during the season of southwesterly winds, and diminished when the northeasterly winds are prevalent.

The Kuroshio (Japanese for “Black Stream”) is so named because of the dark color of its water. It is sometimes called the Japan Current. In many respects it is similar to the Gulf Stream of the Atlantic. Like that current, it carries large quantities of warm tropical water to higher latitudes, and then curves toward the east as a major part of the general clockwise circulation in the Northern Hemisphere. As it does so, it widens and slows, continuing on between the Aleutians and the Hawaiian Islands, where it becomes known as the North Pacific Current.

As this current approaches the North American continent, most of it is deflected toward the right to form a clockwise circulation between the west coast of North America and the Hawaiian Islands called the California Current. This part of the current has become so broad that the circulation is generally weak. Near the coast, the southeastward flow intensifies and average speeds are about 0.8 knot. But the flow pattern is complex, with offshore directed jets often found near more prominent capes, and pole ward flow often found over the upper slope and outer continental shelf. It is strongest near land. Near the southern end of Baja California, this current curves sharply to the west and broadens to form the major portion of the North Equatorial Current.

During the winter, a weak countercurrent flows northwestward, inshore of the southeastward flowing California Current, along the west coast of North America from Baja California to Vancouver Island. This is called the Davidson Current. As in the Atlantic, there is in the Pacific a counterclockwise circulation to the north of the clockwise circulation. Cold water flowing southward through the western part of Bering Strait between Alaska and Siberia, is joined by water circulating counterclockwise in the Bering Sea to form the Oyashio. As the current leaves the strait, it curves toward the right and flows southwesterly along the coast of Siberia and the Kuril Islands. This current brings quantities of sea ice, but no icebergs. When it encounters the Kuroshio, the Oyashio curves southward and then eastward, the greater portion joining the Kuroshio and North Pacific Current.

The northern branch of the North Pacific Current curves in a counterclockwise direction to form the Alaska Current, which generally follows the coast of Canada and Alaska. When the Alaska Current turns to the southwest and flows along the Kodiak Island and the Alaska Peninsula, its character changes to that of a western boundary current and it is called the Alaska Stream. When this westward flow arrives off the Aleutian Islands, it is less intense and becomes known as the Aleutian Current. Part of it flows along the southern side of these islands to about the 180^{th} meridian, where it curves in a counterclockwise direction and becomes an easterly flowing current, being augmented by the northern part of the Oyashio. The other part of the Aleutian Current flows through various openings between the Aleutian Islands, into the Bering Sea. Here it flows

in a general counterclockwise direction. The southward flow along the Kamchatka peninsula is called the Kamchatka Current which feeds the southerly flowing Oyashio. Some water flows northward from the Bering Sea through the eastern side of the Bering Strait, into the Arctic Ocean.

PART II

Sampling and Methods

Chapter 2

Sampling and Methods

2.1 Sampling, Sample Pretreatment and Isolation

2.1.1 Isolation Humin from Organic Substances.

Peat soil was obtained from South Sumatra, Indonesia. Humin was extracted following the procedures recommended by the International Humic Substances Society (IHSS). Peat soil (100 mg) was treated with a 0.1 M HCl solution equal to 10 times the sample weight. The mixture was shaken for 1 h, and the suspension left undisturbed until the solid component of the sample settled. The solid and supernatant were fully separated by centrifugation at 2500 rpm for 15 min. The solid residue was neutralized to pH 7.0 by a 1.0 M NaOH solution, and a 0.1 M NaOH volume equal to 10 times the sample weight was added under the nitrogen atmosphere. The alkaline suspension was shaken for 4 h, and the suspension sample subsequently left undisturbed overnight. The supernatant was separated from the solid residue by centrifugation at 2500 rpm for 15 min. Humin purification was conducted by 0.5% HF-HCl solution, and washed by distilled water until the sample was Cl^- free. Humin characterization included determination of: (1) ash content; (2) functional group content by Fourier transform infrared spectroscopy, FTIR (Shimadzu 8201 PC, Japan); and (3) total acidity, carboxylic, and phenolic-OH group content by barium and

calcium acetate methods (Stevenson 1994).

2.1.2 Trace Elemetns in Surface Sediment of the East China Sea and the Northwestern Pacific Ocean

The sediment samples from seven locations in the East China Sea (outer shelf continent) were selected on 24-28 September 2012 (KT-12-25) and July 2013 (KH-13-04), while the Northwestern North Pacific Ocean were selected on August 23rd to September 16th 2012 with the cruise name KH-12-04 (Fig. 5, 6 and 7), collected from the bottom of the sea by multi core sediment sampling. The top sediments (0-3 cm) was taken and sub sampled by plastic spatula then sealed in PTFE bags and storage at low temperature (-5 degree Celsius). The dry sample are easier to be treat than wet sample, so in our work, I used cold dryer that can dry the samples at -40 degree Celsius. Dry sample were used for the sequential extraction procedure analytical method.

Inductively Coupled plasma-mass spectrometry (ICP-MS HP 4500, Japan) was applied to determination of traces metals and rare earth elements in this work. A horizon shaker was used for the extraction and pH meter was used to measurement pH value of the extraction. An ultracentrifuge was used for centrifugation of the extract. All the teflon, glass and plastic containers used was cleaned by aqua regia (HCl : HNO3 = 3:1) and rinse with MilliQ water (deionized water). The extract of the sample were stored in PTFE tubes and stored at 4^{o}C before analysis.

2.2 Interaction of Cd(II) with Organic Substances

2.2.1 Solubility of Cd(II) in Water Media

The effects of adding humin to Cd(II) solubility in various acidic water media were measured. Twenty-five mL aliquots of aqueous 100 $mg.L^{-1}$ Cd(II) solution were transferred by pipette into 100 mL polyethylene bottles; solution pH was adjusted to 2, 3, 4, 5, 6, 7, 8, 9, 10, 11, and 12 by the addition of HCl and NaOH. Fifty mg of isolated humin was added to each bottle shaken for 120 min, and subsequently left undisturbed for 24 h to reach equilibrium. The filtrate and solid residue were separated by centrifugation at 2500 rpm for 15 min, and filtered through 1 µm Millipore filters. The concentration of Cd(II) in filtrate was determined by atomic adsorption spectroscopy, AAS (Perkin Elmer 3110, USA).

2.2.2 Kinetic and Thermodynamic Parameters of Interaction Cd(II) on Organic Substances

The constant Cd(II) adsorption rate onto humin in freshwater (pH= 6.32) and seawater (pH= 7.31) media was determined by transferring 25 mL aliquots of aqueous 100 $mg.L^{-1}$ Cd(II) solution by pipette into 100 mL polyethylene bottles. Fifty mg of humin was added to each bottle and shaken over the following time course: 2, 5, 10, 20, 40, 90, 120 and 180 min.

The mechanism of Cd(II) adsorption onto humin in freshwater and seawater media was determined using 25 mL aliquots of aqueous 100 $mg.L^{-1}$ Cd(II) solution transferred by pipettes into 100 mL polyethylene bottles. Five hundred mg of humin was added to the prepared solution, shaken for 1 h, and

left undisturbed for 24 h until the solid sample settled. The filtrate and solid residue were separated by decantation, and filtered through 1 μm Millipore filters. The Cd(II) concentration in the filtrate was determined by AAS. The residue was air-dried followed by sequential fractionation. MilliQ water was used to determine the contribution of physical interaction (trapping mechanism); sodium acetate and ammonium acetate were used to determine the ion exchange contribution; hydroxylamine hydrochloride to determine hydrogen bond formation contribution; and sodium pyrophosphate was used to determine the contribution of the complex formation mechanism.

Cd(II) energy and adsorption capacity onto humin in freshwater and seawater media were determined using 25 mL aliquots of aqueous Cd(II) with the following concentrations: 20, 40, 60, 80, 140, 180, and 200 $mg.L^{-1}$, transferred by pipette into 100 mL polyethylene bottles. Fifty mg of humin was added to the solution in each bottle, shaken for 2 h, and subsequently left undisturbed to settle for 24 h to reach equilibrium.

2.3 Trace Elemetns in Surface Sediment of The East China Sea and Northwestern Pacific Ocean

2.3.1 Pseudo Total Trace Metal Digestion

Total concentration of trace metals in sediment were determined by digestion with mixture of aqua regia and HF. One gram of the sediment sample and 20 mL of mixture acid (15 mL HNO3 + 5 mL HCl + 2 mL HF) were heated in sand-bath heater. Digests were filtered by Whatman filter paper into the 50

mL of volumetric flasks.

2.3.2 Sequential Extraction Methods for Trace Metals and Rare Earth Elements in Surface Sediment

Sequential extraction was performed using three stage modified procedure recommended BCR plus the residual fraction presented in Table 5 (Nemati et al., 2011). All extraction was carry-out for 16 h (overnight) at room temperature using mechanical shaker. The extract separated by centrifugation for 25 minutes at 3000 rpm, and resultant supernatant liquid was transferred into a polyethylene volumetric flask. The residue was washed by adding 20 mL of deionized water, shaken for 15 minutes on the end-over-end shaker, and centrifuged for 20 minutes at 3000 rpm.

Step 1 (Acid extractable /exchangeable fraction): 40 mL of 0.11 M acetic acid (Solution I) was added to 1 gram sediment sample in centrifuge tube and shaken for 16 h at room temperature. The extract was then separated from the solid residue by centrifugation and filtrate was separated by decantation as previously described

Step 2 (easy reducible fraction): 40 mL of a freshly prepared hydroxylammonium chloride (solution II) was added to the residue from step 1 in the centrifuge tube, and re-suspendid by mechanical shaking for 16 h at room temperature. The separation of the extract, collection of supernatant, and rinsing of residues were the same as describe in step 1.

Step 3 (Oxidizable fraction): the residue from step 2 was treated twice with 10 mL of 8.8 M hydrogen peroxide (solution III). First, 10 mL of hydrogen

peroxide was added to the residue from step 2 in the centrifuge tube. The digestion was allowed to proceed at the room temperature for 1 h with occasional manual shaker, followed by digestion at 85±2 ^{o}C for another 1 h in a water bath. During the digestion, the centrifuge tube was loosely covered to prevent the substantial loss of hydrogen peroxide. Following that, the centrifuge tube was uncovered and heating was continued until the volume reduced to about 2-3 mL. An additional 10 mL of hydrogen peroxide was added to the tube, covered, and digested with cover at the volume reduced to 2-3 mL. Finally, 50 mL of 1.0 M ammonium acetate (solution IV) was added to the cold mixture and shaken for 16 h at room temperature. The separation of the extract, collection of supernatant, and rinsing of residues were the same described in step 1

Step 4 (residual fraction): The residue from step 3 was digested using a mixture of *aqua regia* (HCl:HNO_3 = 3:1) and HF

2.3.3 Silica Analysis

a. Principal

The molybdenum-yellow was applied to analyze for dissolved silica in the solution each fraction (carbonate, oxides, organic matter and residue) of sediment sample. Silicon is usually ionized when dissolved; it is present as orthosilicic acid (H_4SiO_4 or $Si(OH)_4$) which react with acidic ammonium molybdate to form a blue silico-molybdate complex. This is then compared to standard of known concentration using spectrometer at 380 nm in a 1 cm cell.

b. Preparation of reagents and standard

Reagents 0.01 M sodium-hexa fluorosilicate (Na_2SiF_6), 6 N Sulfuric acid, and 10% ammonium molybdate are required for analysis. Solution of Na_2SiF_6 was prepared by dissolved 1.8804 g of Na_2SiF_6 with 1 liter of de-ionized water to make the concentration 0.01 M. The 10% ammonium molybdate solution was prepared by dissolving 50 g of ammonium molybdate in 500 ml of de-ionized water and the 6N H_2SO_4 was prepared from 36N H_2SO_4 in 100 ml flask.

Standards were prepared 0, 50, 100, 150, 200, 250, and 300 µM of concentration from the 10 mM sodium hexa- fluorosilicate solution in 100 ml flasks. All the sample tubes were properly labeled, 20 ml of water sample and standards were poured into the test tube. Into all the samples and standards, 1 ml of the 6N H_2SO_4 was added. After that 1 ml of the 10% ammonium molybdate solution was also added but toking not of the time of addition into the first tube because analysis must be began in 45 minutes. In a serial order the set of standards in increasing order (from 0-300 µM were arranged in a racket, followed by the samples and the standards again but in a decreasing order (300-0 µM). The tubes were shook until well mixed of sample and reagents.

c. Spectrophotometer principal, data analysis and output

A spectrophotometer is an instrument that measures the fraction of the incident light transmitted through a solution. In other words, it is used to measure the amount of light that passes through a sample material. The amount

of light absorbed is directly proportional to the concentration of absorbing sample.

Before analysis, a spectrometer was always switched on for at least 1 hour and adjusted to 380 nm. Analyte was put into cuvette and place it in the spectrophotometer. Light of 380 nm wavelength passes through the analyte inside the cuvette, and the amount of light transmitted (passes through the solution-*Transmittance*) or absorbed (*Absorbance*) by the analyte is measured by a light meter. A relationship between standard concentration and absorbance were prepared to obtain linear equation, which was used to determine the concentration of H_4SiO_4 in the samples in micromole unit.

2.3.4 Carbonate Analysis

The sample is treated with diluted acid and the residual acid (not consumed by carbonate) is titrated. The results are referred to as "calcium carbonate equivalent" since the dissolution is not selective for calcite, but also carbonates such as dolomite will be dissolved to some extent.

Five (5) gram of sample, add 100 ml 0.2 M HCl by pipette and swirl inside shaking bottle. Loosely screw on the lid and swirl occasionally during the next hour. Let then stand overnight. The next day, indent the bottle by hand, tighten the lid and shake for 2 hours in reciprocating shaker. Let the suspension settle, pipette 10 ml supernatant solution into 100 ml Erlenmeyer flask and add about 25 ml water. Then add a few drops phenolphthalein indicator and titrate with 0.1 M NaOH

Calculation:

$$\% \ CaCO_3 \text{ equivalent} = N \times [(a-b)/s] \times 50 \times mcf$$

where,

a = ml NaOH used for blank;

b = ml NaOH used for sample;

s = air-dry sample weight in gram;

M = molarity of NaOH solution; 50 = 50 x 10^{-3} x 10 x 100% (equivalent weight of $CaCo_3$);

mcf = moisture correction factor.

2.3.5 Trace Metals and Rare Earth Elements Analysis by Inductively Coupled Plasma Mass Spectrometry (ICP-MS)

Inductively Coupled Plasma Mass Spectrometry or ICP-MS is an analytical technique used for elemental determinations. The technique was commercially introduced in 1983 and has gained general acceptance in many types of laboratories. Geochemical analysis labs were early adopters of ICP-MS technology because of its superior detection capabilities, particularly for the rare-earth elements (REEs). ICP-MS has many advantages over other elemental analysis techniques such as atomic absorption and optical emission spectrometry, including ICP Atomic Emission Spectroscopy (ICP-AES), including:

- Detection limits for most elements equal to or better than those obtained by Graphite Furnace Atomic Absorption Spectroscopy (GFAAS).
- Higher throughput than GFAAS
- The ability to handle both simple and complex matrices with a minimum of matrix interferences due to the high-temperature of the ICP source

- Superior detection capability to ICP-AES with the same sample throughput. The ability to obtain isotopic information

An ICP-MS combines a high- temperature ICP (Inductively Coupled Plasma) source with a mass spectrometer. The ICP source converts the atoms of the elements in the sample to ions. These ions are then separated and detected by the mass spectrometer. Argon gas flows inside the concentric channels of the ICP torch. The RF load coil is connected to a radio-frequency (RF) generator. As power is supplied to the load coil from the generator, oscillating electric and magnetic fields are established at the end of the torch. When a spark is applied to the argon flowing through the ICP torch, electrons are stripped off of the argon atoms, forming argon ions. These ions are caught in the oscillating fields and collide with other argon atoms, forming an argon discharge or plasma. The sample is typically introduced into the ICP plasma as an aerosol, either by aspirating a liquid or dissolved solid sample into a nebulizer or using a laser to directly convert solid samples into an aerosol. Once the sample aerosol is introduced into the ICP torch, it is completely dissolved and the elements in the aerosol are converted first into gaseous atoms and then ionized towards the end of the plasma. The most important things to remember about the argon ICP plasma are:

- The argon discharge, with a temperature of around 6000-10000 K, is an excellent ion source.

- The ions formed by the ICP discharge are typically positive ions, M or M , therefore, elements that prefer to form negative ions, such as Cl, I, F, etc.

are very difficult to determine via ICP-MS.

- The detection capabilities of the technique can vary with the sample introduction technique used, as different techniques will allow differing amounts of sample to reach the ICP plasma.

- Detection capabilities will vary with the sample matrix, which may affect the degree of ionization that will occur in the plasma or allow the formation of species that may interfere with the analyte determination.

Once the elements in the sample are converted into ions, they are then brought into the mass spectrometer via the interface cones. The interface region in the ICP-MS transmits the ions traveling in the argon sample stream at atmospheric pressure (1-2 torr) into the low pressure region of the mass spectrometer (<1 x 10-5 torr). This is done through the intermediate vacuum region created by the two interface cones, the sampler and the skimmer. The sampler and skimmer cones are metal disks with a small hole (~1mm) in the center. The purpose of these cones is to sample the center portion of the ion beam coming from the ICP torch. A shadow stop or similar device blocks the photons coming from the ICP torch, which is also an intense light source. Due to the small diameters of the orifices in the sampler and skimmer cones, ICP-MS has some limitations as to the amount of total dissolved solids in the samples. Generally, it is recommended that samples have no more than 0.2% total dissolved solids (TDS) for best instrument performance and stability. If samples with very high TDS levels are run, the orifices in the cones will eventually become blocked, causing decreased sensitivity and detection capability and

requiring the system to be shut down for maintenance. This is why many sample types, including digested soil and rock samples must be diluted before running on the ICP-MS. The ions from the ICP source are then focused by the electrostatic lenses in the system. Remember, the ions coming from the system are positively charged, so the electrostatic lens, which also has a positive charge, serves to collimate the ion beam and focus it into the entrance aperture or slit of the mass spectrometer. Different types of ICP-MS systems have different types of lens systems. The simplest employs a single lens, while more complex systems may contain as many as 12 ion lenses. Each ion optic system is specifically designed to work with the interface and mass spectrometer design of the instrument.

Once the ions enter the mass spectrometer, they are separated by their mass-to-charge ratio. The most commonly used type of mass spectrometer is the quadrupole mass filter. In this type, 4 rods (approximately 1 cm in diameter and 15-20 cm long) are arranged. In a quadrupole mass filter, alternating AC and DC voltages are applied to opposite pairs of the rods. These voltages are then rapidly switched along with an RF-field. The result is that an electrostatic filter is established that only allows ions of a single mass-to-charge ratio (m/e) pass through the rods to the detector at a given instant in time. So, the quadrupole mass filter is really a sequential filter, with the settings being change for each specific m/e at a time. However, the voltages on the rods can be switched at a very rapid rate. The result is that the quadrupole mass filter can separate up to 2400 amu (atomic mass units) per second. This speed is why the

quadrupole ICP-MS is often considered to have simultaneous multi-elemental analysis properties. The ability to filter ions on their mass-to-charge ratio allows ICP-MS to supply isotopic information, since different isotopes of the same element have different masses.

Typical quadrupole mass spectrometers used in ICP-MS have resolutions between 0.7 –1.0 amu. hThis is sufficient for most routine applications. However, there are some instances where this resolution is NOT sufficient to separate overlapping molecular or isobaric interferences from the elemental isotope of interest. The use of high resolution or magnetic sector mass spectrometers has become more common in ICP-MS, allowing the user to eliminate or reduce the effect of interferences due to mass overlap. Figure 2 shows a typical instrumental configuration used in high resolution (HR) ICP-MS. In this type of instrument, both a magnetic sector and an electric sector are used to separate and focus the ions. The magnetic sector is dispersive with respect to both ion energy and mass and focuses all the ions with diverging angles of motion coming from the entrance slit of the spectrometer. The electric sector is dispersive only to ion energy and focuses the ions onto the exit slit. Such an arrangement is called a double-focusing high resolution mass spectrometer. In ICP-MS, reverse Nier-Johnson geometry‑where the magnetic sector is before the electric sector – is commonly used in order to decouple the electric fields in the electric sector from any electric field originating by the ICP RF generator.

The resolution of high-resolution instruments can be changed by adjusting the width of the entrance and exit slits into the spectrometer. Typical

HR-ICP-MS instruments have resolving powers up to 10,000 and are typically operated at preset resolution settings for low, medium or high-resolution to make their operation easier for the user. High resolution instruments also have several limitations. First of all, they typically cost 2-3 times that of a quadrupole ICP-MS instrument. They are also more complex to operate and maintain. In addition, for every 10-fold increase in resolving power, there is a concomitant decrease in signal intensity. This may limit the actual detection capabilities if the concentration of the analyte of interest is very low. Finally, they are much slower than a quadru-pole system. Due to the longer settling times required by the magnet when the voltages are adjusted for large mass jumps, HR-ICP-MS instruments typically are 4-5 times slower than a quadrupole instrument. This makes them unsuitable for the rapid, high-throughput, multi elemental analyses that are routine in production-type laboratories. They are also not the instrument of choice for transient signal analysis, including those obtained using Laser Ablation techniques for elemental profiling or chromatographic separations as their scan speeds are too slow to look at more than 1-3 elements of similar mass in an analysis. As a result, this type of instrument is generally found in research institutions and in laboratories with highly specialized needs for a low number of samples. A second type of HR-ICP-MS instrument is also available that uses multiple detectors–this type is called a Multi-Collector HR-ICP-MS or MC-ICP-MS. These instruments are generally designed and developed for the purpose of performing high-precision isotope ratio analyses. Since an array of 5-10 detectors can be positioned around the exit slit of a double-focusing system, the isotopes of a single element can generally all be determined simultaneously,

leading to the technique's high-precision. The disadvantage of this type of system is that the isotopes must all be in a narrow mass range (± 15-20% of the nominal mass) as the magnetic sector settings remained fixed while only the electric sector settings are scanned. This generally means that each elemental isotopic system must be measured in a separate analysis. This type of instrument is generally not suitable for routine multi-elemental analysis for major and minor constituents and is typically only used for performing isotope ratio measurements.

Once the ions have been separated by their mass-to-charge ratio, they must then be detected or counted by a suitable detector. The fundamental purpose of the detector is to translate the number of ions striking the detector into an electrical signal that can be measured and related to the number of atoms of that element in the sample via the use of calibration standards. Most detectors use a high negative voltage on the front surface of the detector to attract the positively charged ions to the detector. Once the ion hits the active surface of the detector, a number of electrons is released which then strike the next surface of the detector, amplifying the signal. In the past several years, the channel electron multiplier (CEM), which was used on earlier ICP-MS instruments, has been replaced with discrete dynode type detectors. Discrete dynode detectors generally have wider linear dynamic ranges than CEMs, which is important in ICP-MS as the concentrations analyzed may vary from sub-ppt to high ppm. The discrete dynode type detector can also be run in two modes, pulse-counting and analog, which further extends the instrument's linear range

and can be used to protect the detector from excessively high signals.

PART III

Results and Discussion

Chapter 3

Trace Elements (Cadmium) Interaction with Organic Substances (Humin)

3.1 Isolation of Humin from Peat Soil and Characterization

Rice and MacCarthy (1990) reported that humin contains four components, including bitumen, which is the largest humin component; bound lipids; bound humic acids; and impurities. Functional groups include -COOH, -OH, and hydroxyphenol. These functional groups are active sites in Cd(II) adsorption onto humin. The isolated humin FTIR spectra (Fig.1) revealed the hydroxyl group centered at 3421.5 cm^{-1}, and aliphatic CH stretching vibration at 2918.1 cm^{-1} and 2850 cm^{-1}. The carboxylic group (-COOH) was observed in bands at <1700 cm^{-1}. These bands were derived from C=O stretching vibrations of hydrolyzable chemical groups. Weak absorptions indicated low humin carboxylic content. Bands observed at <1618.2 cm^{-1} were interpreted as C=C aromatic or hydrogen stretching vibrations attached to the C=O (conjugated ketone). The bands at 1164.9 cm^{-1} in purified humin were derived from C-O stretching vibrations of carboxylate groups. These results indicated that -COOH and phenolic -OH were present in isolated humin.

It was important to elucidate the quantitative composition of functional groups at humin active sites (Table 1), and the amounts of -COOH and phenolic -OH that served as active sites for Cd(II) adsorption. Stevenson (1994) reported total acidity in acidic soils ranged from 560-890 cmol/kg, with the -COOH

group content of the acidic soil in the range of 150-570 cmol/kg. Results of isolated humin ash content are provided in Table 2. A purification process using HF/HCl releases metals and minerals in humin. Ash content is applied as a parameter to determine the purity of the isolated humin. The lower the ash content the more effective the purification process.

Purified humin addition into the water media influenced the solubility of metal ions. The humin active sites, i.e. -COOH and hydroxyphenol, in water were hydrolyzed based on the following equations (Huheey et al. 1993):

$$-COOH + H_2O \leftrightarrows -COO^- + H_3O^+$$

$$-OH + H_2O \leftrightarrows -O^- + H_3O^+$$

At very low media acidity, humin active site protonation occurred according to the following equations:

$$-COOH + H^+ \leftrightarrows -COOH_2^+$$

$$-OH + H^+ \leftrightarrows -OH_2^+$$

At high pH, increased OH^- concentration resulted in competition between the humin active site ($-COO^-$ and $-O^-$) and OH^- in binding Cd(II). OH^- is a stronger ligand than the carboxylate ion ($-COO^-$) and hydroxide ions ($-O^-$) (Huheey et al. 1993). The interaction between cadmium and hydroxide ions to form cadmium hydroxide was dominant.

3.2 Solubility of Cd(II) in the water media.

The effects of humin addition to Cd(II) solubility in water media are

shown in Fig. 2. At pH < 7 without humin present, all Cd(II) was soluble in the water media as free cations or the aquo complex $Cd(H_2O)_6^{2+}$. Between pH 7 and 10, dissolved Cd(II) decreased gradually because most Cd(II) was in the form of $Cd(OH)_2$, which was not soluble in the water media. The $Cd(OH)_2$ Ksp value was 4.5 x 10^{15}, and Cd(II) will hypothetically be precipitated as $Cd(OH)_2$ at pH ≥ 7.555; at pH ≥ 10, no Cd(II) will be detected in solution, as it will all be precipitated as $Cd(OH)_2$.

3.3 Kinetic Parameter of Cd(II) Interaction with Humin

Schnoor (1996) indicated aquo ($Cd(H_2O)_6^{2+}$) and chloro ($CdCl^+$ and $CdCl_2$) complexes were responsible for Cd(II) adsorption onto humin in freshwater and seawater media, respectively. Increased Cl^- concentrations in seawater media resulted in a rise in the chloro complex. The Cd(II) adsorption amount onto humin in seawater media was less than freshwater media (Fig. 3). In freshwater, the adsorption of ($Cd(H_2O)_6^{2+}$) was more rapid than the chloro complex ($CdCl^+$ and $CdCl_2$); and because $Cd(H_2O)_6^{2+}$ size was relatively larger than the chloro complex, i.e. $CdCl^+$ and $CdCl_2$, ion charge was the dominant factor relative to the size of the ion (Fig. 3).

Kinetic parameters for adsorption of Cd(II) onto humin are provided in Table 3. The calculation method proposed by Santosa et al. (2001) was applied to obtain the data consistent with the Langmuir-Hinshelwood kinetics model (Schnoor 1996). In the method, the constant adsorption rate values were obtained from the linear slope of the curve ln(Co/C)/C against t/C from the following equation:

$$\ln(Co/C)/C = k1\,.\,t/C + Q$$

where Co is the initial metal ion concentration, C is the remaining metal ion concentration after sorption at *t* time, *k*1 is the constant sorption rate, and Q represents sorption-desorption constants.

Cd(II) adsorption onto humin in freshwater media only occurred through a single phase. As previously indicated, Cd(II) adsorption onto humin primarily involved two Cd species, in the aqua and chloro complexes, and the two Cd species adsorption rates (aqua and chloro complexes) were relatively similar (Table 3). In seawater media, an increase in chloro and decrease in aqua complex concentrations caused adsorption processes to occur in two different phases. The first phase was considered a fast phase reaction rate constant, which showed a 63-fold reaction rate increase, while the second phase was slow, and exhibited a 12-fold increase compared to the fresh water.

The percent contributions of interaction mechanisms between Cd(II) and humin are shown in Fig. 4. Results indicated two factors affected the adsorption process. (1) Adsorbent: In freshwater media, the -COOH active site contributed to Cd(II) adsorption on humin. This condition caused an interaction tendency to complex bonding. In seawater media, the -COONa active site contributed to Cd(II) adsorption on humin. This condition caused an interaction tendency to cation bonding. (2) Adsorbate: The $-COO^-$ active site involved in the adsorption process was a strong acid, which served as a suitable strong base for adsorbate (Huheey et al. 1993).

Cd(II) adsorption onto humin in freshwater media was dominated by hydrogen bonding and ion exchange. This result indicated that the most stable Cd(II) species in freshwater media was $Cd(H_2O)_6^{2+}$, which therefore showed a tendency to form hydrogen bonding with humin active sites. In addition, Cd(II) species are not strong bases, so the species elicit interactions, which form ion exchanges. However, Cd(II) species do not fit via complex bonding with the humin active site. In seawater media, results showed increased contributions to hydrogen bonding and decreased contributions to cation exchange, indicating that in seawater media, $Cd(H_2O)_6^{2+}$ played an important role in the Cd(II) adsorption process onto humin, which exhibited a propensity to develop hydrogen bonds with the humin active site. The decline in cation exchange suggested that in seawater media, humin binding Na(II) and Cd(II) active sites formed stable $CdCl^-$,, which are poor contributors to adsorption processes.

3.4 Thermodinamic parameter of Cd(II) interaction with humin

Evaluations were performed using the adsorption properties of the Langmuir and Freundlich adsorption isotherm linear equations. We compared results to obtain a conclusion best suited to the pattern of Cd(II) adsorption onto humin in freshwater and seawater media. The following Langmuir isotherm sorption model was used to determine the capacity (b) and sorption equilibrium constant (K); sorption energy (E) was subsequently calculated according to the equation $E = RT \ln K$ (Jain et al. 2004; Dader 2003):

$$\frac{C}{m} = \frac{1}{b.K} + \frac{C}{b}$$

where *C* is the concentration of metal ions remaining in solution at equilibrium, *m* is the adsorbed metal ion on 1g sorbent, *K* is the sorption equilibrium constant, and *b* is the sorption capacity.

The adsorption capacity of Cd(II) onto humin decreased from freshwater to seawater media, as values for *b* were 2 x 10^{-4} mol/g and 1.256 x 10^{-4} mol/g respectively (Table 4). Reduced adsorption capacity indicated that Cd(II) adsorption onto humin was particularly influenced by $Cd(H_2O)_6)^{2+}$ species. In seawater media, the number of $Cd(H_2O)_6^{2+}$ species decreased, causing a reduction in adsorption capacity.

A comparison of Langmuir and Freundlich isotherm parameters (Table 4) showed that the Langmuir model was more closely followed, as may be seen from the higher R^2 values. Therefore, results showed adsorption of Cd(II) onto humin followed a Langmuir isotherm model (monolayer adsorption), with humin active sites dominated by -COOH and phenolic -OH functional groups.

In conclusion, Cd was in the form of Cd(II) and $Cd(H_2O)_6^{+2}$, and soluble in water media. At pH > 7.55, cadmium precipitated as $Cd(OH)_2$. The adsorption processes of aquo $(Cd(H_2O)_6)^{2+}$ and chloro ($CdCl^+$ dan $CdCl_2$) complexes functioned simultaneously in freshwater and individually in seawater media.

Chapter 4

Trace Elements in Surface Sediment from the East China Sea as Marginal Sea

4.1 Reproducibility and Accuracy of BCR Sequential Extraction Method

To evaluate the reproducibility and accuracy of the method, a reference sediment material (GBW-07309) was subjected to BCR protocol. Three sub samples (set A, B, C) were taken through BCR sequential extraction method in parallel. The result and the relative standard deviation (RSD) are listed in Table 6. Result was indicated that method had a good reproducibility and accuracy (RSD < 7.8%).

4.2 Internal Check Recovery

An internal check was performed on the result of the sequential extraction by comparing the total amount of elements extracted by different reagents during the sequential extraction procedure with the result of the total digestion. The recovery was calculated as follow the equation

$$\text{Recovery} = \frac{\text{C fraction 1+C fraction 2+C fraction 3+C fraction 4}}{\text{C total digestion}} \text{ x } 100\%$$

Result showed in Table 7 indicated that the sum of the four fractions are in a good agreement with the total digestion and the methods used is reliable and repeatable

4.3 Hydrographic Setting of Research Area

Hydrographic condition is an important factor to affect the physical properties of sediment; furthermore, it affects the concentration and the spatial distribution of trace elements, which mean that understanding the hydrographic condition is the one key to study trace elements spatial distribution in surface sediments. Based on the references on the division of different water masses (Liu et al., 1992; Chu et al., 2005; Zhang et al., 2007), our study area was divided into three groups (Fig. 8) as follows: group I, the northern of OSECS (station 5, 6 and 7) with the water depths around 41-81 m were bound to the Yellow Sea. The cold, fresh, oxygen-rich, sigma-t (density-1000, $kg.m^{-3}$) close to 25 known as Yellow Sea bottom cold water (YSCW) and the warm, fresh, oxygen-rich, sigma-t less than 22 known as Yellow Sea mixed water (YSMW) influence this group. Group II, at the middle of OSECS (station 4, 8, and 9) with the water depths 54-93 m were influenced by East China Sea surface water (ECSSW) characteristics of the warm, saline, oxygen-poor and sigma-t less than 25 $kg.m^{-3}$ and Kuroshio subsurface water (KSSW) which is cold, saline, oxygen-medium and sigma-t less than 25 $kg.m^{-3}$. Group III, the southern OSECS (station 1, 2, and 3) with the water depths 552-1677 m were strong influenced by Kuroshio Current (KC).

4.4 Spatial Distributions of Trace Elements and Correlation with TOC, Carbonate, SiO_2, and Al

Total concentration ranges of trace elements, TOC, carbonate, SiO_2 and Al in surface sediment of the OSECS were as follows: Fe, 34230-57614 $\mu g.g^{-1}$; Pb, 20.1-98.1 $\mu g.g^{-1}$; Mn, 667-7119 $\mu g.g^{-1}$; Zn, 126-215 $\mu g.g^{-1}$; Cd, 0.1-1.06

µg.g^{-1}; Co, 9.16-30.1 µg.g^{-1}; TOC, 0.67-3.51 %; Carbonate, 8.56-27.5 %; SiO_2, 0.69-1.9 % and Al, 2.81-8.45% (Table 8 and Table 9). The concentration range of trace elements in surface sediment of OSECS are comparable with some reference (Yuan et al., 2012; Fang et al., 2009) characterized by different group depend on the hydrographic setting of research area. Higher concentration of trace elements generally found in the group III, relative to the group II and group I (Fig. 9). This finding is in a good agreement with general distribution of TOC, carbonate, and SiO_2, indicating that biogenic process influenced trace elements concentration and distribution. In contrast, the distribution trend of Aluminum was opposite with the trace elements, TOC, carbonate and SiO_2. For most of sedimentary deposits, aluminum can be considered an indicator of alumino-silicates fraction of sediment, with very little ability to move during diagenesis (Morford and Emerson, 1999; Piper and Perkins, 2004) and aluminum also can act as indicator of lithogenic origin from the continent. Lower concentration of Al at the southern OSECS compared with middle and northern, suggesting lithogenic effect on the group III was not as strong as group I and II (Fig. 10).

In addition, higher concentration of Mn in group III (average: 5004 µg g^{-1}) compared with other groups (average group II, 1084 µg g^{-1}; and group I, 906 µg g^{-1}) indicated special geochemical process happened in this area. Since this area was close with the Okinawa Trough, some submarine volcano in this area likely produce hydrothermal plume to influence the Mn concentration. It is well established that hydrothermal fluxes can represent a potentially important source of trace elements. Trace elements of Pb, Zn, and Mn are enriched in this

environment, commonly hosted by suite of minerals such as barite, celestite, galena, blende and rhodochrosite (Tribovillard et al., 2006 and references therein).

Pearson's correlation coefficient given an idea about possible relations between elements: common origin, uniform distribution, similar behavior and relationships amongst trace elements. Good correlation coefficient value between each trace elements can be indication come from the same origin. The result shown in Table 10 generally trace elements had a significant positive correlation between each other. This data indicated that trace elements in the sediment of OSECS generally come from the same origin.

The relationships between concentration of trace elements with TOC, carbonate, SiO_2, and Al by Pearson's correlation coefficient was shown in the Table 10 give us information about control factor of trace elements distribution. TOC had a good correlation coefficient with Cd, Pb, Mn, and Zn (0.92, 0.72, 0.87, and 0.90) indicated that the concentration of these four trace elements strongly influenced by TOC. While carbonate correlated well with the Cd and Zn (0.77 and 0.77) indicated that the distributions of these two trace elements also influenced by carbonate. In addition total SiO_2 had a good correlation with all trace elements (Cd, 0.88; Pb: 0.93; Mn, 0.88; Fe, 0.76; Co, 0.81; and Zn, 0.80) indicated that SiO_2, TOC and carbonate lead to the increase of trace elements concentration in the surface sediment of the OSECS. In other words, trace elements in surface sediment of OSECS mainly come from the ocean biogenic process.

4.5 Source of Trace Elements by Using Fractionation and Correlation with TOC, SiO_2, Carbonate, and Al

To further identify various sources of trace elements in sediment, chemical fractionation can give complete information about potential source and bioavailability of trace elements in surface sediment. Trace element in carbonate phase is indication of natural ocean biogenic (diatom and foraminifera) or anthropogenic origin and easy re-mineralization to the pore water or bottom sea water (good bioavailability). Oxide phase represents Mn/Fe oxides origin and may be released to the pore water or bottom sea water if the sediment is subjected to more reducing condition (more difficult to re-mineralization relative to carbonate phase). Organic phase is deemed biogenic origin (bond to organic matter or sulfides) and may be released into environment if conditions become more oxidizing (difficult to re-mineralization). Trace element in residual fraction denotes lithogenic origin from continent which has very strong bonding with sediment (the most difficult phase to re-mineralization).

To facilitate discussion of the distribution of trace elements, fractionation of trace elements in surface sediment were divided into two types (Fig. 11 and Table 9): 1) by the degree of their association with the different phases; and 2) by the area. By the degree of their association with the different phases, trace elements in surface sediment of OSECS divided into three groups. Manganese (Mn), Zinc (Zn) and Lead (Pb) existed in all phases indicated that they come from various sources. Cadmium (Cd) presented mainly in carbonate phase (average 72.8%), suggesting natural biogenic or anthropogenic source. While

Iron (Fe) and Cobalt (Co) were dominated by residual phase (average Fe: 83.6% and Co: 72.7%) indicated that these two trace elements were strongly influenced by lithogenic source from continent. By the area, the southern ECS had special feature which the proportion of oxides phase (average Cd: 32.4; Pb: 64.4; Mn: 84.1; Fe: 21.6; Co: 37.1 and Zn: 36.6%) was bigger than that in the middle ECS (average Cd: 6.3; Pb: 46.8; Mn: 38.7; Fe: 6.4; Co: 9.2; and Zn: 22.7%) and the northern ECS (average Cd: 4.3; Pb: 40.8; Mn: 30.8; Fe: 7.4; Co: 10.0 and Zn: 22.8%).

The marine geochemistry of manganese (Mn) has been studied rather extensively (e.g. Bruland and Franks, 1983; Donat and Bruland, 1995; Wei et al., 2000) not only because Mn participates in wide variety of geochemical processes but also because it's geochemical behavior may co-precipitate and scavenge other trace elements. The distribution and fractionation of Mn in the water and the sediment are strongly affected by external origin and sink (Klinkhammer et al., 1997), hydrothermal processes (Mottl et al., 1995) and redox condition (Martin et al., 1985). Generally, Mn in all stations has relatively big portion of the oxides phase (Fig. 11), indicating Mn in our study area is liable to deposit in coarse sediment to form hydrate manganese oxides ($MnO_2.nH_2O$) and may be released if the sediment is subjected to more reduced condition (Panda et al., 1995). Especially for the group III (station 1, 2, and 3), the dominant fraction of Mn was oxides phase. Since this group was close with volcano area (Okinawa trough) (Wei et al., 2000; Hsu et al., 2003), domination in oxides phases indicated that Mn was strong influence by hydrothermal plume become hydrate manganese oxides. Good correlation (0.84) existed in the oxides phase between Mn and SiO_2 (Table

7) indicated that distribution of Mn in oxides phase was influenced by SiO_2. In addition, Mn concentration in oxides and organic matter phase correlated well with other trace elements but not for carbonate and residual phase, demonstrating Mn and other trace elements in oxides and organic matter phase come from the same origin.

Similar with Mn, Pb also had a big portion of oxides phase at all stations. In other words, Pb in this phase was liable to deposit in coarse sediment to form hydrate lead oxide ($nPbO.H_2O$). Pb had good correlation with SiO_2 and TOC in the oxides phase (0.97 and 0.85) (Table 11), indicating that the distribution of Pb in oxides phase was influenced by SiO_2 and TOC. Dissolved Pb in water from aerosol deposition could be scavenged by Mn oxides, whose seaward decreasing trend in the ECS might contribute to the similar distribution of oxides phase Pb (Lin et al., 2002). Lead at the group III had the biggest proportion of oxides phase compared with other station, likely hydrothermal plume also influenced the fractionation of Pb.

Zinc could have various sources (Fig. 11) since it comparably existed in all phases. Similar with Mn, the proportion of oxides phase in the southern part (group III) was bigger than in the middle and northern (group I and II), indicating that Zn distribution in group III was influenced by manganese oxides as scavenging for other trace elements. Strong positive Pearson's correlation coefficient between Zn and other trace elements in oxides and organic matter phase indicated that Zn in these two phases probably come from the same origin with other trace elements. Moreover, good correlation between Zn with SiO_2 and TOC in oxide phase (0.79 and 0.97) and organic matter phase (0.77 and 0.92)

suggested that Zn in these two phases come from the biogenic sources. Zinc as trace nutrient, is typically depleted in the upper layer of water column because of biological uptake by marine phytoplankton and are strongly correlated with macronutrients (Frew et al., 2001; Hendry et al., 2008; Sun et al., 2011), e.g. Zn and silicate

The result of sequential extraction for Cd showed that the dominant proportion of Cd (more than 78% except S4) was carbonate phase, implying that most of Cd in the surface sediment of the OSECS is exchangeable. The trace elements in this phase are adsorbed on sediments or on their essential components namely clay and humic acids (Yuan et al, 2004). Weakly adsorbed Cd on the surface sediment by relatively weak electrostatic interaction may be released by ion-exchange processes and dissociation of Cd-carbonate phase (Tersier et al. 1979). Extremely high oxides phase of Cd in group III denoted that other processes influence fractionation of Cd, such as authigenic processes besides ocean biogenic input. Furthermore, some cadmium in the seawater or surface sediment can be scavenged by Mn oxides dominant in group III. Since Cd is a nutrient type element and could be delivered to sediment with marine organic matter (Tribovillard et al., 2006), biogenic Cd is often associated with calcium organism and biogenic carbonate in sediment (Lin et al., 2002), a good correlation coefficient of Cd with carbonate and SiO_2 in the carbonate phase (0.87 and 0.86) (Table 7) indicated that distribution of Cd in the OSECS was controlled by carbonate and SiO_2. Moreover, good correlation of Cd with SiO_2 and TOC in the oxides and organic matter phases give more evidence that Cd in the surface sediment of OSECS was from the biogenic process.

The distribution of Fe and Co in the surface sediment ECS mainly were found in the residual phase (Fig. 11). This pattern was similar with the result reported by Yuan et al., 2004 and Yu et al., 2013, who found that Fe and Co in the surface sediment of inner shelf ECS mostly retained in the residual phase. High proportion of residual phase implied that Fe and Co in OSECS dominant from natural lithogenic origin via Changjiang River, yellow sea, and Korean coastal current sediment load and atmospheric input. Trace elements associated with the residual phase are likely to be incorporated in alumino-SiO_2 minerals and unlikely released to pore-water through dissociation. These elements are unlikely to pose direct and significant threaten to surrounding. Moreover, Fe and Co had a good correlation coefficient with Al in the residual phase (0.71 and 0.84) (Table 11), indicated that the distribution of these two trace elements strong influence by Al in the form of alumino-silicates. Similar with other trace elements, Fe and Co at the southern ECS (group III) also had a biggest proportion of oxides phase compare with other group likely hydrothermal plume or manganese oxides as scavenging also influenced the fractionation of Fe and Co.

To further evidence multi sources of various trace elements, we compared trace elements in different endmembers and our samples. Here, we chosen Fe and Mn as indicators of hydrothermal and lithogenic source, we plotted a graph between Fe vs. Mn (Fig. 12.A). The result showed that the stations 1, 2, and 3 (group III) tend to be influenced by these two sources. Hydrothermal activity releases large quantities of manganese and deposited in coarse sediment to form hydrate manganese oxides ($MnO_2.nH_2O$), which can influence the

sedimentary accumulation of other trace elements through their redox cycling in oxygen-deficient environment (Morford et al, 2005). In contrast, groups I (station 5, 6 and 7) and II (station 4, 8 and 9) overlap with lithogenic endmember, clearly indicating Fe and Mn in these two groups were influenced by lithogenic origin. To differentiate other trace element sources in group I and II, Zn and Co are used to trace biogenic sources. Zn and Co in these two groups located two endmember mixing line between biogenic and lithogenic source (Fig. 12.B), indicating they are affected by these two sources.

4.6 Trace Elements Sediment Flux, Atmospheric Input and Potential Re-mineralization

About 40–50% of the sediment (~ 2.3×10^8 t y^{-1}) load from the Changjiang River deposits in the estuary, while the remaining is delivered to the ECS shelf during flood seasons, but much is re-suspended and carried southward by winter storms and coastal currents (Milliman et al., 1985b; Zhang and Liu, 2002; Liu et al., 2010). An elongated subaqueous mud wedge is formed extending from the river mouth southward off the Zhejiang and Fujian coast (Liu et al., 2007). This illustrated that sediment load from the Changjiang River could be a significant trace elements source in sediments of the East China Sea. In addition, the Yellow Sea Current and Korean Coastal Current provided important trace elements into the OSECS, which annually carries Fe: 1.5×10^9 kg y^{-1}; Mn: 2.7×10^7 kg y^{-1}; Cd: 1.9×10^4 kg y^{-1}; Pb: 8.3×10^5 kg y^{-1}; and Zn: 5×10^6 kg y^{-1} from the south Yellow Sea and Korean coast into the northeastern ECS (Yuan et al., 2012). Lower concentrations of TOC and most trace elements in the northeastern OSECS (group I) compared with the middle (group II) and the southern OSECS (group

III) indicated contribution of Yellow sea and Korean coast was smaller than input from the Changjiang River in the OSECS. This information is also proved that the sediment input from Changjiang River do not have a significant influence to the station 5, 6 and 7 (group I).

The sedimentation rate in the ECS and southern Yellow Sea were comprehensively evaluated by the previous studies (0.17 to 2.31 cm y^{-1} and 0.01 to 0.86 cm y^{-1}), respectively (Alexander et al., 1991; Huh and Su, 1999; Su and Huh, 2002; Fang et al., 2009; Yuan et al., 2012; Yu et al., 2013). The average trace element sedimentation fluxes were calculated from the product among the trace element concentrations, mass accumulation rate (MAR), and average core size of each group (50.2 cm^2). Group I, very close with the southern Yellow Sea, MAR value was taken from Yuan et al. (2012). Group II, located in the middle of the ECS, MAR value was taken from Yu et al. (2013). While group III, located in the southern ECS, MAR value was taken from Fang et al. (2009), respectively (Table 8). The average annual sedimentation fluxes of trace elements in three groups were listed in Table 8. The sediment fluxes of Fe, Co, and Zn were concentrated in the middle OSECS (group II) accounting for ~43 % of the total fluxes of each trace elements. Manganese and cadmium were concentrated in the southern OSECS (group III) accounting 51 % of total fluxes each trace elements, while Pb distributed evenly in all groups.

The frequency and scale of dust events giving rise to kosa aerosol has increased rapidly in the East Asian region since 2000 (Nishikawa and Mori, 2003). Thus, Asian countries suffer from the dust storms generated in the late

winter and spring in this decade. Asian dust storm impacts on the biogeochemistry of sediment in the East China Sea, especially to biological bloom and budget of nutrients and trace elements (Yuan and Zhang 2006; Hsu et al., 2010). Fluxes of total trace elements concentration from atmosphere in each group were calculated by dividing the flux of soluble species by the solubility of these trace elements. Dry deposition fluxes of Fe, Mn, Cd, Pb, and Zn from atmosphere at the group I were as follows: 2252, 64, 2, 130, and 213 mg m^{-2} y^{-1} (Yuan et al., 2012). At group II, dry deposition of Co, Zn, Cd, and Pb were reported as follows: 0.03, 6.94, 0.07, and 0.91 mg m^{-2} y^{-1} (Hsu and Lin 2010), while dry deposition of Fe, Mn, Pb, and Zn from atmosphere in the group III were as follows: 1.4 x 10^{-3}, 2.4 x 10^{-4}, 9.1 x 10^{-5} and 6.9 x 10^{-4} mg m^{-2} y^{-1} (Fang et al. 2009), respectively. Atmospheric fluxes of Cd, Pb, and Zn (1.93 x 10^{7}, 1.09 x 10^{9}, and 1.78 x 10^{9} g y^{-1}) (Table 12) strongly influence the sediment flux in group I (station 5, 6, and 7). In contrast, trace elements flux from the atmosphere was very low contributed to the total annual sediment flux in group II and III.

Some trace elements such as Fe, Zn, and Cd play very important roles in microorganism growth at sea to maintain the balance of the food chain. Trace elements that can be used as micronutrients, either come from the atmosphere input as particles which soluble or insoluble in water and can also be derived from the surface sediment. Trace element in the carbonate or exchangeable phase is considered to be weakest binding with sediment which may equilibrate with the pore water and thus diffuse to the bottom water. We can see that exchangeable trace element concentrations originating from the surface sediment is quite significant compared with the atmospheric input (Table 12), implying the

potentially important micronutrients source from sediment. Despite our calculated exchangeable sediment fluxes are not the real trace elements entering into the eutrophic zone involved in primary productivity, they are potential re-mineralization flux to the pore water or bottom water, the potential re-mineralized zinc 3 order magnitude higher than the atmospheric input in station 2. In particular in group III, there is no atmospheric trace element input, sediment contribution (Fe, $1.9x10^3$; Mn, 789; Pb, 0.51; and Zn, 66.8 μg y^{-1}) might be the exclusively significant source. Water depth in group III ranged from 550-1667 m, trace elements (micronutrient) in the bottom water released from sediment can enter into the upper layer (eutrophic zone) via upwelling etc, which has important implications for the promotion of phytoplankton production in the northwestern Pacific Ocean.

4.7 Conclusions

Trace elements in surface sediment of the outer shelf continent East China Sea come from various sources including lithogenic, ocean biogenic hydrothermal (submarine volcano). The northern and the middle part, Pb, Mn, Zn and Cd were dominated by ocean biogenic (carbonate and organic phase) while Fe and Co were dominated by lithogenic (residual phase). The proportion of oxides fraction in the southern was bigger than the middle and the northern of OSECS indicated another geochemical processes influenced the fractionation compositions besides ocean biogenic and lithogenic. Since this area was close with Okinawa where submarine volcanoes have been found, hydrothermal plume likely influenced trace elements composition. Potential re-mineralization of Fe

and Zn from surface sediment to the pore water or bottom water as micronutrient was bigger compare with atmospheric input in the southern of OSECS, implying that sediment may be an important micronutrient source to the northwestern Pacific Ocean.

Chapter 5

Trace Elements in Surface Sediment of the Northwestern Pacific Ocean as Open-Ocean

5.1 Internal check recovery

An internal check was performed on the result of the sequential extraction by comparing the total amount of elements extracted by different reagents during the sequential extraction procedure with the result of the total digestion. A reference sediment material (GBW-07309) was subjected to BCR protocol. The recovery was calculated as follow the equation

$$\text{Recovery} = \frac{\text{C fraction 1+C fraction 2+C fraction 3+C fraction 4}}{\text{C total digestion}} \text{ x } 100\%$$

to evaluate the reproducibility and accuracy of the method. Result showed in Table 19 indicated that the sum of the four fractions are in a good agreement with the total digestion and the methods used is reliable and repeatable

5.2 Spatial distribution

The distribution of trace elements at sampling station(S) were presented in Fig. 13 and Table 17. The mean contents of the trace elements in surface sediment NwPO were: Cd: 0.03; Pb: 14.76; Mn: 3116.01; Fe: 44974.01; Co: 11.89; and Zn: 80.40 $\mu g.g^{-1}$, allowing to arrange the trace elementns concentration from higher to lower were in the following order: Fe > Mn > Zn > Pb > Co > Cd.

The marginal sea such as East China Sea (ECS), source containing terrigenous and marine inputs played an important role in controlling trace metal. But for the open-ocean such as Northwestern Pacific Ocean (NwPO), the atmosphere deposition of mineral dust is the one of the most important pathway by which trace elements reach the open-ocean. Most of atmospheric deposition which reached the open ocean settles in the water column. Whereas, their

dissolved fraction would be transported to the other area by water circulation, while some of trace metal and REEs will be deposit in the sediment in a long time. The North Pacific Ocean receives a huge amount of mineral dust that contains anthropogenic materials from Asian continent, especially in spring (Uematsu et al. 1983). In the western North Pacific, approximately 50% of the total dust deposition is supplied by wet deposition (Uematsu, 2003), which implies that the trace elements in wet deposition may be crucial to the western North Pacific. Besides atmospheric deposition as main approaches, possibility for trace elements enter to the NwPO included material transport by ocean current and biological activity. To facilitate discuss the influence and contribution of source on trace metal distribution, the study area was divided into two groups (Fig. 16): group I, close with coastal (station 1, 2, 3 and 4) which influence by Kuroshio Current (KC) and influence by land input ;group II, station 5, 6, 7 and 8 which bound to the Kuroshio Ekstension Current (KE), Oyashio Current (OC) and Western Subarctic Gyre (WSG).

Almost trace elements (except Fe and Co) had higher concentration in the station group II which bound to Kurishio current and Oyashio current and closer with land. Cobalt, had the highest concentration at the station 8 (group II) which bound with Western Subarctic Gyre. The highest concentration of carbonate is at the station 6 which far from the land. Further away, the concentration carbonate at the station 1, 2 and 3 which closer with the land are lower compare with the station 4, 5, 6, 7 and 7. This data indicated that carbonate in the sediment is increased in the deeper area. The concentration distribution of aluminum was different with the carbonate. Aluminum at the station which closer with the land (S1, S2 and S3) had higher concentration compare with another station which farther from the land (Table 20 and Fig. 18). Since aluminum is the one of parameter to state that the sediments derived from lithogenic source, this data indicated that the surface sediment in the stations near land likely come from the lithogenic source and the sediment at stations far from the land likely come from the authigenic or anthropogenic source.

The relationship between every two elements and each trace metal with aluminum, carbonate and SiO_2 were analyzed and the Pearson correlation coefficient shown in Table 22. Almost each trace elements no any significant correlation, only Cd had a significant correlation with Zn (0.79) and Fe had a significant correlation with total aluminum (0.81). A significant correlation between Cd and Zn indicated that the distribution of Cd was similar with Zn and also the source of this two trace elements likely same. Significant correlation between Fe and aluminum likely indicated that distribution of Fe was influence by the concentration of aluminum. Since we know that almost aluminum in the sediment of the sea is come from the lithogenic source, from this data also cant interpretation that Fe probably come from the lithogenic source (as natural source).

5.3 Sequential Extraction Result

The trace elements concentration in the surface sediment sample from each step of extraction methods are shown in Table 21. The distribution of trace elements are divided into four groups depending on the degree of their association with the different phases. Manganese (Mn) and Cobalt (Co) at the station 1, 2 and 3 were mainly in the residual fraction (more than 60% of total concentration), while at the station 4 to 8 were mainly in the oxide fraction (more than 50% of total concentration). Cadmium (Cd) is present mainly in acid soluble and reducible fractions. Lead (Pb) and Zinc (Zn) are in the group with presenting distributed in all fractions. Iron (Fe) was found in a group with mainly in residual fraction (more than 74% of total concentration) in all station.

5.3.1. Manganese and cobalt

The pattern of distribution Mn and Co in the surface sediment of Northwestern Pacific ocean mainly were found in the residual fraction at the station close with the land (S1, S2, and S3) but at the station far from the land (S4, S5, S6, S7 and S8) the mainly found in the oxides fraction (see Fig. 19). High

proportion of residual fraction at the S1, S2 and S3 implied that Mn and Co in these three stations were mainly from natural lithogenic origin. Trace elements in residual fraction are likely to be incorporated in alumino-silicate minerals and unlikely released to pore-water through dissociation. Decrease in the proportion of residual fractions and increasing the proportion of oxide fractions indicate that the Mn and Co in the station located far from the land or the open ocean come from the authigenic or anthropogenic sources. Higher proportion in oxide fraction was comparable with the Mn and Co data from the surface sediment of southern of the outer shelf East China Sea. Mn in that area has relatively big portion of the oxides phase, indicating deposit in sediment to form hydrate manganese oxides ($MnO_2.nH_2O$) and may be released if the sediment is subjected to more reduced condition (Panda et al., 1995). A big proportion of Cobalt in oxide fraction indicated that hydrate manganese oxides also influenced the distribution of Cobalt. Since we known that geochemical behavior of manganese may co-precipitate and scavenge other trace elements.

5.3.2 Cadmium

Although the concentration of Cd was the lowest compared to other metal trace, but levels of Cd in sediments or sludge were much concern for a long time because of its high toxicity. Several sequential extraction procedures, including the BCR protocol have been used to obtain information on the distribution of Cd in sediment (Naji et al. 2010; Serife et al. 2000). In this study, Cd was also detected in the marine sediment following the BCR sequential extraction. The result of sequential extraction for Cd is illustrated at Fig. 19 and Table 21.

The concentration of Cd in the S5 is bigger than S1 even the S5 is far from the land compare with S1 indicated that distribution of trace elements in the northwestern Pacific Ocean was strong influence by atmospheric deposition. The dominant proportion of Cd was found in the carbonates, indicated that most of Cd in the surface sediment is bound to carbonate and exchangeable. The trace elements in this fraction are adsorbed on sediments on their essential components

namely clay, Fe and Mn hydrated oxides, and humic acids (Yuan et al, 2004). Weakly adsorbed Cd on the surface sediment by relatively weak electrostatic interaction maybe released by ion-exchange processes and dissociation of Cd-carbonate phase (Tersier et al. 1979). The Cadmium in this fraction is the most labile, hence and easy to take up from sediment by the biota. A big proportion of Cd in the oxides fraction also indicated that some part of Cd is bound to amorphous Fe and Mn oxides hydrate which easy to take up by biota if the condition become reduction. By using Pearson correlation coefficient we try to understand correlation Cd with other trace metal in each fraction. The result shown in Table 23, Cd had a good correlation with Zn in two fraction (carbonate fraction is 0.97 and oxides fraction is 0.95). This result indicated that in this two fractions, Cd and Zn likely come from the same source (ocean biogenic source).

5.3.3 Lead and Zinc

The distribution pattern of these two trace elements are illustrated in Fig. 19. Pb and Zn were distributed in all fractions, indicated that Pb and Zn come from the various sources. Big proportion lead in oxides fraction indicated that Pb and Zn exist as oxides and may be released if the sediment is subjected to more reduction condition (Panda et al. 1995). This fraction also indicated that Pb and Zn were labile and easy to take up from sediment. Big proportion of oxides fraction in a group II was comparable with the data of Pb and Zn from the surface sediment in the southern of outer shelf East China Sea, which indicating that Pb and Zn liable to deposit in sediment to form hydrate lead oxide and hydrate zinc oxide and the distribution in this group was influenced by manganese oxides as scavenging for other trace elements. Base on the Pearson correlation coefficient (Table 23), Lead in the carbonate and residual fraction have no good correlation with another trace elements indicated Pb in this two fractions likely not come from the same source. Lead in oxides and organic matter fraction had a good relation with Mn (0.73 and 0.74), this result indicated that Pb in this two fraction likely come the same source.

By using the same method with lead (Pearson correlation coefficient), Zn

in the carbonate and oxides fractions had a good correlation with the Cd (0.97 and 0.95), indicated that Zn and Cd in this two fractions probably come from the same source (authigenic source). Zn in the organic matter fraction had a good correlation with the Fe, indicated that Zn and Fe in this fraction come from the same organic source. To make its evidence we need to major silica in this fraction and also total organic carbon (TOC). Zn also had a good correlation with silica and aluminium (0.85 and 0.68) at the residual fraction, indicated that Zn in this fraction controlled by aluminosilicate mineral from the lithogenic source.

5.3.4 Iron

The pattern of distribution Fe in the surface sediment of Northwestern Pacific Ocean mainly found in the residual fraction. This pattern was similar with the result reported by Yuan C et al. 2004, who found that Fe in the surface sediment of the East China Sea mostly retained in the residual fraction. High proportion of residual fraction in the surface sediment from NwPO implied that Fe indicated mainly from natural lithogenic. Trace elements associated with the residual fraction are likely to be incorporated in alumino-silicate minerals and unlikely released to pore-water through dissociation. These elements are unlikely to pose direct and significant threaten to surrounding.

Correlation coefficient of Fe in the carbonate fraction have a good correlation with the Co, indicated that the distribution of Fe and Co in this fraction influence by the same source. Fe in the residual fraction had a good correlation with the aluminum, indicated that distribution of Fe in this fraction controlled by the aluminum as derived from the lithogenic. Since the residual fraction is the biggest proportion of the Fe in surface sediment of the NwPO, means that the main source of Fe is come from the lithogenic or natural.

Oxide fraction of Fe was increased from the station close with the land (S1, S2 and S3) to the station far from the land or open ocean (S4 to S8) was comparable with the data of Pb and Zn from the surface sediment of the East China Sea. Pb and Zn at the station 1 of the East China Sea (as open-ocean), proportion of the oxides fraction were higher than other stations (as marginal sea).

To further evidence multi sources of various trace elements, trace elements was compared in different endmembers and our samples. Here, Fe and Mn were chosen as indicators of hydrothermal and lithogenic source, a graph was plotted between Fe vs. Mn (Fig. 20). The result showed that the stations 4, 5, 6, 7, and 8 (group I) tend to be influenced by these two sources. Hydrothermal activity releases large quantities of manganese and deposited in coarse sediment to form hydrate manganese oxides ($MnO_2.nH_2O$), which can influence the sedimentary accumulation of other trace elements through their redox cycling in oxygen-deficient environment (Morford et al, 2005). In contrast, groups I (station 1, 2, and 3) was higher than lithogenic endmember, clearly indicating Fe and Mn in these two groups were influenced by lithogenic origin and another sources like anthropogenic source.

5.4 Environmental Implication

Contaminant factor (Cf) of elements and risk assessment code (RAC) were calculated to know environmental implication in the surface sediment from the Northwestern Pacific Ocean.

5.4.1 Contamination Factor

To know degree of trace elements risk to the environment in relation with its retention time, we need to calculate contaminant factor. A high contamination factor of trace elements shows low retention time and high risk to the environment. The individual contamination factor (Cf) was used to estimate the relative retention time of trace elements retained in the sediment. Its determined by dividing of the sum of each trace metal concentration in the mobile fraction (acid soluble, easy reducible and oxidizable) by its concentration in the residual fraction.

Contamination factor of the each trace elements in the surface sediment in all station were shown in the Fig. 23. Almost trace elements (except Mn at the station 4 and 5) have low contamination factor, that's mean the mobility of almost

trace elements in surface sediment of the Northwestern Pacific Ocean was low..

5.4.2 Risk Assessment Code (RAC)

The risk assessment code (RAC), defined as the fraction of metal exchangeable and/or associated with carbonates (% F1 for BCR), was determinate for the six traces elements, and the value interpreted in accordance with the RAC classification described by Perin et al. (1985). The RAC was determined base on the percentage of the total trace metal content that was found in the first sediment fraction in BCR method (% acid soluble fraction). This indicated trace metal are weakly bound to the solid phase. This condition means that the trace metal pose greater risk to the aquatic environment due to their greater potential (Jain et al. 2004). When this percentage mobility less than 1% , the sediment has no risk to aquatic environment. Percentage of 1-10% reflect low risk, 11-30% medium risk, and 31-50% high risk. Above 50%, the sediment poses a very high risk and in considered dangerous, with elements easily able to enter the food chain (Perin et al. 1985 and Jain et al. 2004)

In General, the data on Fig. 24 shown all trace elements at all station were low risk with RAC less than 10%., so, there is not any significant trace elements mobility for these trace elements. A medium risk is indicated for Zn at S5 and S6, Mn at S2 and S4, and Cd at S1 that it can be noticeable in the early future.

PART IV

General Conclusions

Chapter 6

General Conclusions

1. Cadmium was in the form of Cd(II) and $Cd(H_2O)_6^{+2}$, and soluble in water media. At pH > 7.55, cadmium precipitated as $Cd(OH)_2$. The adsorption processes of aquo $(Cd(H_2O)_6)^{2+}$ and chloro ($CdCl^+$ dan $CdCl_2$) complexes functioned on the humin simultaneously in freshwater and individually in seawater media.
2. Based on the chemical fractionation, the trace metals in surface sediment of the outer shelf continent East China Sea and Northwestern Pacific Ocean come from various sources including lithogenic, ocean biogenic, hydrothermal (submarine volcano) and anthropogenic.
3. The northern and the middle part of outer shelf East China Sea, Pb, Mn, Zn and Cd were dominated by ocean biogenic (carbonate and organic phase) while Fe and Co were dominated by lithogenic (residual phase).
4. The proportion of oxides fraction in the southern was bigger than the middle and the northern of OSECS indicated hydrothermal plume likely influenced trace metals composition since this area was close with Okinawa where submarine volcanoes have been found,
5. Potential re-mineralization of Fe and Zn from surface sediment to the pore water or bottom water as micronutrient was 4 to 5 times bigger than atmospheric input in the southern of OSECS, implying that surface sediment may be an important micronutrient source to the Yellow Sea, Japan Sea and northwestern Pacific Ocean.
6. Trace metal fractionation in surface sediment from the NwPO: Manganese (Mn) and Cobalt (Co) at the station 1, 2 and 3 were mainly in the residual fraction, while at the station 4 to 8 were mainly in the reducible fraction. Lead (Pb) and Zinc (Zn) are in the group with presenting distributed in all fractions.

Cadmium (Cd) is present mainly in acid soluble and reducible fractions. Iron (Fe) was found in a group with mainly in residual fraction. Trace metal fractionation in surface sediment of the Northwestern Pacific Ocean mainly controlled by aluminum (Al) as lithogenic source and carbonate as authigenic source.

7. Potential mobility and bioavailability of trace metal in the surface sediment of Northwestern Pacific Ocean almost metal in all stations are low (except Mn at stations 4 and 5). Second parameter is risk assessment code (RAC): almost trace metals (except Co and Fe) at almost station in the East China Sea have high value (more than 25%), while in the Northwestern Pacific Ocean at all stations were low (less than 25%).

References

Aja S.U. 1998. The sorption of the rare earth element, Nd, onto kaolinite at 25 degrees C. Clays and Clay Minerals 46(1): 103-109.

Alexander, C.R., DeMaster, D.J., Nittrouer, C.A. 1991. Sediment accumulation in a modern epicontinental-shelf setting: The Yellow Sea. Mar. Geol. 98, 51-72.

Ankley, GT; Phipps, GL; Leonard, EN; Benoit, DA; Mattson, VR. 1991. Acid-volatile sulfide as a factor mediating cadmium and nickel bioavailability in contaminated sediments. Environ Toxicol Chem 10:1299B1307.

Baig JA, Kazi TG, Arain MB, shah AQ, Sarfraz RA, Afrizi HI. 2009. Arsenic fraction in sediments of different origins using BCR sequential and single extraction methods. J Hazard Mater 167: 745-751

Billen, G. and Garnier, J. 2007. River basin nutrient delivery to the coastal sea: Assessing its potential to sustain new production of non-siliceous algae. *Marine Chemistry*, 106(1–2), 148–160.

Bruland, K. W., and R. P. Frank. 1983. Mn, Ni, Cu, Zn, and Cd in the western North Atlantic. In: Wong, C.S., Boyle, E., Bruland, K.W., Burton, J.D. and Golberg, E.D. (Eds.), Trace metals in water. (pp. 395-414). (New York: Plenum Press)

Brumbaugh, WG; Ingersoll, CG; Kemble, NE; May, TW; Zajicek, JL. 1994. Chemical characterization of sediments and pore water from the Upper Clark Fork River and Milltown Reservoir, Montana. Environ Sci Chem 13:1971-1983.

Casas, A. M., Crecelius, E. A. 1994. Relationship between acid volatile sulfide and the toxicity of zinc, lead and copper in marine-sediments. Environ Toxicol Chem 13:529B536.

Chegrouche S., Mellah A., Telmoune S. 1997. Removal of lanthanum from aqueous solutions by natural bentonite. Water Research 31(7): 1733-1737.

Chester, R. 2003. *Marine Geochemistry*. Blackwell Science, Malden

Chu, P., Chen, Y., Kuninaka, A., 2005. Seasonal variability of the Yellow Sea/East China Sea surface fluxes and thermohaline structure. Advance. Atmos. Sci. 22(1), 1-20.

Conley, D.J., Schelske, C.L. and Stoermer, E.F. 1993. Modification of the biogeochemical cycle of silica with eutrophication. *Marine Ecology Progress Series*, 81, 121–128.

Coppin F, Berger G, Bauer A, Castet S, Loubet M. 2002. Sorption of lanthanides on smectite and kaolinite. Chemical Geology 182(1), 57-68.

Dader, M., Colilla, M., Hitzky, E. R. 2003. Biopolymer−clay nanocomposites based on chitosan intercalated in montmorillonite, Chem. Mater. 15, 3774-3780.

Di Toro, D.M; Mahony, JD; Hansen, DJ; Scott, KJ; Hicks, MB; Mayr, SM; Redmond, MS. (1990) Toxicity of cadmium in sediments: the role of acid volatile sulfide. Environ Toxicol Chem 9:1487B1502.

Di Toro, DM; Mahony, JD; Hansen, DJ; Scott, KJ; Carlson, AR; Ankley, GT. 1992. Acid volatile sulfide predicts the acute toxicity of cadmium and nickel in sediments. Environ Sci Tech 26(1):96-101.

Donat, J. R., and K. W. Bruland. 1995. Trace elements in the oceans. In: Salber, B. and Steinnes, E. (Eds.), Trace elements in natural waters. (pp. 247-281). (Boca raton: CRC press).

Fang TH, Li JY, Feng HM, and Chen HY. 2009. Distribution and contamination of trace metals in surface sediment of the East China Sea. Mar Environ Res 68: 178-187

Forstner, U., 1995. Non-linear release of metals from aquatic sediments. In:

Salomons, W; Stigliani, WM, eds. Biogeodynamics of pollutants in soils and sediments. Germany: Springer-Verlag

Frew, R.D., Bowie, A., Croot, P., Pickmere, S., 2001. Macronutrient and trace metal geochemistry of an in situ iron-induced Southern Ocean bloom. Deep Sea Res. Part II. 48, 2467-2481.

Gallet, S., Jahn, B., Torii, M., 1996. Geochemical characterization of the Luochuan loess-paleosol sequence, China, and paleoclimatic implication. Chem. Geol. 137, 67-88.

Gaillardet, J. Viers, J. and Dupre, B. 2004. Trace elements in river waters. In: Drever, J.I. (ed.) *Surface and Ground Water, Weathering and Soils*. Vol. 5 in *Treatise on Geochemistry*, H.Holland, Turekian, KK, Editor. Elsevier, Amsterdam, pp. 225–272.

Haley TJ, in Handbook on the Physics and Chemistry of Rare Earths, Karl A. Gschneidner, Jr., LeRoy E, Eds. (North-Holland Publishing Company, 1979), vol. 4, 553-585.

Hare, L; Tessier, A; Borgmann, U. 2003. Metal sources for freshwater invertebrates: pertinence for risk assessment. Human Ecol Risk Assess 9: 779-793.

Hendry, K.R., Rickaby, R.E.M., De Hoog, J.C.M., Keith, W., Mark, R., 2008. Cadmium and phosphate in coastal Antartic seawater: implication for Southern Ocean nutrient Cycling. Mar. Sci. 112, 149-157.

Ho, T.Y., Wen, L.S., You, C.F, Lee, D.C., 2007. The trace-metal composition of size fractionated plankton in the South China Sea: Biotic versus abiotic sources. Limnol. Oceanogr. 52(5), 1776-1788.

Hsu, S.C., Lin, F.J., 2010. Elemental characteristics of surface suspended particulates off the Changjiang estuary during the 1998 flood. J. Mar. Sys. 81, 323-334.

Hsu, S.C., Lin, F.J., Jeng, W.L., Chung, Y.C., Shaw, L.M. 2003. Hydrothermal

signatures in the southern Okinawa Trough detected by sequential extraction of settling particles. Mar. Chem. 84, 49-66.

Hsu, S.C., Wong, G.T.F., Gong, G.C., Shiah, F.K., Huang, Y.T., Kao, S.J., Tsai, F., Lung, S.C., Lin, F.J., Lin, I.I., Hung, C.C., Tseng, C.M., 2010. Source, solubility, and dry deposition of aerosol trace elements over the East China Sea. Mar. Chem. 120, 116-127.

Hu Y, Vanhaecke F, Moens L, Dams R, Castilho Pd, Japenga J. 1998. Determination of the aqua regia soluble content of rare earth elements in fertilizer, animal fodder phosphate and manure samples using inductively coupled plasma mass spectrometry. Analytica Chimica Acta 373: 11.

Hu Z, Haneklaus S, Sparovek G, Schnug E. 2006. Rare earth elements in soils. Communications in Soil Science and Plant Analysis 37: 1381-1420.

Huh, C.A., Su, C., 1999. Sedimentation dynamics in the East China Sea elucidated from ^{210}Pb, ^{137}Cs and ^{239,240}Pu. Mar. Geol. 160, 183-196.

Huheey, J. E., Keiter, E. A., and Keiter, R. L. 1993. Inorganic chemistry, Ed 4th, Harper Collins College Publisher, California, CA, USA

Ichihashi H, Morita H, Tatsukawa R. 1992. Rare earth elements (REEs) in naturally grown plants in relation to their variation in soils. Environmental Pollution 76(2): 157-162.

Ishibashi, J.I., Noguchi, T., Toki, T. Miyabe, S., Yamagami, S., Onishi, Y., Yamanaka, T., Yokoyama, Y., Omori, E., Takahashi, Y., Hatada, K., Nakaguchi, Y., Yoshizaki, M., Konno, U., Shibuya, T., Takai, K., Inagaki, F., Kawagucci, S., 2014. Diversity of fluid geochemistry affected during fluid upwelling in active hydrothermal field in the Izena Hole, the middle Okinawa Trough back-arc basin. Geochemical Journal. 48, 357-369.

Jahn, B., Gallet, S., Han, J., 2001. Geochemistry of the Xining, Xifeng and Jixian sections, Loess Plateau of China: eolian dust provenance and paleosol evolution during the last 140ka. Chem. Geol.

Jain, A. K., Gupta, V. K., Jain, S., and Suhas. 2004 Removal of chlorophenols using industrial wastes, Environ. Sci. Technol. 38, 1195

Jarvis K.E. 1988. Inductively coupled plasma mass spectrometry: A new technique for the rapid or ultra-trace level determination of the rare-earth elements in geological materials. Chemical Geology 68: 31-39.

Jiang, Z.H. and Peng, Z.H., 1999. Evaluating the inundation of Changjiang River Valley in 1998 and countermeasures for fl ood control, Journal of Nanjing Forestry University, 23(2): 1-5 (in Chinese).

Kazi, T.G., Jamali, M.K., Kazi, G.H., Arain, M.B., Arfidi, H.I., Siddiqui, A., 2005. Evaluating the mobility of toxic metals in untreated industrial wastewater sludge using BCR sequential extraction procedure and leaching test. Anal. Bioanal. Chem. 383, 297-304.

Kimoto A, Nearing M, Zhang X, Powell D. 2006a. Applicability of rare earth element oxides as a sediment tracer for coarse-textured soils. Catena 65(3): 214-221.

Kimoto A, Nearing M.A., Shipitalo M.J., Polyakov V.O.. 2006b. Multi-year tracking of sediment sources in a small agricultural watershed using rare earth elements. Earth Surface Processes and Landforms 31(14): 1763-1774.

Klinkhammer, G.P., Chin, C.S., Wilson, C., Rudnicki, M.D., German, C.R., 1997. Distribution of dissolved manganese and fluorescent dissolved organic matter in the Columbia River estuary and plume as determined by in situ measurement. Mar. Chem. 56, 1-14.

Koeppenkastrop D, De Carlo EH. 1992. Sorption of rare-earth elements from seawater onto synthetic mineral particles: An experimental approach. Chemical Geology 95: 251-263.

Laufer F, Yariv S, Steinberg M. 1984. The adsorption of quadrivalent cerium by kaolinite. Clay Minerals 19(2): 137-149.

Leybourne M, Johannesson K. 2008. Rare earth elements (REE) and yttrium in stream waters, stream sediments, and Fe–Mn oxyhydroxides: Fractionation, speciation, and controls over REE+Y patterns in the surface environment. Geochimica et Cosmochimica Acta 72(24): 5962-5983.

Lin S, Hsieh IJ, Huang KM, Wang CH., 2002. Influence of the Yangtze River and grain size on the spatial variations of heavy metals and organic carbon in the East China Sea continental shelf sediment. Chem Geol 182: 377-394

Liu, C.Q., Masuda, A., Okada, A., Yabuki, S., Zhang, J., Fan, Z.L., 1993. A geochemical study of loess and desert sand in northern China: Implication for continental crust weathering and composition. Chem. Geol. 106, 359-374.

Liu, H., He, Q., Wang, Z., Weltje, G. J., Zhang, J., 2010. Dynamics and spatial variability of near-bottom sediment exchange in the Yangtze Estuary, China. Estuarine. Coast. Shelf. Sci. 86, 322-330.

Liu, J., Xu, K., Li, A., Milliman, J., Velozzi, D., Xiao, S., Yang, Z., 2007. Flux and fate of Yangtze River sediment delivered to the East China Sea. Geomorphology. 85: 208–224.

Liu, L.S., Zhou, J., Zheng, B.H., Cai, W.Q., Lin, K.X., Tang, J.L., 2013. Temporal and spatial distribution of red tide outbreak in the Yangtze River Estuary and adjacent waters, China. Mar. Pollut. Bull. 72, 213-221.

Liu P-L, Tian J-L, Zhou P-H, Yang M-Y, Shi H. 2004. Stable rare earth element tracers to evaluate soil erosion. Soil and Tillage Research 76(2): 147-155.

Liu, S., Shen, X., Wang, Y., Han, S., 1992. Preliminary analysis of distribution and variation of perennial monthly mean water masses in the Bohai Sea, the Huanghai (Yellow) Sea and the East China Sea. Acta Ocearologica Sinica. 11, 483–498.

Liu, S., Shi, X., Liu, Y., Zhu, Z., Yang, G., Zhu, A., Gao, J., 2011. Concentration, distribution and assessment of heavy metals in sediments of mud area

from inner continental shelf of the East China Sea. Environ. Earth. Sci. 64, 567- 579.

Loveland W, “Hydrospheric trace elements and their application in tracing water pollutants” (Oregon State University, Water Resources Research Institute, 1978). Loveland W, in Lanthanide Probes in Life, Chemical and Earth Sciences: Theory and Practice, Bunzli JCG, Choppin GR, Eds. (Elsevier Science Ltd, 1989), 391-411.

Mahler B. J., Bennett P. C., Zimmerman M. 1998a. Lanthanide-labeled clay: A new method for tracing sediment transport in karst. Ground Water 36(5): 835-843.

Markert B. 1987. The pattern of distribution of lanthanide elements in soils and plants. Phytochemistry 26(12): 3167-3170.

Martin, J.H., Knauer, G.A., Broenkow, W.W., 1985. VERTEX: the lateral transport of manganese in the northeast Pacific. Deep. Sea. Res. 32, 1405-1427.

Matisoff G, Ketterer ME, Wilson CG, Layman R, Whiting PJ. 2001. Transport of rare earth element-tagged soil particles in response to thunderstorm runoff. Environmental Science & Technology 35(16): 3356-3362.

Maybeck, M. (2004) Global occurence of major elements in rivers. In: Drever, J.I. (ed.) *Surface and Ground Water, Weathering and Soils*. Vol. 5 in Holland, H.D. and Turekian, K.K. (Exec.eds) *Teatise on Geochemistry*. Elesevier, Amsterdam, pp. 207–223.

MCA-DSD, Department of Disaster Aid, Ministry of Civil Aff airs of PRC., 2003. A disaster survey of China in 2002, with direct economic losses of 171.7 billion RMB (Yuan). Journal of Disaster Reduction, (1): 31-35 (in Chinese).

Michaelides K, Ibraim I, Nord G, Esteves M. 2010. Tracing sediment redistribution across a break in slope using rare earth elements. Earth Surface Processes and Landforms 35: 575-587.

Milliman JD, Shen HT, Yang ZS, Meade R.H., 1985b. Transport and deposition of river sediment in the Changjiang Estuary and adjacent continental-shelf. Cont. Shelf. Res. 4: 37–45.

Mudroch A, Azcue JM, Mudroch P., 1997. Manual of physico-chemical analysis of aquatic sediments. Boca Raton, FL: Lewis Publishers.

Mudroch, A, Azcue JM, Mudroch P., 1999. Manual of bioassessment of aquatic sediment quality. Boca Raton, FL: Lewis Publishers.

Morford, J.L., Emerson, S., 1999. The geochemistry of redox sensitive trace metals in sediment. Geochim. Cosmochim. Acta. 63, 253-261.

Morford, J.L., Emerson, S.R., Breckel, E.J., Kim, S.H., 2005. Diagenesis of oxyanions (V, U, Re, and Mo) in pore waters and sediment from a continental margin. Geochim. Cosmochim. Acta. 63, 3373-3378.

Mottl, M.J., Sansone, F.J., Wheat, C.G., Resing, J.A., Baker, E.T., Lupton, J.E., 1995. Manganese and methane in hydrothermal plume along the East Pacific Rice, $8^0$40` to $11^0$50` N. Geochim. Cosmochim. Acta. 59, 4147-4165.

Naji A, Ismail A, Ismail AR (2010) Chemical speciation and contamination assessment of Zn and Cd by sequential extraction in surface sediment of Klang River, Malaysia. Microchem J 95: 285-292

Nemati K, Abu Bakar NK, Abas MR, Sobhanzadeh E., 2011. Speciation of heavy metals by modified BCR sequential extraction procedure in different depths of sediments from sungai buloh, Selangor, Malaysia. J Hazard Mater 192: 402-410

Nishikawa, M., Mori, I., 2003. Characteristic of kosa phenomena between Japan and China. J. Arid. Land. Studies. 13, 21-34 (in Japanese)

Panda D, Subramanian V, Panigrahy RC., 1995. Geochemical fractionation of heavy metal in Chilka Lake (east coast of India)- a tropical coastal lagoon. Environ Geol 26: 199-210

Perin G, Craboledda L, Lucchese M, Cirrilo R, Dotta L, Zanette ML, Orio AA ., 1985. Heavy metal speciation in the sediments Northern Adriatic Sea-new approach for environmental toxicology determination. Heavy Metals in the Environment 2: 454-456

Piper, D.Z., Berkins, R.B., 2004. A modern vs. Permian black shale-the hydrography, primary productivity, and water-column chemistry of deposition. Chem. Geol. 206, 177-197.

Polyakov VO, Nearing MA, Shipitalo MJ. 2004. Tracking sediment redistribution in a small watershed: Implications for agro-landscape evolution. Earth Surface Processes and Landforms 29(10): 1275-1291.

Polyakov VO, Kimoto A, Nearing MA, Nichols MH. 2009. Tracing sediment movement on a semiarid watershed using rare earth elements. Soil Science Society of America Journal 73(5): 1559-1565.

Qiandao Lake Online., 2004. Retrieved November 2004, from http://www.qdh.gov.cn/cagk/cagk_gk.asp

Qin, Y.S. and Zhao, Y.Y., 1987. Geology of the East China Sea. Science Publisher, Beijing (in Chinese).

Reuther, R., 1999. Trace metal speciation in aquatic sediments: methods, benefits, and limitations. In: Manual of bioassessment of aquatic sediment quality. Mudroch, A; Azcue, JM; Mudroch, P, eds. Boca Raton, FL: Lewis Publishers; pp. 1B54.

Rice, J. A and MacCarthy, P. 1990. A model of humin. Environ. Sci. Technol. 24(12), 1875-1977.

Robinson and K.H. Brink (eds.), The Sea, John Wiley & Sons Inc., New York, Vol. 11: 483-505.

Robinson WO, Bastron H, Murata KJ. 1958. Biogeochemistry of the rare-earth elements with particular reference to hickory trees. Geochimica et Cosmochimica Acta 14: 55-67.

Roy, I; Hare, L., 1999. Relative importance of water and food as Cd sources to the predatory insect Sialis vlata (Magaloptera). Can J Fish Aquat Sci 56(7):1143B1149.

Santosa, S. J., Narsito., Lesbani, A. 2001. The determination of active site, capacity, energy and rate constant on the adsorption of Zn(II) and Cd(II) on chitin. J Ion Exch. 14, 89-92.

Schellenberger, A., Veit, H., 2006. Pedostratigraphy and pedological and geochemical characterization of Las Carreras loess-paleosol sequence, Valley de Tafi, NW-Argentina. Quaternary. Sci. Reviews. 25, 811-831.

Schnoor, J. L. 1996. Environmental modeling. John Wiley & Sons Inc, New York, NY, USA.

Serife T, Senol K, Latif E (2000) Determination of heavy metals and their speciation in the lake sediments by flame atomic absorption spectrometry after a four stage sequential extraction procedure. Anal Chem Acta 413: 33-40.

Spencer KL, Droppo IG, He C, Grapentine L, Exall K. 2011b. A novel tracer technique for the assessment of fine sediment dynamics in urban water management systems. Water Research 45(8): 2595-2606.

Stevens C. J., Quinton J. N. 2008. Investigating source areas of eroded sediments transported in concentrated overland flow using rare earth element tracers. Catena 74(1): 31-36.

Stevenson, F. J. 1994. Humus chemistry: genesis, composition, reactions. John Wiley & Sons Inc. New York, NY, USA.

Su, J.L., 1998. Circulation dynamics of the China Seas north of 18˚N. In: A.R.

Su, C., Huh, C., 2002. ^{210}Pb, ^{137}Cs and ^{239,240}Pu in the East China Sea sediments: sources, pathways and bidget of sediments and radionuclides. Mar. Geol. 183, 163-178.

Sun, W.P., Hu, C.Y., Han, Z.B., Xue, B., Pan, J.M., 2011. Distribution of dissolved

cadmium in Pryrd Bay, Antarctica. Mar. Sci. Bull. 13, 50-59.

Suzuki, R., Ishibashi, J.I., Nakaseama, M., Konno, U., Tsunogai, U., Gena, K., Chiba, H., 2008. Diverse range of mineralization induced by phase separation of hydrothermal fluid: case study of the Yonaguni Knoll IV hydrothermal field in the Okinawa Trough Back-Arc Basin. Res. Goeol. 58(3), 267-288.

Tack, FMG; Verloo, M.G., 1999. Single extractions versus sequential extraction for the estimation of heavy metal fractions in reduced and oxidised dredged sediments. Chem Spec & Bioavail 11(2):43-50.

Taylor, S.R., MnLennan, S.M., McCulloch, M.T., 1983. Geochemistry of loess continental crustal composition and crustal model ages. Geochimica et Cosmochimica Acta. 47, 1897-1905.

Tersier, A., Campbell, P.G.C., Bisson, M., 1979. Sequential extraction procedure for the speciation of particulate trace metals. Anal. Chem. 51, 844-851.

Tribovilard, N., Algeo, T.J., Lyons, T., Riboulleau, A., 2006. Trace metals as paleoredox and paleoproductivity proxies: an update. Chem. Geol. 232, 12-32.

Tripathi, J.K., Rajamani, V., 1999. Geochemistry of the loessic sediments on Delhi ridge, eastern Thar desert, Rajasthan: implication for exogenic processes. Chem. Geol. 155, 265-278.

Tessier A, Campbell P.G.C, Bisson, M., 1979) Sequential extraction procedure for the speciation of particulate trace metals. Anal Chem 51(7):844-851.

Tribovillard N, Algeo TJ, Lyons T, Riboulleau A., 2006. Trace metals as paleoredox and paleoproductivity proxies: an update. Chem Geol 232: 12-32

Tye AM, Young SD, Crout NMJ, Zhang H, Preston S, Barbosa-Jefferson VL, Davison W, McGrath SP, Paton GI, Kilham K, Resende L., 2003. Predicting the activity of Cd^{2+} and Zn^{2+} in soil pore water from the.

Tyler G. 2004. Rare earth elements in soil and plant systems - a review. Plant and Soil 267: 16. USEPA. U.S. EPA sets expectations for Chesapeake Bay states and D.C. to reduce water pollution. 2009. USEPA. 2012. National Summary of State Information. http://www.epa.gov/waters/ir/index.html. Accessed: May 2, 2012.

Uematsu M (2003) Atmospheric input of mineral dust to the western North Pacific region based on direct measurements and a regional chemical transport model. Geophys Res Lett 30: 1342

Uematsu M, Duce RA, Prospero JM, Chen L, Merrill JT, McDonald RL (1983) Transport of mineral aerosol from Asia over the North Pacific Ocean. J Geophys. Res 88: 5343–5352

Wang, G.P., Liu, J.S., Tang, J., 2004. Historical variation of heavy metals with respect to the different chemical forms in recent sediments from Xianghai Wetlands, Northeast China. Wetlands. 24, 608-619.

Wang, S.M. and Dou, H.S., 1998. Chinese Lake Notes. Science Press, Beijing (in Chinese)

Wang ZG, Yu XY, Zhao ZH, Rare earth elements geochemistry (in chinese). (Scientific Publishing Company, Beijing, China, 1989).

Wei, C.L.,Wong G.T.F., Sun S.J., Gong G.W., 2000. Extractable manganese in the southeastern East China Sea shelf and the Okinawa Trough. Oceanol. Acta. 24, s99-111.

Wutscher HK, Perkins RE. 1993. Acid extractable rare earth elements in Florida citrus soils and trees. Communications in Soil Science and Plant Analysis 24: 2059-2068.

Yu, Y., Jinming, S., Xuegang, L., Huamao, Y., Ning, L., 2013. Fractionation, origins and budgets of potential harmful elements in surface sediment of the East China Sea. Mar. Pollut. Bull. 68, 157-167.

Yuan, H., Jinming, S., Xuegang, L., Ning L., Liqin, D., 2012. Distribution and contamination of heavy metals in surface sediments of the South Yellow Sea. Mar. Pollut. Bull. 64, 2151-2159.

Yuan, C., Shi, J., He, B., Liu, J., Liang, L., Jiang, G., 2004. Speciation of heavy metals in marine sediments from the East China Sea by ICP-MS with sequential extraction. Environ. Int. 30, 769-783.

Yuan, W., Zhang, J., 2006. High correlation between Asian dust and biological productivity in the western North Pacific. Geophysical. Res. Let. 33, L07603, doi:10.1029/2005GL025174.

Zhang, J., Liu, C.L., 2002. Riverine composition and estuarine geochemistry of particulate metals in China–weathering features, anthropogenic impact and chemical fluxes. Estuar. Coast. Shelf. Sci. 54, 1051–1070.

Zhang, J., Liu, S.M., Ren, J.L., Wu, Y., Zhang, G.L., 2007. Nutrients from the eutrophic Changjiang (Yangtze River) estuary to the oligotrophic Kuroshio waters and re-evaluation of budget for the East China Sea shelf. Progress. Oceanography. 74, 449-478.

Zhang X.C., Friedrich J.M., Nearing M.A., Norton L. D., 2001. Potential use of rare earth oxides as tracers for soil erosion and aggregation studies. Soil Science Society of America Journal 65(5): 1508-1515.

Zhang XC, Nearing MA, Polyakov VO, Friedrich JM. 2003. Using rare-earth oxide tracers for studying soil erosion dynamics. Soil Science Society of America Journal 67: 10.

Zhao, Y.Y., Li, F.Y., 1991. Preliminary studies on sedimentation rate and sediment flux of the South Huanghai Sea. Oceanol. Limnol. Sin, 22 (1), 38-43 (in Chinese).

Zhang, J., 2002. Biogeochemistry of Chinese estuaries and coastal waters: Nutrients, trace metals and biomarkers. Regional Environmental Change, 3: 65-76.

Zhu, D.Q., 1993. Water System Thesaurus of China, Qindao Publication Press (in Chinese).

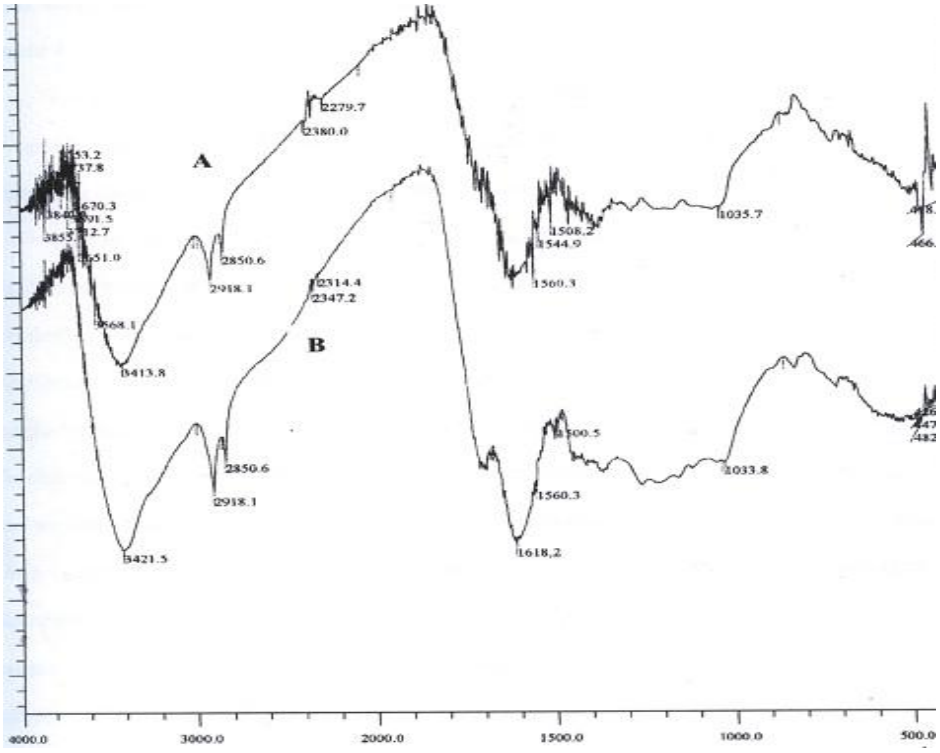

Figure. 1. FTIR spectra of isolated humin from peat soil. (A) Before purification; (B) After purification.

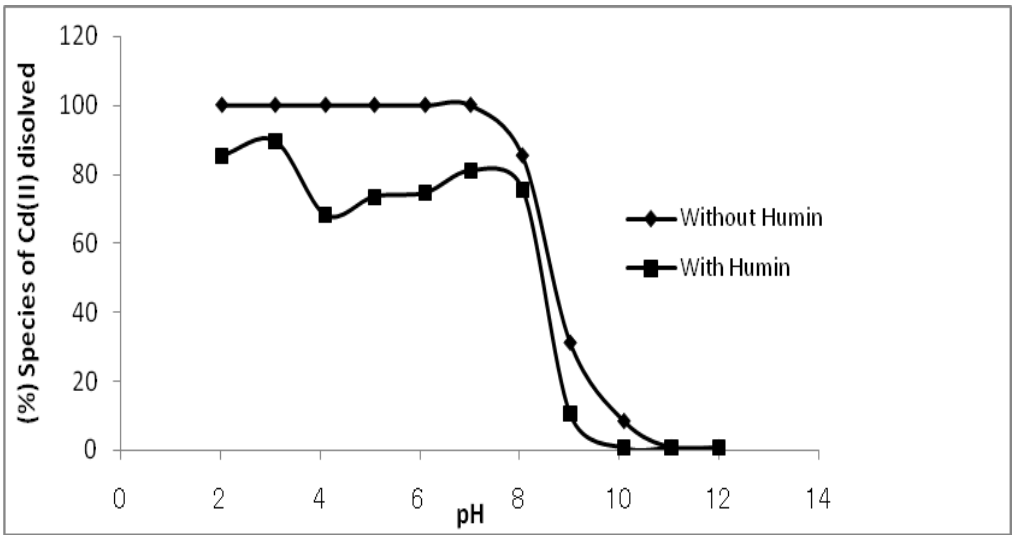

Figure. 2. Effects of adding humin on Cd(II) solubility in water media.

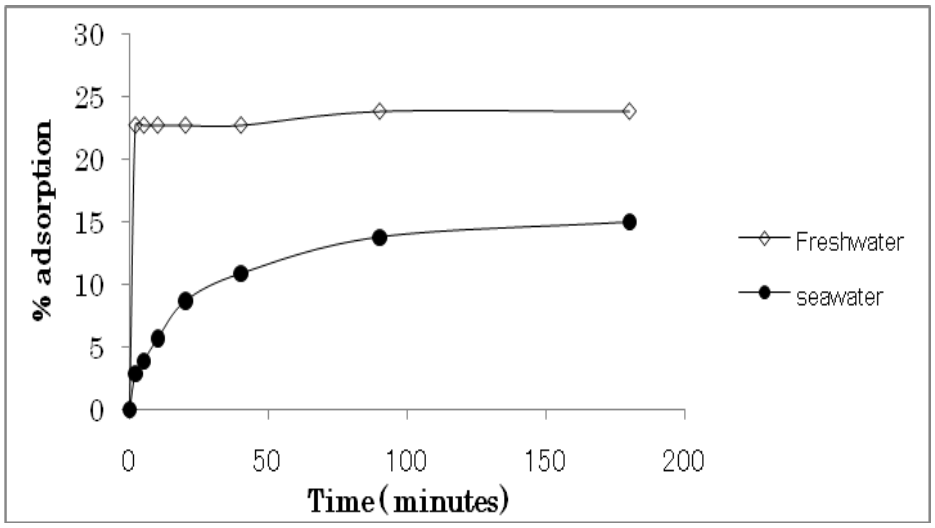

Figure. 3. Adsorption time of Cd(II) on humin in freshwater (pH= 6.32) and seawater (pH= 7.21) media.

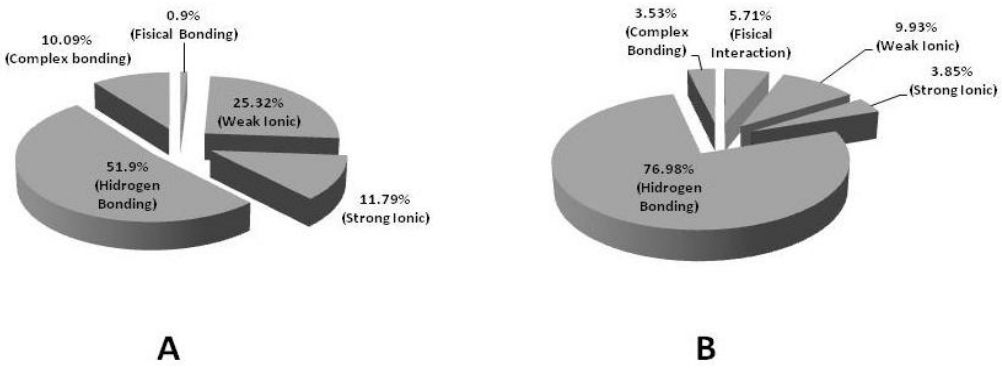

Figure. 4. Contribution of several interaction mechanisms between Cd(II) and humin. (A)Freshwater media; (B) Seawater media.

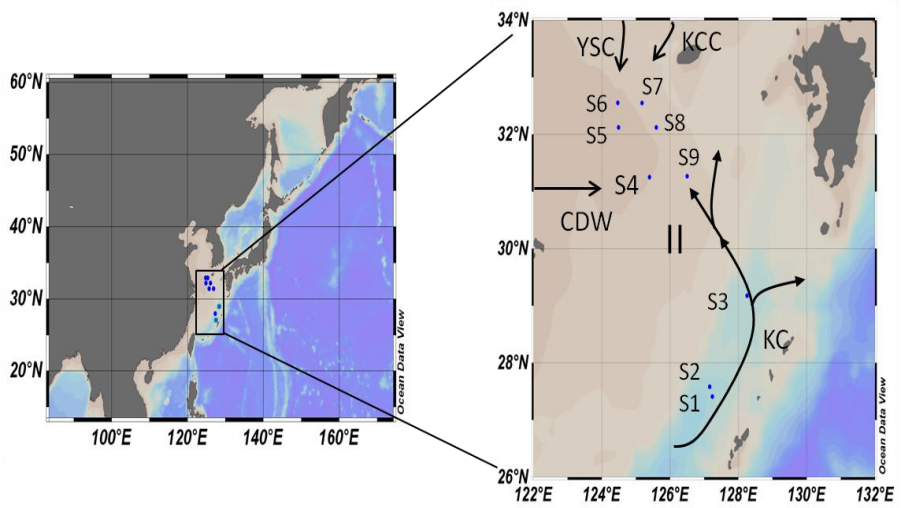

Figure 5 Location of sediment sampling in the East China Sea with current sytem: KWC: Kuroshio warm current; KCC: Korean coastal current; YSC: Yellow sea current; CDW: Changjiang Dilute Water; TWC: Taiwan warm current.

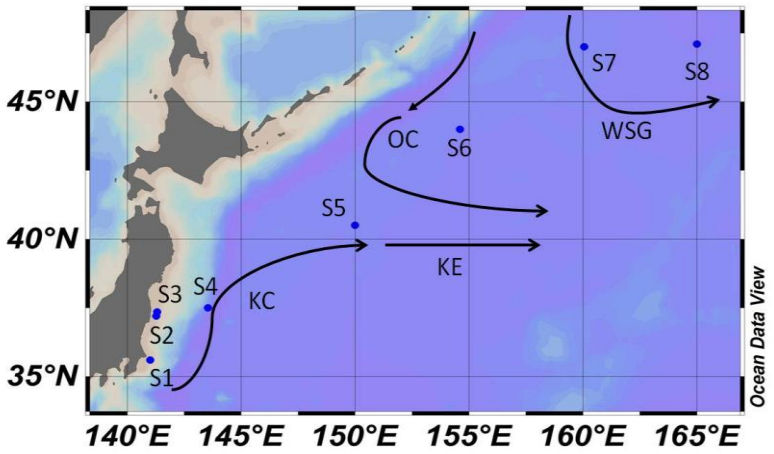

Figure 6. Location of sediment sampling in the Northwestern Pacific Ocean with current sytem: KC: Kuroshio Current; KE: Kuroshio Extension; OC: Oyashio Current; and WSG: Western Subartic Gryre

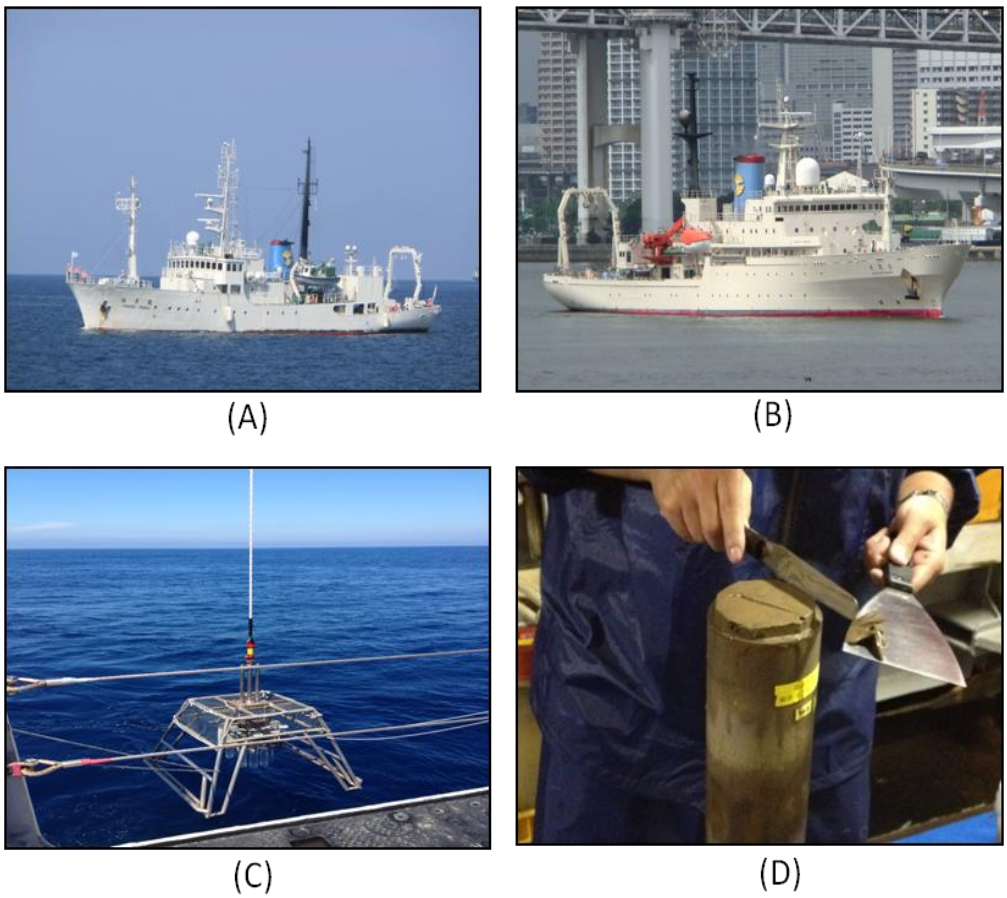

Figure 7.A) R/V Tansei Maru; B) R/V Hakuho Maru; C) Multiple core sampler; D) Sediment cutting process

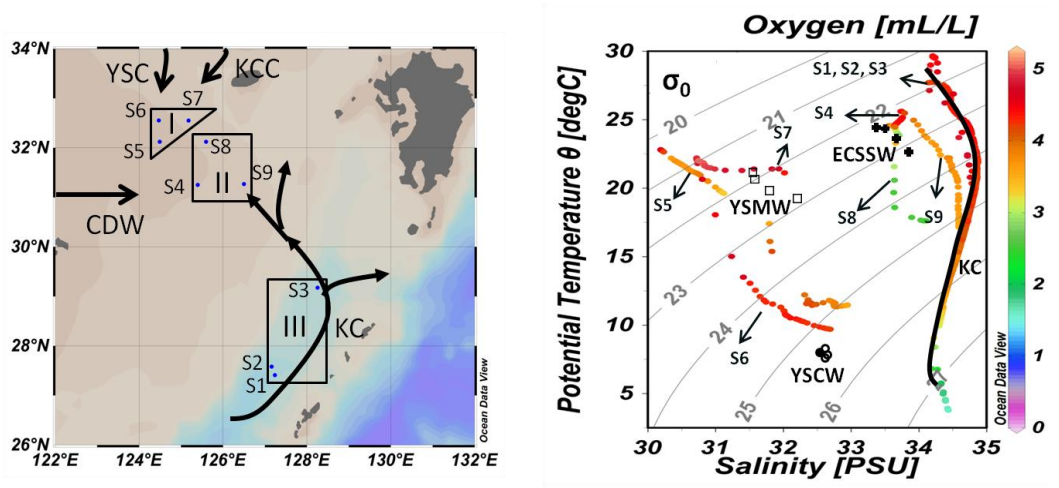

(A) (B)

Figure 8. (A) Location of sediment sampling in the East China Sea with current system: Kuroshio current (KC); Korean coastal current (KCC); Yellow Sea current (YSC); and Changjiang Dilute Water (CDW).
(B) T-S diagram with water mass clasification: Kuroshio Current (KC); East China Sea surface water (ECSSW); Yellow Sea mixed water (YSMW); and Yellow Sea cold water (YSCW). Color bar showed the oxygen concentration.

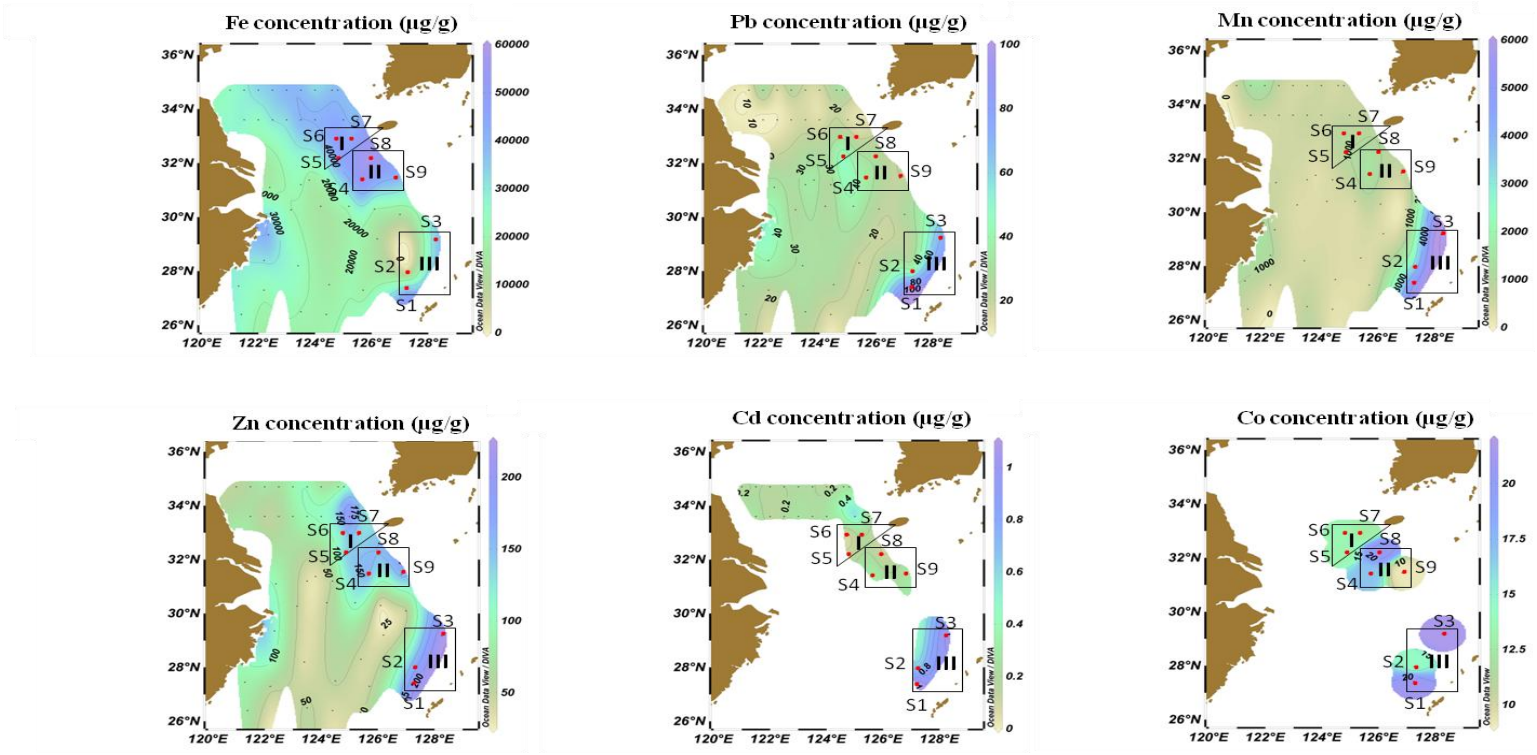

Figure 9. Distribution of trace metals in surface sediments in the outer shelf East China Sea

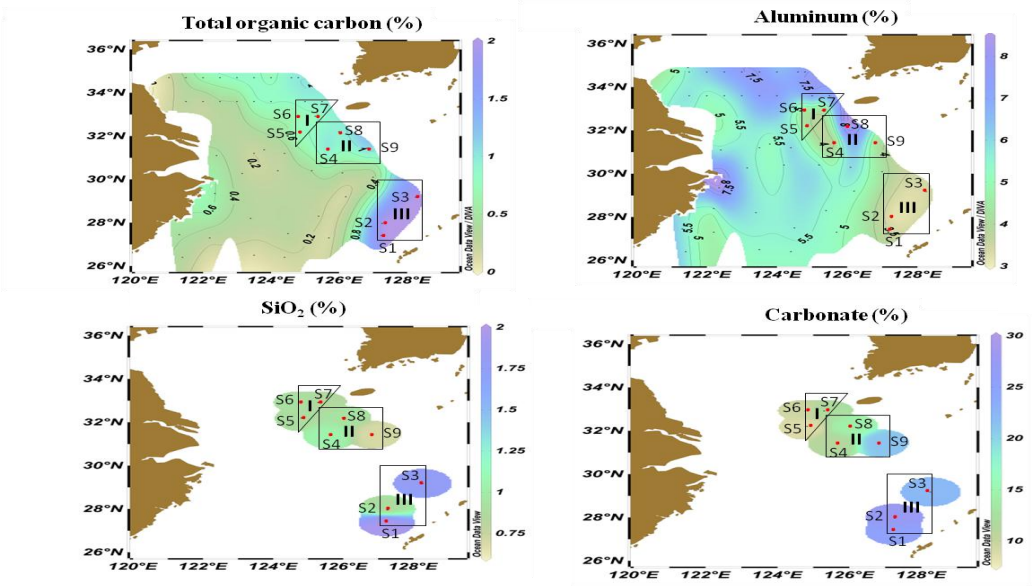

Figure 10.Distribution of total organic carbon (TOC), aluminum, SiO_2 and carbonate in surface sediments of the outer shelf East China Sea

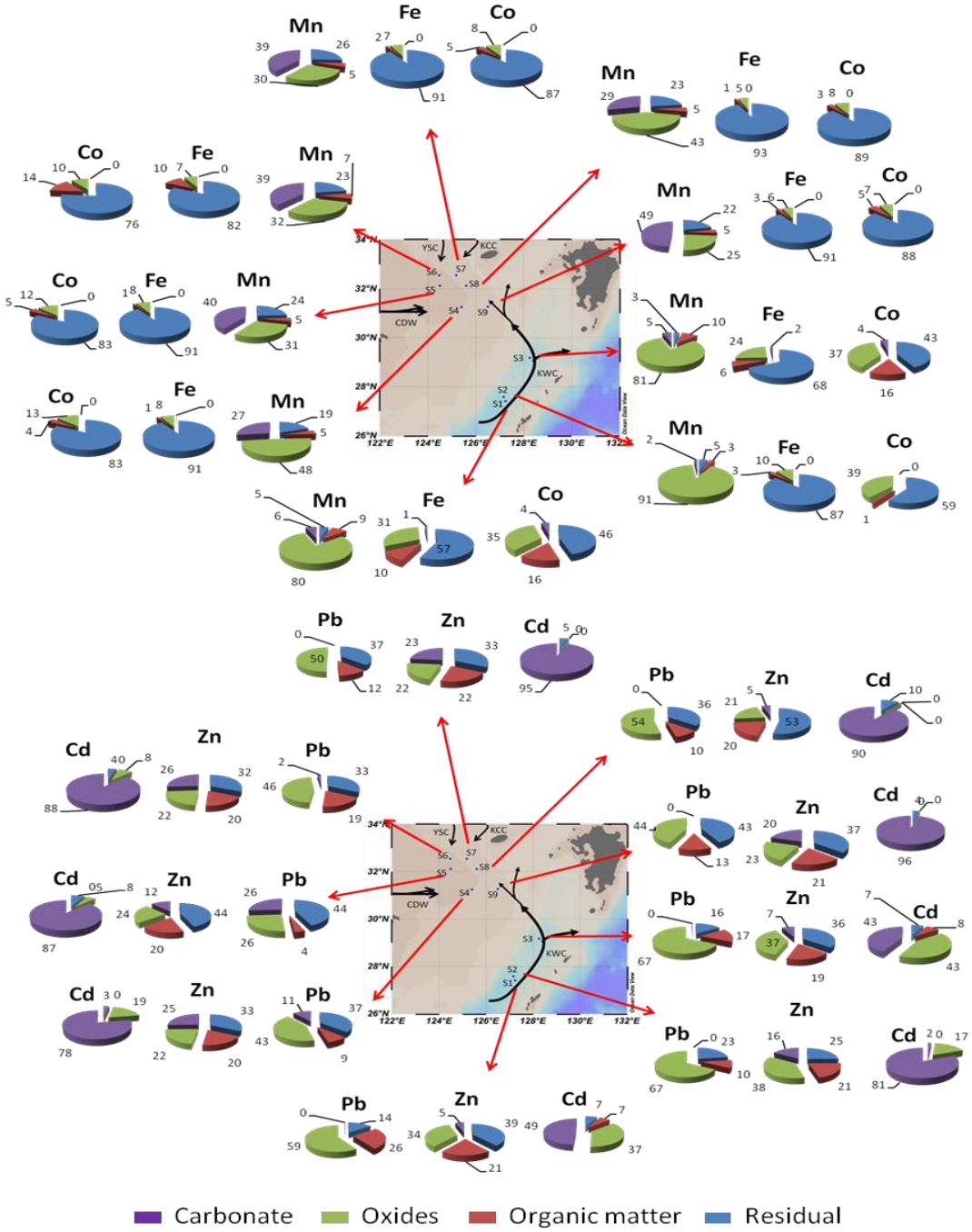

Figure 11. Distribution of trace metal phases in surface sediment of the outer shelf East China Sea.

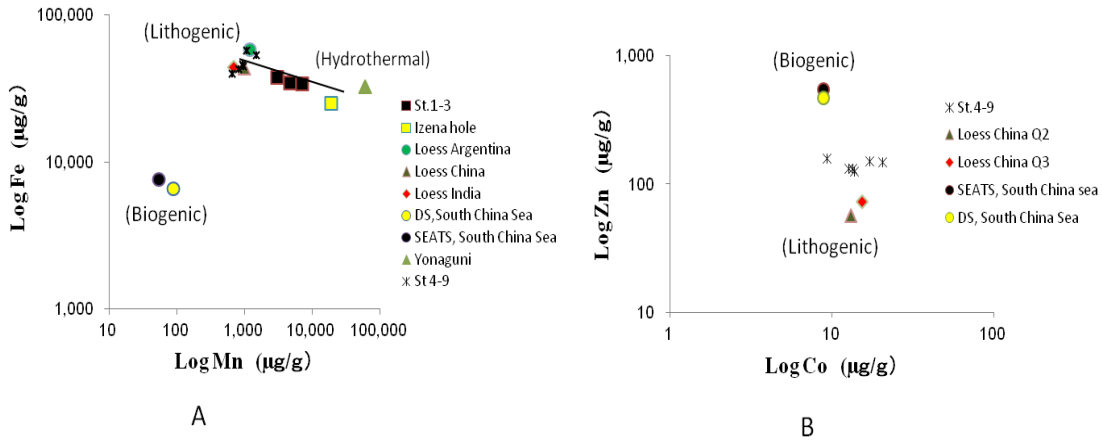

Figure 12. A) Relationship between Iron (Fe) and Manganese (Mn) for the samples at the stations 1, 2 and 3 (group III) and three endmembers from lithogenic, hydrothermal, and biogenic origin (Izena hole, Ishibashi et al., 2014; Loess Argentina, Schellenberger and Veit, 2006; Loess China, Taylor et al., 1983; Gallet et al., 1996; Jahn et al., 2001; Loess India, Tripathi and Rajamani, 1999; DS and SEATS South China Sea, Ho et al., 2007; Yonaguni, Suzuki et al., 2008).

B) Relationship between Zn and Co for the collected samples at stations 4, 5, 6, 7, 8, and 9 (group I and II), combined with biogenic and lithogenic two endmember sources (Loess China Q2 and Q3, Liu et al., 1993; DS and SEATS South China Sea, Ho et al., 2007).

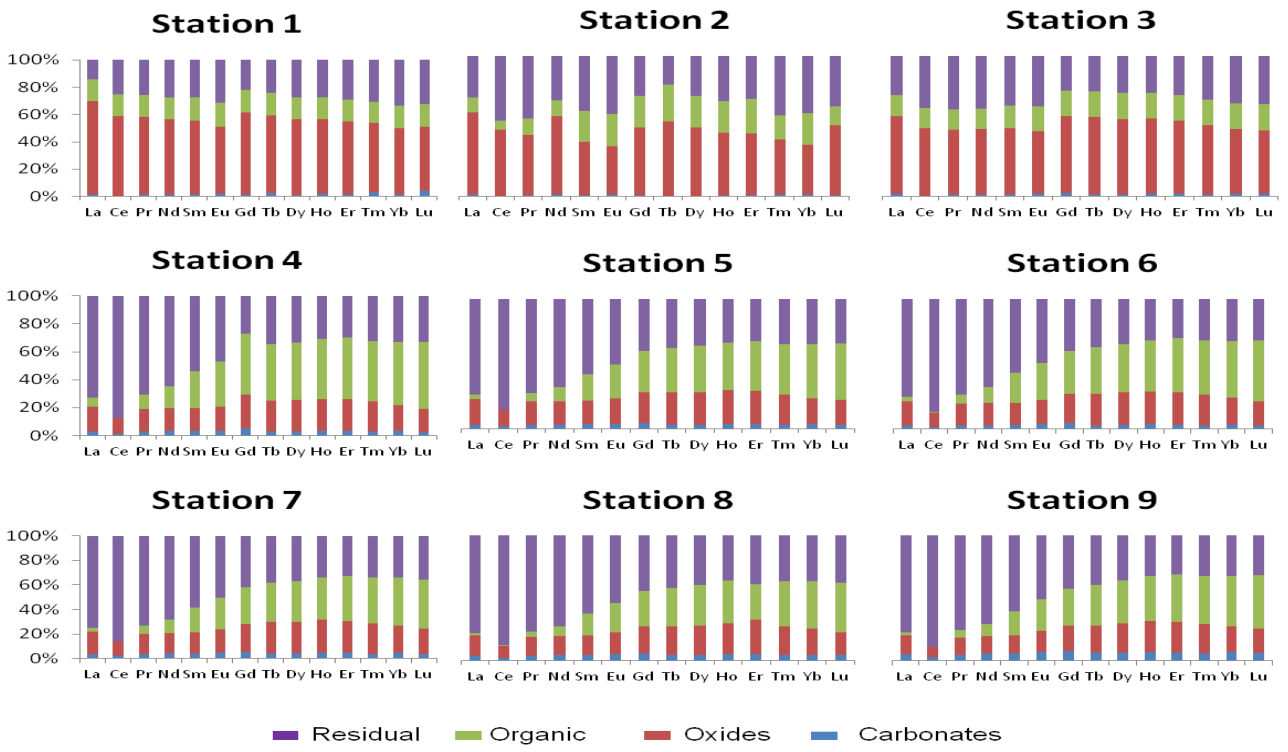

Figure 13. Fractionation of rare earth elements in the surface sediment of the outer shelf continent East China Sea

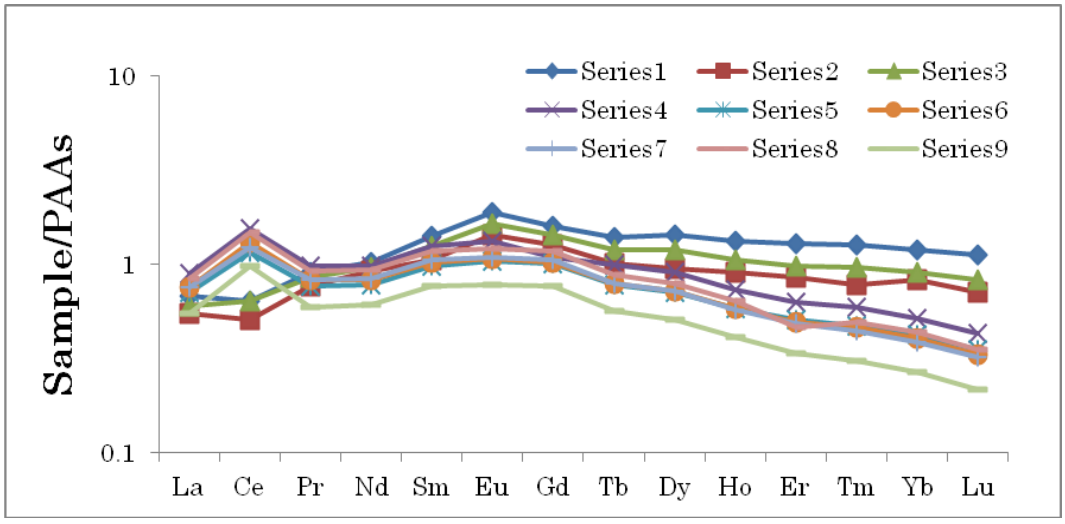

Figure 14. Plot showing the variation of rare earth elements pattern (total concentration) in surface sediment of the outer shelf East China Sea

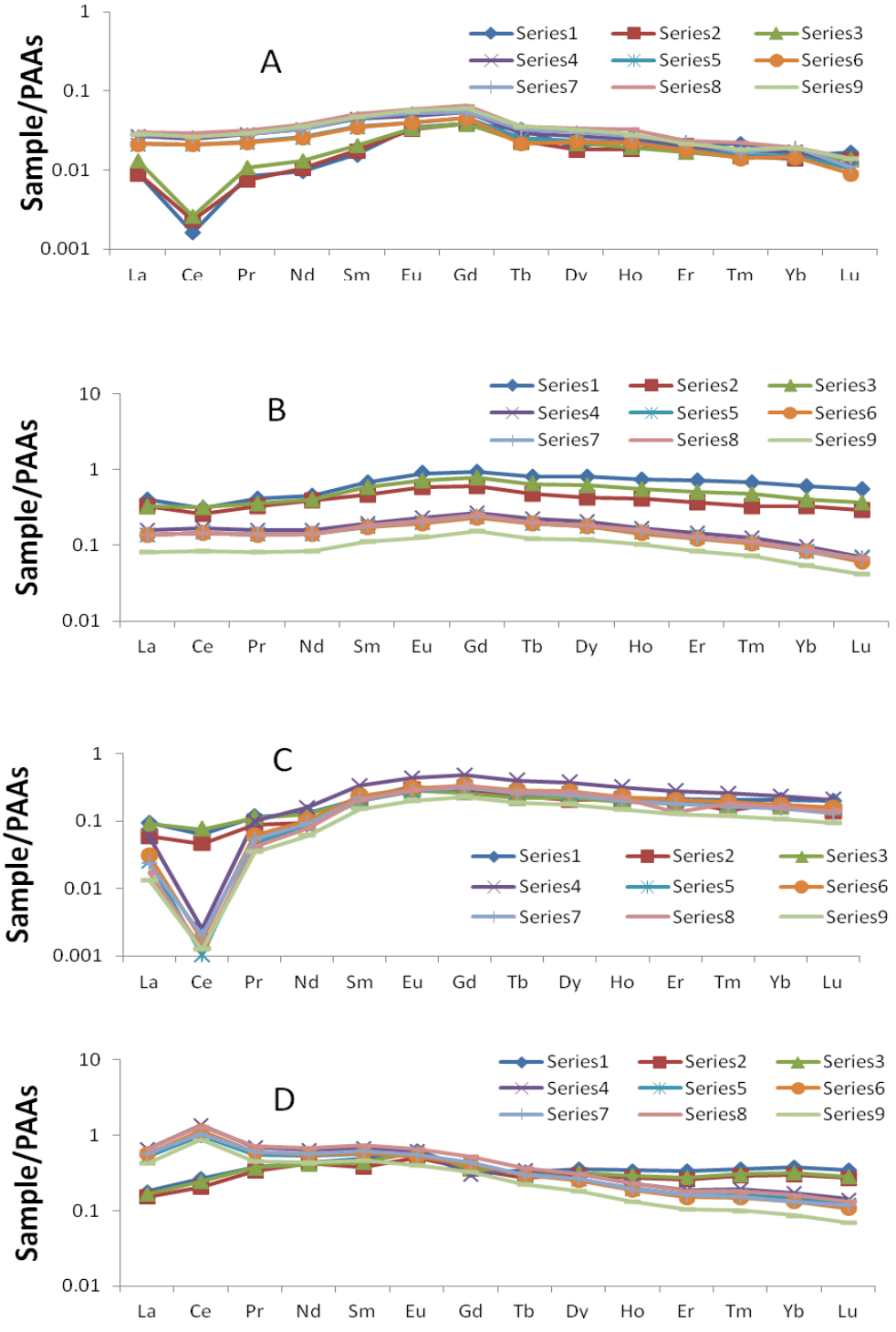

Figure 15. Plot showing the variation of rare earth elements pattern in surface sediment of the outer shelf East China Sea.
A. Carbonate phase: B. Oxides phase; C. Organic Matter Phase;
D. Residual phase

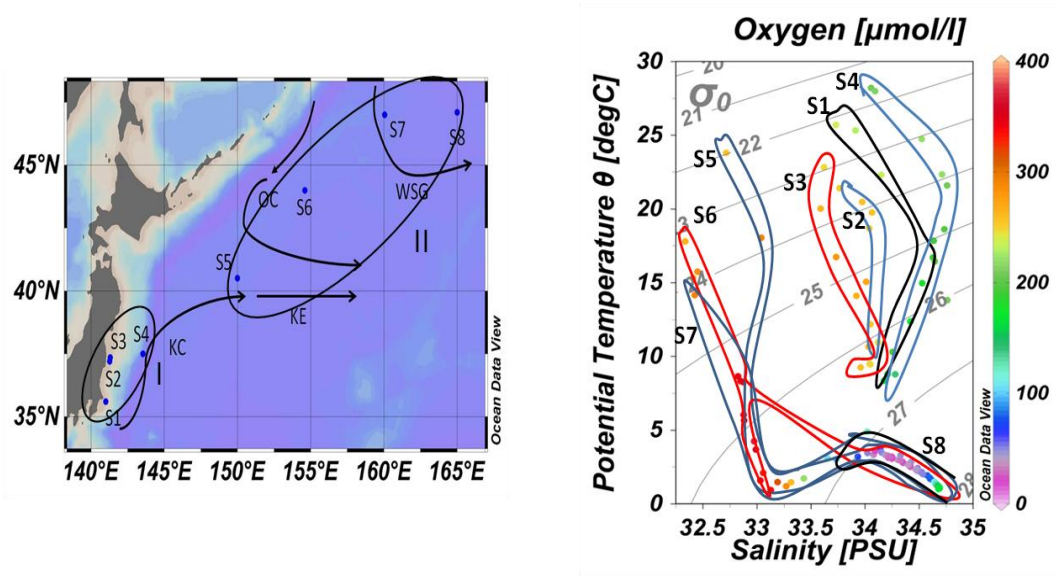

Figure 16. (A) Location of sediment sampling in the Nortwestern Pacific Ocean with current system: Kuroshio current (KC); KE: Kuroshio Extension; OC: Oyashio Current; and WSG: Western Subartic Gryre
(B) T-S-DO diagram of water mass in the Nortwestern Pacific Ocean

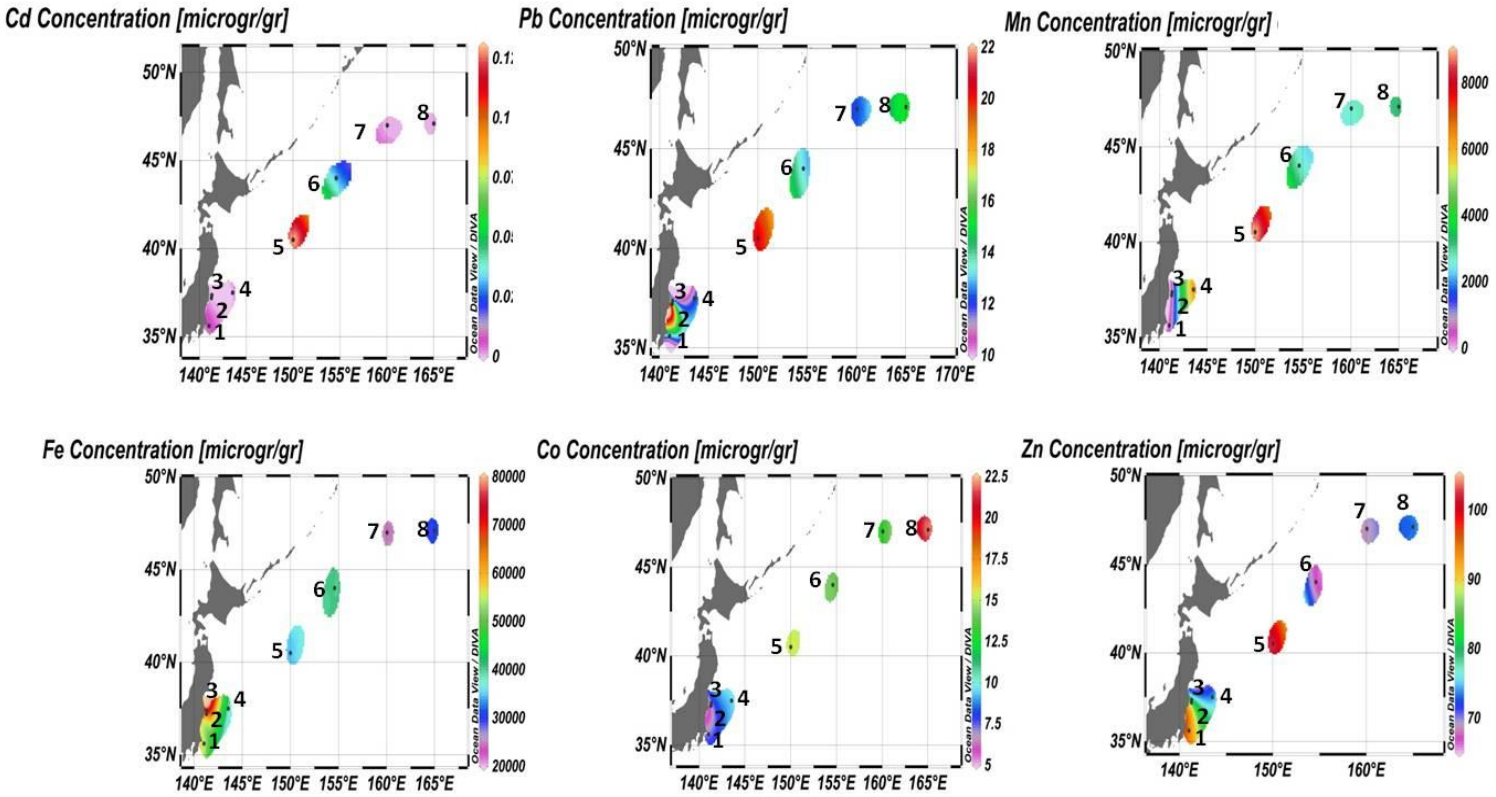

Figure 17. Disribution of trace metal in surface sediment of the Northwestern Pacific Ocean

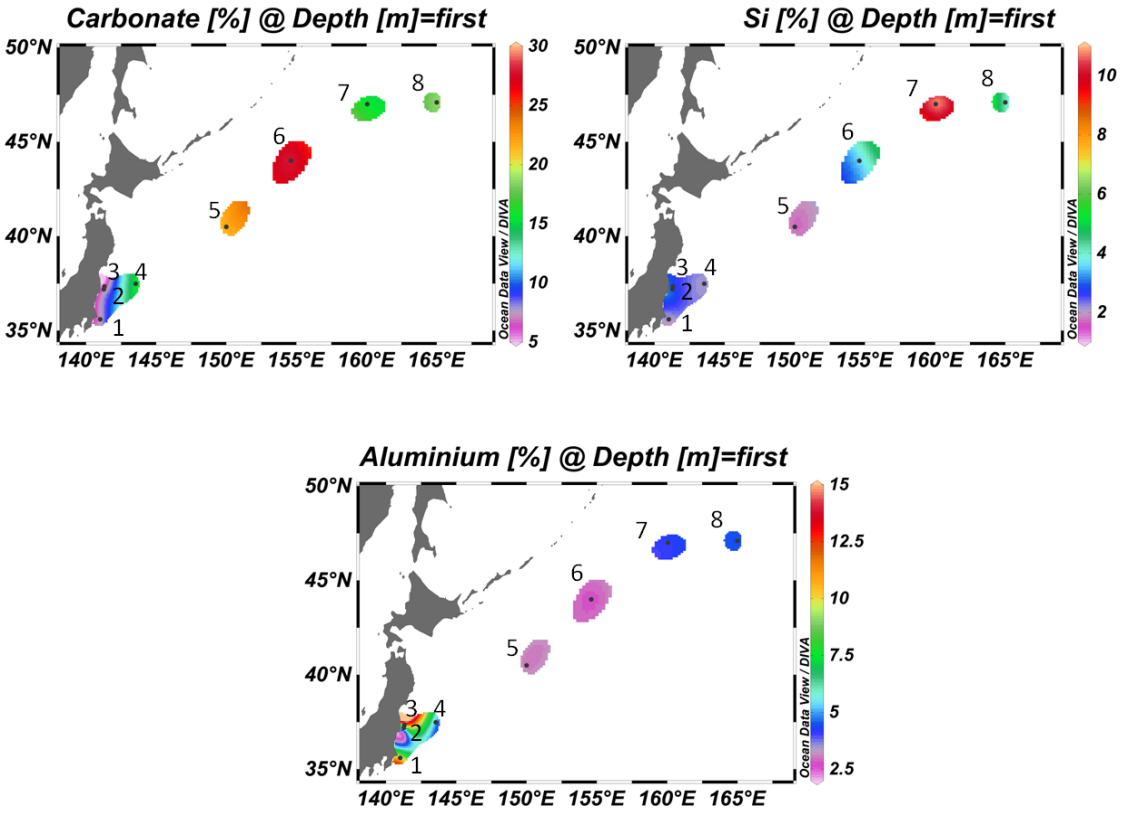

Figure 18. Distribution of carbonate, silica and aluminium in surface sediment of the Northwestern Pacific Ocean

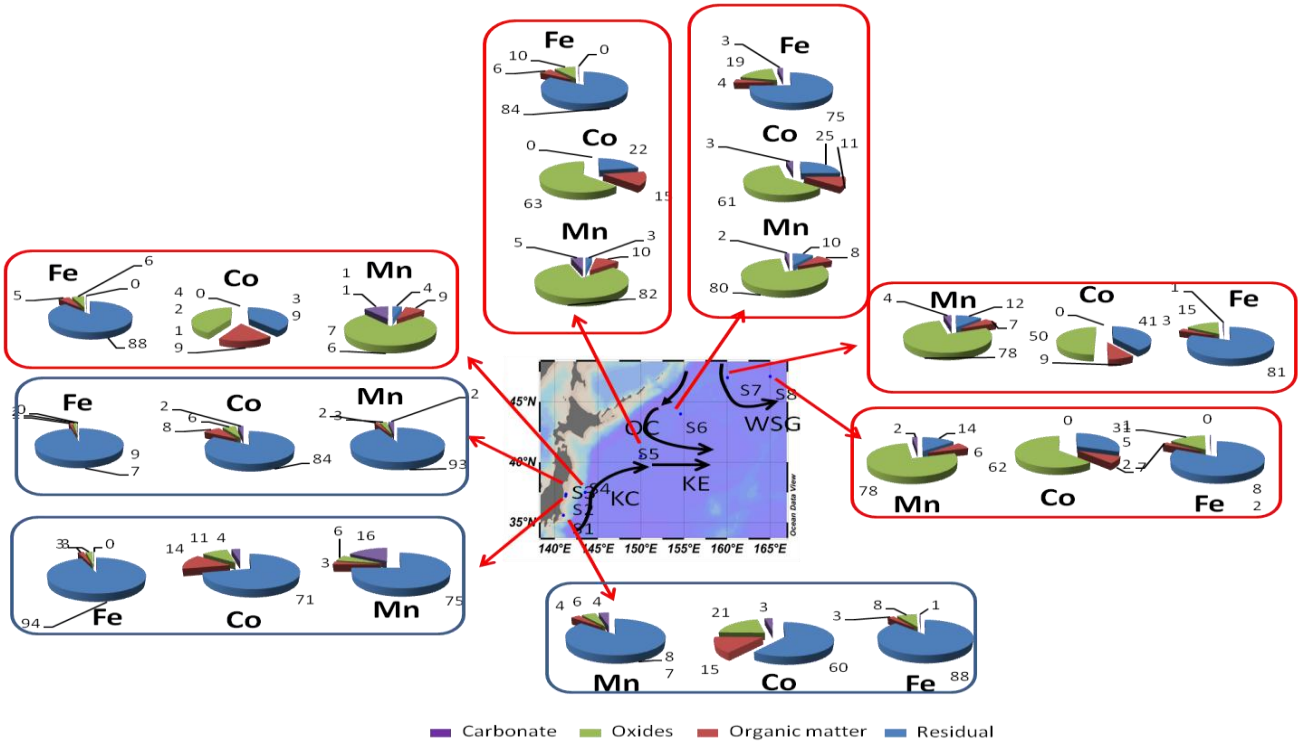

Figure 19. Fractionation of trace metal in surface sediment of the Nortwestern Pacific Ocean in all stations

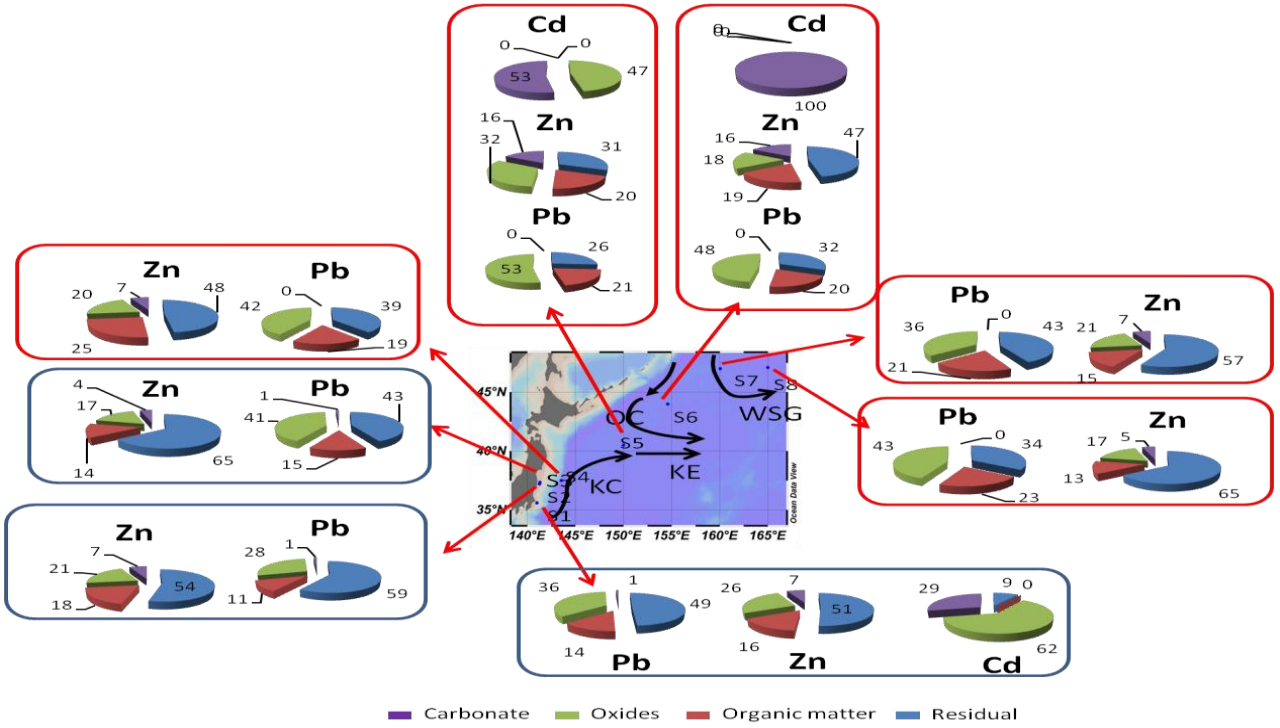

Figure 19. Continue

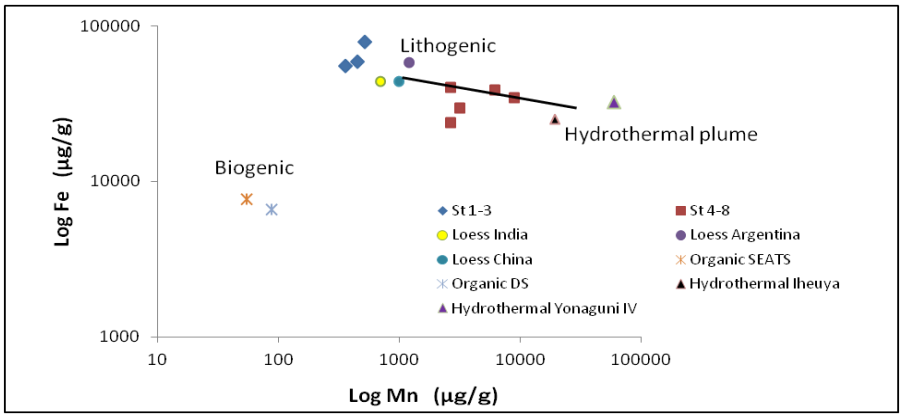

Figure 20. Relationship between Iron (Fe) and Manganese (Mn) for the samples at all stations and three endmembers from lithogenic, hydrothermal, and biogenic origin (Izena hole, Ishibashi et al., 2014; Loess Argentina, Schellenberger and Veit, 2006; Loess China, Taylor et al., 1983; Gallet et al., 1996; Jahn et al., 2001; Loess India, Tripathi and Rajamani, 1999; Organic DS and SEATS, Ho et al., 2007; Yonaguni, Suzuki et al., 2008)

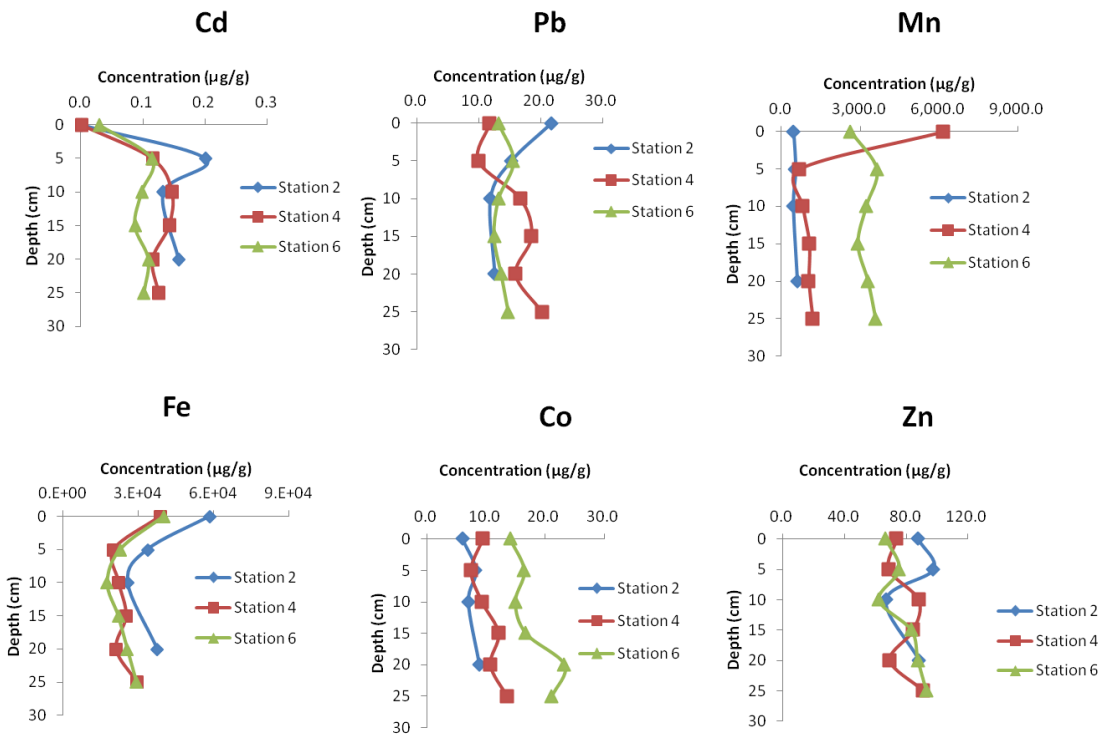

Figure 21. Trace metals concentration with depth in surface sediment at some station of the Northwestern Pacific Ocean

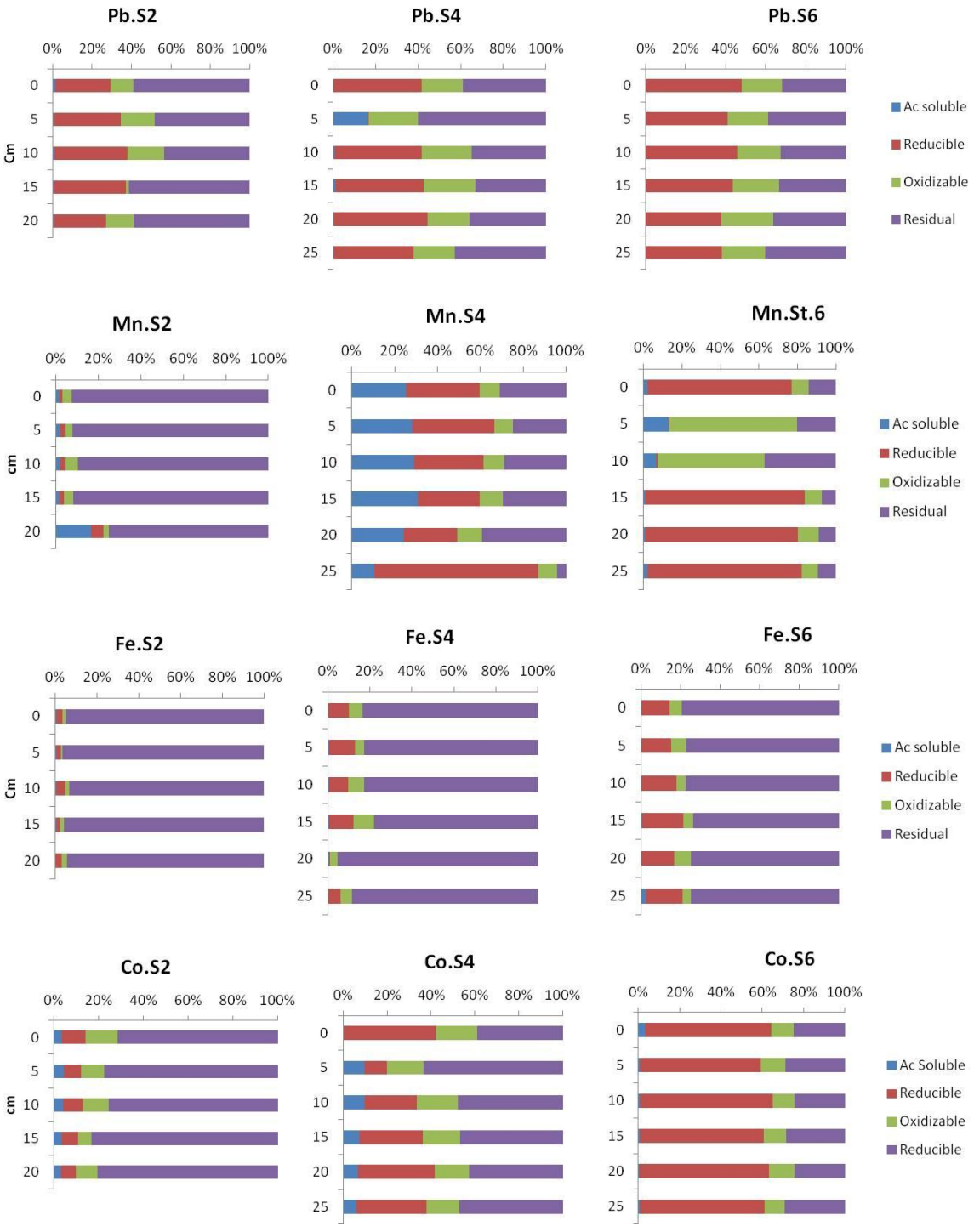

Figure 22. Fractionations of trace metal in surface sediment of the Northwestern Pacific Ocean in station 2, 4 and 6 with depth

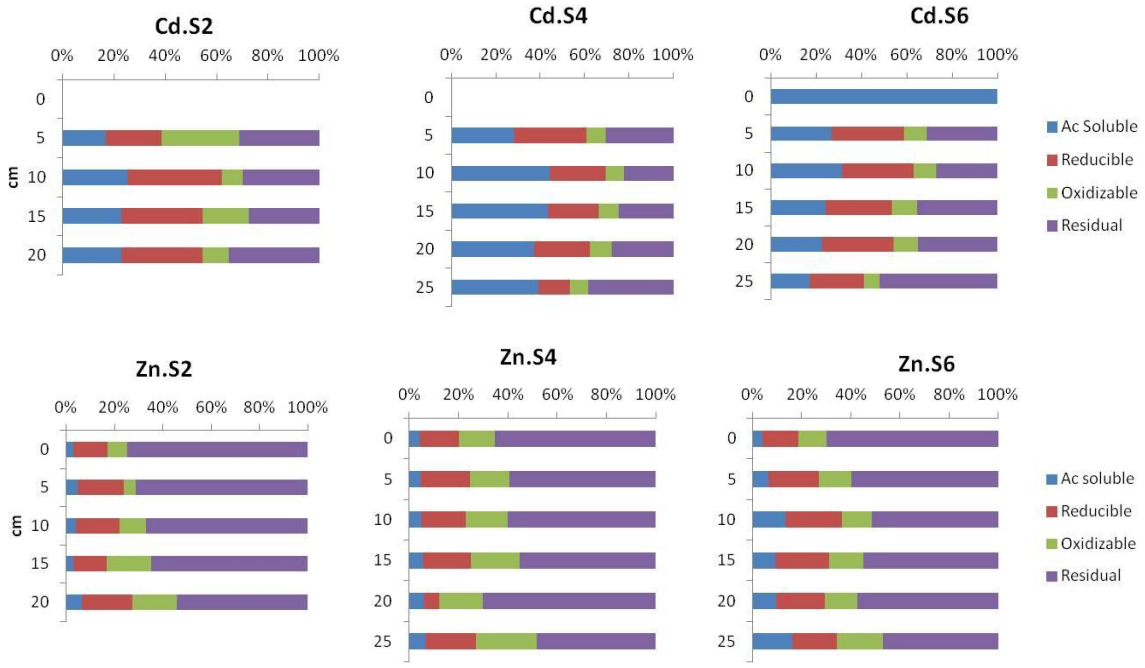

Figure 22. Continued

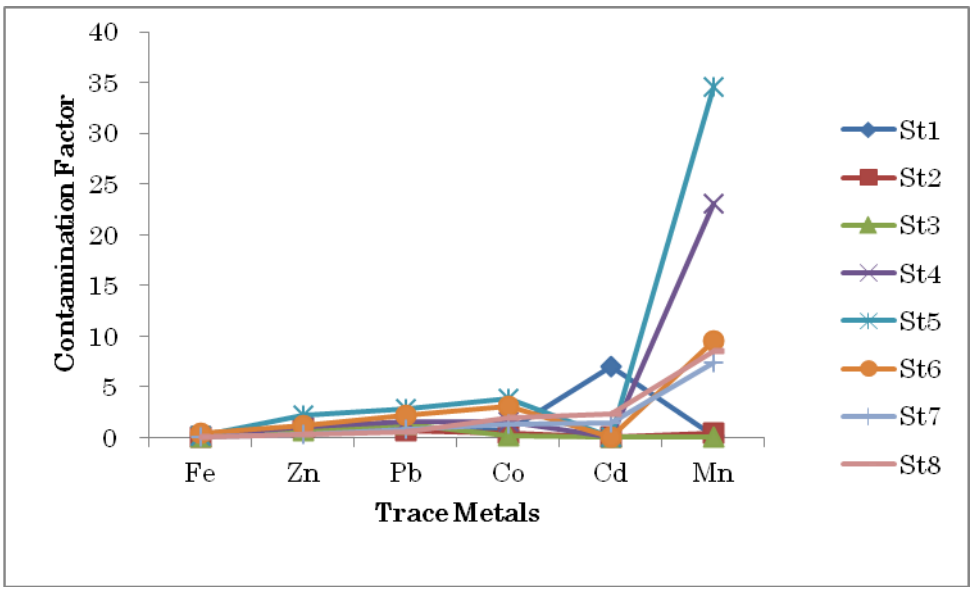

Figure 23. Contamination factor(Cf) of trace metals in surface sediment of the Northwestern Pacific Ocean

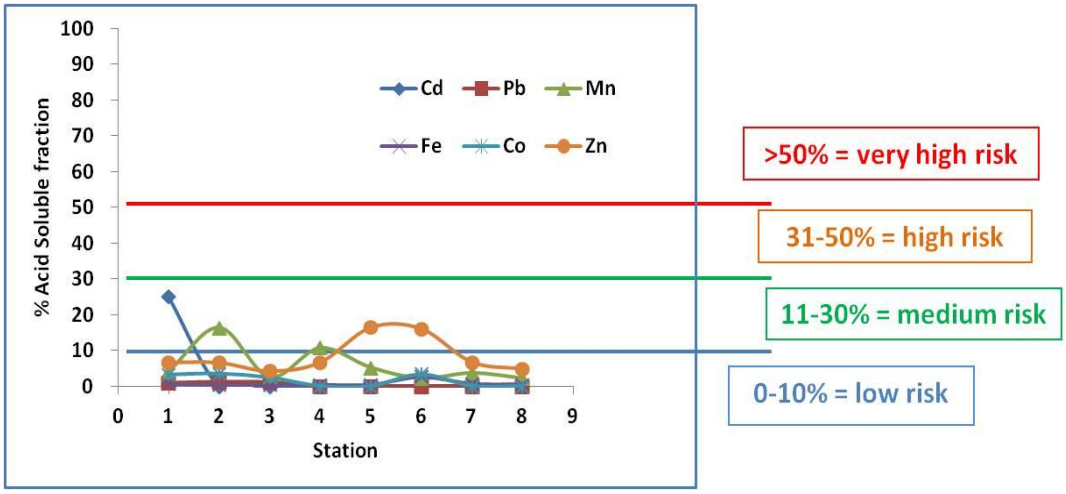

Figure 24. Risk assessment code(RAC) of trace metals in surface sediment of the Northwestern Pacific Ocean

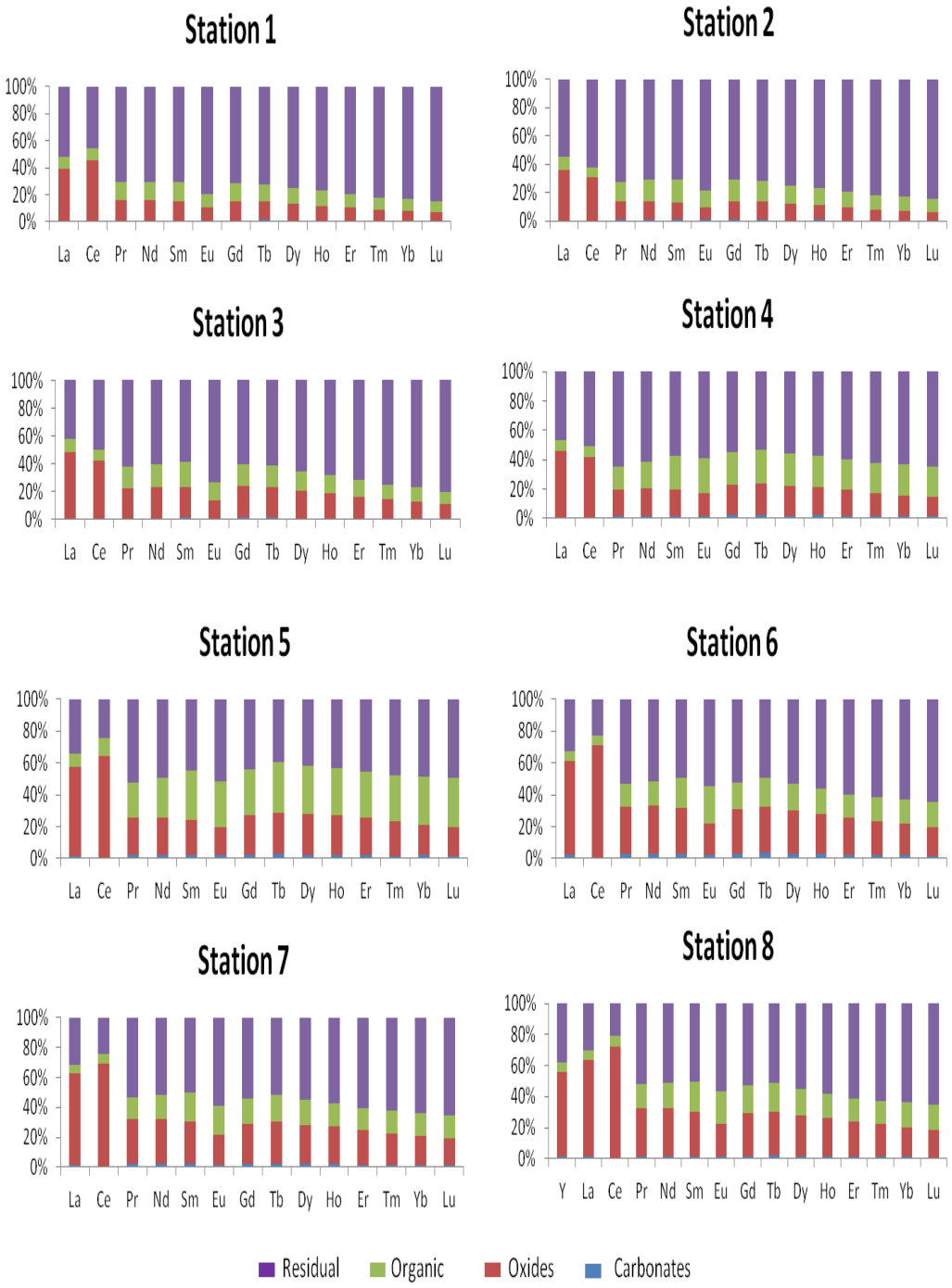

Figure 25. Fractionations of rare earth elements in surface sediment of the Northwestern Pacific Ocean

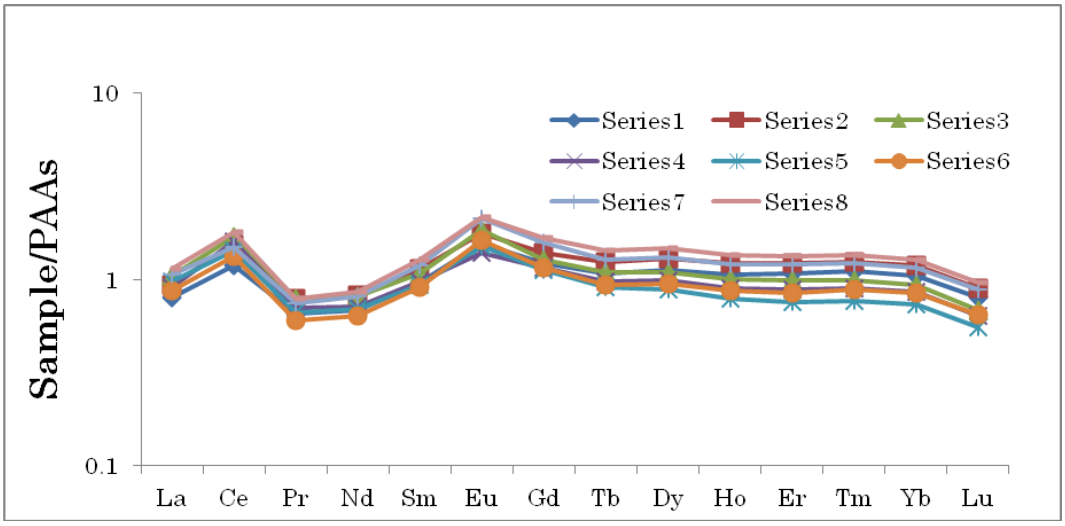

Figure 26. Plot showing the variation of rare earth elements pattern (total concentration) in surface sediment of the Northwestern Pacific Ocean

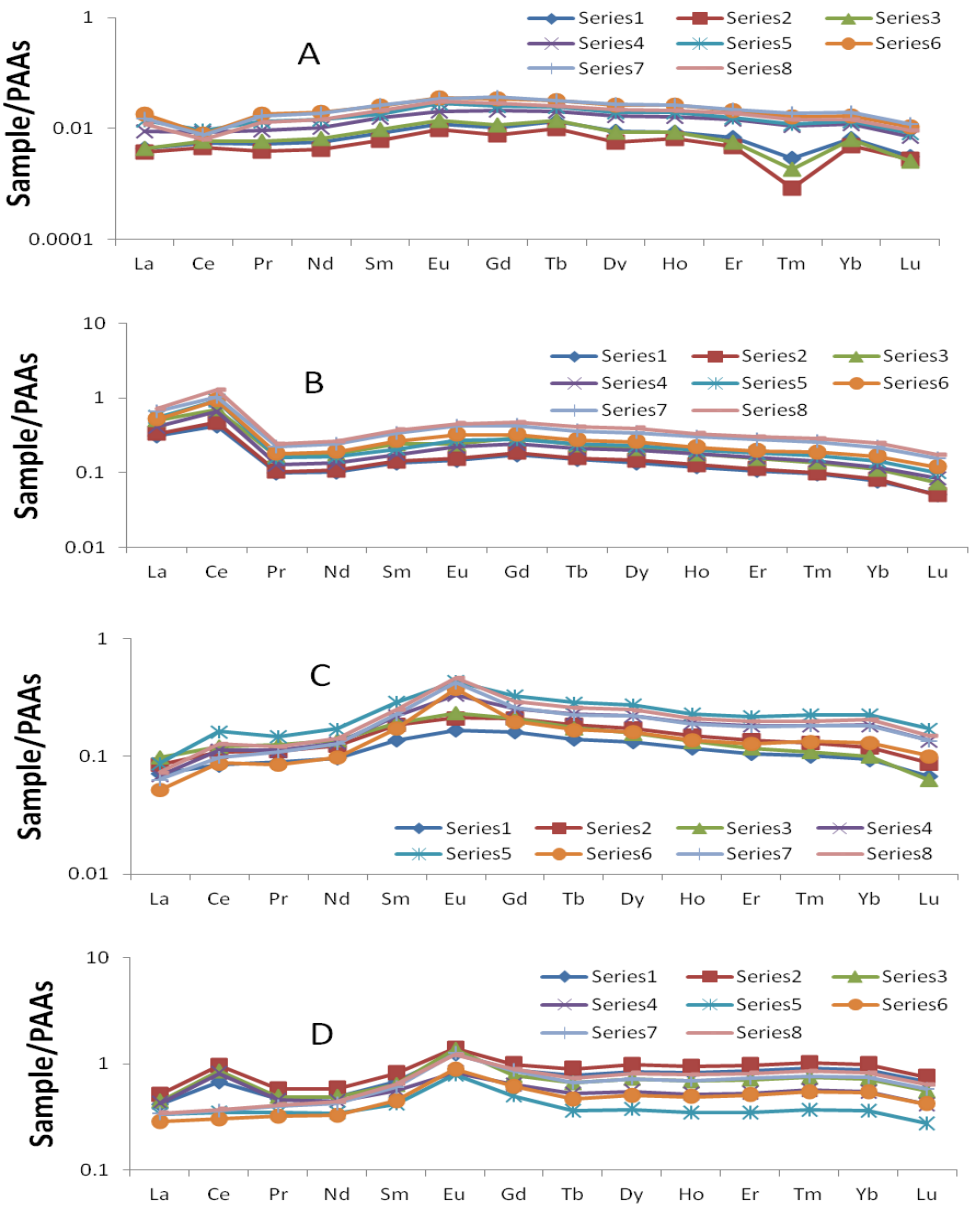

Figure 27. Plot showing the variation of rare earth elements pattern in surface sediment of the Northwestern Pacific Ocean..
A. Carbonate phase: B. Oxides phase; C. Organic Matter Phase;
D. Residual phase

Tables

Table 1. Quantitative composition of functional groups as active sites on isolated humin.

Functional group	Content (cmol/kg) in isolated humin
Total Acidic	677
Carboxylic (-COOH)	115
Hydroxyl (Phenolic-OH)	562

Table 2. Ash content of isolated humin.

Purification Step	Ash Content % (w/w)
Before purification	5.04
After purification	1.54

Table.3 Sorption constant (k1) for plot ln(Co/C)/C *versus* t/C for sorption of Cd(II) onto humin

Medium	k1 (minutes^{-1})	
	Fast Phase	Slow Phase
Freshwater	0.5×10^{-3}	
Seawater	31.88×10^{-3}	6.2×10^{-3}

Table 4. Sorption capacity(b), energy (E), and sorption affinity (K) obtained from Langmuir and Freundlich isotherm models for sorption of Cd(II) onto humin.

Medium	Langmuir model				Freundlich model		
	b(mol/L)	K $(mol/L)^{-1}$	E (kJ/mol)	R^2	1/n	K $(mol/L)^{-1}$	R^2
Freshwater	2×10^{-4}	$5.631 \times 10^{+3}$	21.54	0.9967	0.3473	$5.85 \times 10^{+3}$	0.9373
Seawater	1.256×10^{-4}	$2.733 \times 10^{+3}$	19.74	0.9976	0.4525	$11.09 \times 10^{+3}$	0.9570

Table 5 BCR three-stage plus residual fraction of sequential extraction schem

Extraction step	Reagent(s)	Phases
1	HOAc (0.11 mol/L)	Carbonates, exchangeable metals
2	$NH_2OH.HCl$ (0.1 mol/L)	Oxides Fe/Mn
3	H_2O_2 (8.8 mol/L) Then NH_4OAc (1.0 mol/L) at pH 2	Organic Matter
4	HCl/HNO_3 + HF	Residual Phase

Table 6 Reproducibility of modified BCR sequential extraction method by using standard sediment (GBW-07030)

Element	Fraction	Mean[a]	RSD[b]	Element	Fraction	Mean[a]	RSD[b]
Cd	Carbonate	0.07	3.1	Co	Carbonate	0.55	3.4
	Oxides	0.04	6.2		Oxides	2.63	2.1
	Organic Matter	0.02	6.7		Organic Matter	3.75	7.3
	Residual	0.1	4.6		Residual	6.49	1.3
	SUM	0.23			SUM	13.42	
Pb	Carbonate	0.02	7.8	Zn	Carbonate	5.48	6.3
	Oxides	0.22	5.5		Oxides	9.54	6.6
	Organic Matter	4.68	6.1		Organic Matter	19.72	5.7
	Residual	16.6	4.2		Residual	46.45	7.2
	SUM	21.52			SUM	81.19	
Mn	Carbonate	114	7.5				
	Oxides	245.07	3.7				
	Organic Matter	141	5.5				
	Residual	106.36	3.2				
	SUM	606.43					

Table 7 Recovery of modified BCR sequential extraction method by using standard sediment (GBW-07030)

Element	Concentration ($\mu g.g^{-1}$)		Recovery (%)
	Sum of all fraction	Valued concentration	
Cd	0.23	0.24	95.83
Pb	20.05	21.1	95.02
Mn	606.43	610.1	99.40
Fe	33874.82	33300.5	101.72
Co	13.42	13.6	98.68
Zn	81.2	81.34	99.83

Table 8 Location and concentration of total organic carbon (TOC), aluminum, carbonate, SiO_2 in surface sediment of the outer shelf East China Sea

Station	Long (E)	Lat (N)	Water depth	TOC	Al	Carbonate	SiO_2 (%)				
			(m)	(%)	(%)	(%)	Carbonate	Oxides	Organic matter	Residual	Total
1	127-24.033	27-40.971	1677	3.51	3.23	25.2	0.13	1.09	0.70	0.05	1.97
2	127-16.086	27-58.282	552	3.19	2.81	27.5	0.17	0.33	0.17	0.19	0.86
3	128-25.430	29-17.421	1066	3.36	3.08	22.2	0.14	0.85	0.74	0.05	1.79
4	125-39.869	31-25.154	54	0.99	3.96	11.3	0.08	0.32	0.29	0.35	1.04
5	124-49.332	32-12.052	41	0.79	4.49	8.56	0.07	0.27	0.27	0.28	0.89
6	124-47.007	32-55.138	63	0.67	4.44	9.28	0.12	0.27	0.25	0.28	0.91
7	125-17.977	32-54.993	81	0.76	4.26	12.3	0.05	0.29	0.22	0.29	0.84
8	125-59.829	32-12.045	84	0.92	8.45	14.3	0.04	0.33	0.25	0.32	0.93
9	126-50.044	31-26.814	93	1.13	4.34	21.1	0.07	0.23	0.20	0.20	0.69

Table 9 Concentration of trace metals by modified BCR-sequential methods for surface sediment of the outer shelf East China Sea (unit: $\mu g.g^{-1}$)

	Cd	Pb	Mn	Fe	Co	Zn
Station No.1						
Carbonate	0.52	0.26	288	519	0.88	10.1
Oxides	0.40	57.7	3853	10666	7.35	65.8
Organic Matter	0.07	26	424	3546	3.33	39.9
Residual	0.07	14.1	244	19912	9.69	75.3
TOTAL	1.06	98.1	4809	34643	21.2	191
Station No.2						
Carbonate	0.53	0.00	49.7	31.5	0.00	27.0
Oxides	0.11	27.9	2799	3639	5.56	63.3
Organic Matter	0.00	4.30	88.5	1250	0.19	34.9
Residual	0.02	9.49	146	33094	8.38	41.0
TOTAL	0.66	41.7	3083	38014	14.1	166
Station No.3						
Carbonate	0.43	0.23	390	817	0.86	16.1
Oxides	0.43	47.4	5792	8078	8.16	80.5
Organic Matter	0.08	11.8	690	2054	3.49	413
Residual	0.07	10.9	247	23281	9.25	77.5
TOTAL	1.01	70.4	7119	34230	21.8	215
Station No.4						
Carbonate	0.25	3.85	407	80.1	0.00	38.8
Oxides	0.06	14.9	725	4081	2.14	33.9
Organic Matter	0.00	3.07	286	635	14.0	30.3
Residual	0.01	12.8	286	48695	14.0	50.0
TOTAL	0.32	34.6	1705	53491	30.1	153
Station No.5						
Carbonate	0.12	12.2	388	16.4	0.00	16.1
Oxides	0.01	11.9	293	3551	1.59	32.4
Organic Matter	0.00	2.03	46.5	387	0.62	26.2
Residual	0.01	20.5	232	40868	11.1	59.1
TOTAL	0.13	46.6	959	44823	13.3	134
Station No.6						
Carbonate	0.20	0.66	361	25.4	0.00	33.1
Oxides	0.02	13.6	300	3405	1.30	28.3
Organic Matter	0.00	5.50	60.7	4776	1.94	24.8
Residual	0.01	9.69	210	38201	10.4	39.9
TOTAL	0.23	28.9	932	46407	13.6	126
Station No.7						

Carbonate	0.20	0.00	324	41.5	0.00	31.4
Oxides	0.00	10.2	245	2979	1.07	29.3
Organic Matter	0.00	2.49	60.6	728	0.57	29.8
Residual	0.01	7.48	215	39134	10.9	43.7
TOTAL	0.21	20.1	844	42883	12.6	134
Station No.8						
Carbonate	0.09	0.00	314	28.9	0.00	7.70
Oxides	0.00	15.0	466	3125	1.59	31.9
Organic Matter	0.00	2.86	58.0	725	0.62	30.2
Residual	0.01	10.0	251	53736	18.2	80.2
TOTAL	0.10	27.9	1090	57614	20.4	150
Station No.9						
Carbonate	0.25	0.00	327	3.52	0.00	32.0
Oxides	0.00	8.73	165	2512	0.66	36.9
Organic Matter	0.00	2.69	31.4	1036	0.44	32.9
Residual	0.01	20.0	144	36660	8.06	58.5
TOTAL	0.26	31.4	667	40211	9.16	160

Table 10 Pearson correlation coefficients between total trace metals, total organic carbon (TOC), aluminum, carbonate, and SiO_2 in surface sediments of the outer shelf East China Sea ($0.01 < P < 0.05$)

	Cd	Pb	Mn	Fe	Co	Zn	TOC	Al	Carbonate	SiO_2
Cd	1.00	0.87	0.94	0.43	0.60	0.90	0.92	-0.58	0.77	0.88
Pb		1.00	0.81	0.67	0.70	0.73	0.72	-0.56	0.51	0.93
Mn			1.00	0.44	0.71	0.93	0.87	-0.44	0.65	0.88
Fe				1.00	0.85	0.44	0.24	0.24	0.09	0.76
Co					1.00	0.64	0.50	0.17	0.26	0.81
Zn						1.00	0.90	-0.35	0.77	0.80

Table 11 Pearson correlation coefficients between concentration of trace metals in each phase, TOC, aluminum, carbonate, and SiO_2 in surface sediments of the outer shelf East China Sea ($0.01 < P < 0.05$)

	Cd	Pb	Mn	Fe	Co	Zn	Carbonate	SiO_2	TOC	Al
Carbonate Phase										
Cd	1.00	-0.41	-0.57	0.59	0.64	-0.08	0.87	0.86	-	-
Pb		1.00	0.36	0.58	-0.23	-0.09	-0.53	-0.23	-	-
Mn			1.00	0.19	0.11	0.04	-0.66	-0.51	-	-
Fe				1.00	0.96	-0.45	0.48	0.50	-	-
Co					1.00	-0.53	0.48	0.50	-	-
Zn						1.00	-0.26	-0.02	-	-
Oxides phase										
Cd	1.00	0.97	0.96	0.94	0.95	0.91		0.95	0.84	-
Pb		1.00	0.92	0.96	0.96	0.89		0.97	0.85	-
Mn			1.00	0.82	0.98	0.98		0.84	0.91	-
Fe				1.00	0.86	0.76		0.99	0.70	-
Co					1.00	0.97		0.87	0.93	-
Zn						1.00		0.79	0.97	-
Organic matter phase										
Cd	1.00	0.85	0.97	0.40	0.93	0.84		0.99	0.73	-
Pb		1.00	0.72	0.58	0.83	0.70		0.84	0.63	-
Mn			1.00	0.34	0.89	0.83		0.95	0.74	-
Fe				1.00	0.67	0.10		0.39	0.16	-
Co					1.00	0.61		0.94	0.52	-
Zn						1.00		0.77	0.92	-
Residual phase										
Cd	1.00	0.14	0.28	-0.83	-0.32	0.62		-0.90		-0.38
Pb		1.00	0.40	-0.04	0.07	0.25		-0.01	-	-0.09
Mn			1.00	0.20	0.63	0.42		0.16	-	0.24
Fe				1.00	0.77	-0.19		0.94	-	0.71
Co					1.00	0.33		0.61	-	0.84
Zn						1.00		-0.46	-	0.39

Table 12 The area, average of trace metal concentration, mass accumulation rate (MAR), annual sedimentation flux, atmospheric flux and exchangeable trace metals in sediment flux for each group of the outer shelf East China Sea

			Fe	Mn	Co	Cd	Pb	Zn
Average trace metal concentration (μg/g)								
	Core size (cm^2)	MAR (g cm^{-2} y^{-1})						
Group I	50.2	0.17[a]	4.47x 10^4	0.91x 10^3	13.2	0.19	32.1	131
Group II	50.2	0.17[b]	5.04x 10^4	1.08x 10^3	15.5	0.23	27.5	155
Group III	50.2	0.07[c]	3.56x 10^4	5.00x 10^3	19.0	0.91	70.1	191
Annual trace metal sedimentation flux (μg y^{-1})								
Group I			3.71x 10^5	0.75x 10^4	109	1.57	0.27x10^3	1.09x10^3
Group II			4.31x 10^5	0.93x 10^4	132	1.94	0.24x10^3	1.32x10^3
Group III			1.29x 10^5	1.81x 10^4	68.9	3.29	0.25x10^3	0.69x10^3
Atmosphere trace metals flux (μg y^{-1})								
	Dry deposition flux*							
Group I			1.13x 10^4	0.32x10^3	nd	11.6	0.65x10^3	1.07x10^3
Group II			Nd	nd	0.13	0.35	4.58	1.75
Group III			0.01	0.00	nd	nd	0.00	0.00
Potential of re-mineralization of trace metals from surface sediment to the pore water or bottom water (μg y^{-1})								
Group I			0.23x10^3	2.96x10^3	0.00	1.07	25.2	0.22x10^3
Group II			0.29x10^3	3.24x10^3	0.00	1.71	8.70	0.22x10^3
Group III			1.90x10^3	0.79x10^3	1.85	1.89	0.51	66.8

a Data taken from Yuan et al (2012), references therein Alexander et al. (1991), and Zhao and Li (1991)

b Data taken from Yu et al. (2013), and references therein Hsu and Lin (2010)

c Data taken from Huh and Su (1999), and Su and Huh (2002)

* group I, Fe, Mn, Cd, Pb, and Zn: 2252, 64, 2, 130, and 213 mg m^{-2} y^{-1}; group II, Co, Zn, Cd, and Pb: 0.03, 6.94, 0.07, and 0.91 mg m^{-2} y^{-1}; group III, Fe, Mn, Pb, and Zn: 1.4 x 10^{-3}, 2.4 x 10^{-4}, 9.1 x 10^{-5} and 6.9 x 10^{-4} mg m^{-2} y^{-1}

nd: not determined

Table 13 Comparison ot trace metals concentration in surface sediments of representative seas around East China Sea

Location	Cd(μg/g)	Pb(μg/g)	Mn(μg/g)	Fe(%)	Co(μg/g)	Zn(μg/g)	Reference
East China Sea (Outer Shelf Continental)	0.09-0.66 0.25	20.14-46.61 31.49	667-1495.8 1047.82	3.61-5.30 4.43	7.99-16.88 12.71	20.63-38.07 28.46	This study
The Yellow Sea	0–8.21 0.513	4.80–21.9 12.3	84.7–1593 410	0.61–2.27 1.33	4.11–13.0 8.24	21.9–96.2 47.3	Ziang et al. (2014)
South Yellow Sea	0.06–1.54 0.30	6.20–39.3 17.8	152–1910 789	1.00–5.21 3.54	ND	24.4–244 93.7	Yuan et al. (2012)
Bohay Bay	0.04-0.08 0.24	5.90-97.0 21.2	ND	ND	ND	56.3-309 103	Zhan et al. (2010)
East China Sea	ND	10.0-49.0 27	152-1152 484	0.62-3.97 2.1	ND	18.0-114 60	Fang et al. (2009)
East China Sea	0.2-0.3 0.27	22.3-28.0 25.14	ND	ND	12.1-14.9 13.34	72.9-102.4 86.06	Yu et al. (2013)
Inner continental Shelf of East China Sea	0.09-0.21	24.4-53 34.1	ND	ND	ND	80.2-140.5 116.03	Liu et al. (2011)

Table 14 Total concentration of rare earth elements in surface sediment of the outer shelf continent East China Sea

REEs	Concentration (μg/g)								
	St 1	St 2	St 3	St 4	St 5	St 6	St 7	St8	St9
Y	30.92	20.01	23.48	16.98	13.67	14.65	13.50	14.77	9.77
La	26.01	20.99	23.00	34.29	26.97	28.75	29.00	32.32	21.03
Ce	51.20	40.76	51.16	123.91	91.54	103.88	98.59	118.35	78.24
Pr	8.07	6.73	7.56	8.64	6.78	7.28	7.30	8.13	5.27
Nd	34.65	31.38	32.49	33.38	26.49	28.01	28.45	31.70	20.69
Sm	7.78	5.84	6.93	6.93	5.45	5.71	5.87	6.48	4.28
Eu	2.03	1.54	1.78	1.44	1.13	1.15	1.18	1.32	0.84
Gd	7.45	5.91	6.68	5.10	4.71	4.79	4.91	5.45	3.57
Tb	1.08	0.79	0.92	0.77	0.60	0.62	0.61	0.68	0.44
Dy	6.66	4.41	5.56	4.24	3.34	3.38	3.37	3.71	2.38
Ho	1.32	0.90	1.05	0.73	0.58	0.58	0.56	0.63	0.40
Er	3.66	2.42	2.80	1.80	1.44	1.41	1.39	1.33	0.95
Tm	0.51	0.32	0.39	0.24	0.19	0.19	0.18	0.20	0.13
Yb	3.38	2.32	2.54	1.46	1.19	1.14	1.09	1.22	0.75
Lu	0.48	0.31	0.36	0.19	0.15	0.14	0.14	0.15	0.09
SUM	**185.21**	**144.62**	**166.67**	**240.09**	**184.23**	**201.68**	**196.14**	**226.44**	**148.84**
Lan/Ybn	1.18	1.18	1.18	1.18	1.18	1.18	1.18	1.18	1.18
Smn/Lan	1.68	1.68	1.68	1.68	1.68	1.68	1.68	1.68	1.68
Smn/Ybn	1.98	1.98	1.98	1.98	1.98	1.98	1.98	1.98	1.98
Y/Ho	**23.42**	**22.31**	**22.43**	**23.33**	**23.62**	**25.46**	**23.89**	**23.47**	**24.16**
Nd/Yb	**10.24**	**13.53**	**12.79**	**22.86**	**22.33**	**24.66**	**26.03**	**25.91**	**27.54**
La/Yb	**7.69**	**9.05**	**9.05**	**23.48**	**22.73**	**25.31**	**26.54**	**26.41**	**27.99**

Table 15 The concentration of rare earth elements in carbonates fraction in surface sediment of the outer shelf continent East China Sea

REEs	Concentration (μg/g)								
	St 1	St 2	St 3	St 4	St 5	St 6	St 7	St 8	St 9
Y	0.67	0.47	0.82	0.80	0.69	1.82	0.88	0.95	1.00
La	0.35	0.34	0.50	1.03	0.82	0.81	1.05	1.15	1.10
Ce	0.13	0.18	0.21	1.97	1.66	1.67	2.12	2.31	2.11
Pr	0.07	0.07	0.09	0.25	0.20	0.20	0.25	0.28	0.26
Nd	0.33	0.35	0.44	1.11	0.88	0.87	1.12	1.29	1.20
Sm	0.09	0.10	0.11	0.25	0.19	0.19	0.26	0.28	0.26
Eu	0.04	0.04	0.04	0.05	0.04	0.04	0.06	0.06	0.06
Gd	0.18	0.18	0.18	0.25	0.21	0.21	0.25	0.30	0.28
Tb	0.03	0.02	0.02	0.02	0.02	0.02	0.03	0.03	0.03
Dy	0.09	0.08	0.10	0.13	0.11	0.11	0.14	0.16	0.15
Ho	0.03	0.02	0.02	0.02	0.02	0.02	0.03	0.03	0.03
Er	0.05	0.06	0.05	0.06	0.05	0.05	0.07	0.07	0.06
Tm	0.01	0.01	0.01	0.01	0.01	0.01	0.01	0.01	0.01
Yb	0.04	0.04	0.04	0.05	0.04	0.04	0.05	0.05	0.05
Lu	0.01	0.01	0.01	0.00	0.00	0.00	0.00	0.01	0.01
SUM	**2.10**	**1.96**	**2.63**	**6.01**	**4.95**	**6.06**	**6.32**	**6.97**	**6.63**
Lan/Ybn	1.18	1.18	1.18	1.18	1.18	1.18	1.18	1.18	1.18
Smn/Lan	1.68	1.68	1.68	1.68	1.68	1.68	1.68	1.68	1.68
Smn/Ybn	1.98	1.98	1.98	1.98	1.98	1.98	1.98	1.98	1.98
Y/Ho	**25.72**	**25.56**	**42.37**	**32.76**	**31.04**	**81.91**	**32.74**	**29.22**	**36.03**
Nd/Yb	**7.80**	**9.00**	**10.16**	**22.75**	**20.37**	**21.22**	**20.71**	**23.53**	**22.22**
La/Yb	**8.24**	**8.77**	**11.55**	**21.21**	**18.92**	**19.86**	**19.32**	**21.14**	**20.44**

Table 16 The concentration of rare earth elements in oxides fraction in surface sediment of the outer shelf continent East China Sea

REEs	Concentration (μg/g)								
	St 1	St 2	St 3	St 4	St 5	St 6	St 7	St 8	St 9
Y	23.43	13.99	16.87	5.15	4.45	4.39	4.48	4.61	3.15
La	15.27	12.56	12.65	6.10	5.30	5.23	5.25	5.22	3.11
Ce	24.83	20.72	25.38	13.50	11.77	11.66	11.71	11.70	6.67
Pr	3.66	2.89	3.19	1.40	1.23	1.21	1.24	1.23	0.72
Nd	15.20	13.39	13.59	5.38	4.75	4.74	4.84	4.82	2.84
Sm	3.83	2.56	3.23	1.10	0.98	0.97	1.01	1.01	0.61
Eu	0.97	0.64	0.79	0.25	0.22	0.21	0.22	0.23	0.14
Gd	4.41	2.79	3.63	1.26	1.11	1.08	1.14	1.17	0.71
Tb	0.62	0.37	0.50	0.17	0.15	0.15	0.16	0.16	0.10
Dy	3.77	2.00	2.93	0.96	0.83	0.84	0.87	0.87	0.55
Ho	0.74	0.41	0.55	0.17	0.15	0.14	0.15	0.16	0.10
Er	2.03	1.05	1.46	0.41	0.36	0.35	0.36	0.37	0.24
Tm	0.28	0.13	0.19	0.05	0.04	0.04	0.05	0.05	0.03
Yb	1.69	0.93	1.15	0.27	0.24	0.23	0.24	0.25	0.15
Lu	0.24	0.13	0.16	0.03	0.03	0.03	0.03	0.03	0.02
SUM	**100.98**	**74.57**	**86.29**	**36.20**	**31.62**	**31.28**	**31.72**	**31.85**	**19.14**
Lan/Ybn	1.18	1.18	1.18	1.18	1.18	1.18	1.18	1.18	1.18
Smn/Lan	1.68	1.68	1.68	1.68	1.68	1.68	1.68	1.68	1.68
Smn/Ybn	1.98	1.98	1.98	1.98	1.98	1.98	1.98	1.98	1.98
Y/Ho	**31.64**	**34.26**	**30.67**	**30.88**	**29.60**	**30.83**	**29.38**	**29.61**	**31.33**
Nd/Yb	**8.98**	**14.38**	**11.86**	**19.71**	**20.20**	**20.24**	**20.35**	**19.01**	**18.57**
La/Yb	**9.02**	**13.48**	**11.04**	**22.32**	**22.51**	**22.34**	**22.07**	**20.59**	**20.37**

Table 17 The concentration of rare earth elements in organic fraction in surface sediment of the outer shelf continent East China Sea

REEs	Concentration (μg/g)								
	St 1	St 2	St 3	St 4	St 5	St 6	St 7	St 8	St 9
Y	5.29	3.64	4.44	6.58	4.67	4.80	4.29	4.72	3.10
La	3.55	2.27	3.42	2.22	0.96	1.15	0.89	0.66	0.50
Ce	5.05	3.66	5.99	0.20	0.08	0.14	0.16	0.10	0.10
Pr	1.01	0.79	0.98	0.88	0.41	0.53	0.47	0.36	0.30
Nd	4.42	3.15	4.29	5.33	2.82	3.43	3.11	2.60	2.04
Sm	1.18	1.10	1.14	1.83	1.11	1.30	1.18	1.13	0.83
Eu	0.35	0.31	0.31	0.47	0.29	0.33	0.30	0.31	0.21
Gd	1.25	1.27	1.22	2.20	1.48	1.57	1.47	1.56	1.07
Tb	0.18	0.18	0.17	0.31	0.21	0.22	0.20	0.21	0.14
Dy	1.12	0.95	1.02	1.73	1.19	1.27	1.12	1.23	0.83
Ho	0.21	0.20	0.19	0.31	0.21	0.23	0.20	0.22	0.15
Er	0.61	0.58	0.51	0.79	0.56	0.58	0.51	0.38	0.36
Tm	0.08	0.06	0.07	0.10	0.07	0.08	0.07	0.07	0.05
Yb	0.57	0.51	0.45	0.66	0.50	0.49	0.43	0.47	0.30
Lu	0.08	0.06	0.07	0.09	0.07	0.07	0.06	0.06	0.04
SUM	**24.96**	**18.73**	**24.25**	**23.72**	**14.64**	**16.18**	**14.45**	**14.08**	**10.01**
Lan/Ybn	1.18	1.18	1.18	1.18	1.18	1.18	1.18	1.18	1.18
Smn/Lan	1.68	1.68	1.68	1.68	1.68	1.68	1.68	1.68	1.68
Smn/Ybn	1.98	1.98	1.98	1.98	1.98	1.98	1.98	1.98	1.98
Y/Ho	**24.65**	**18.06**	**23.58**	**21.13**	**22.03**	**21.23**	**21.96**	**21.92**	**21.26**
Nd/Yb	**7.71**	**6.21**	**9.53**	**8.08**	**5.69**	**6.99**	**7.26**	**5.57**	**6.78**
La/Yb	**6.20**	**4.46**	**7.60**	**3.37**	**1.93**	**2.35**	**2.09**	**1.41**	**1.66**

Table 18 The concentration of rare earth elements in residual fraction in surface sediment of the outer shelf continent East China Sea

REEs	Concentration (μg/g)								
	St 1	St 2	St 3	St 4	St 5	St 6	St 7	St 8	St 9
Y	1.53	1.92	1.36	4.45	3.86	3.64	3.85	4.50	2.52
La	6.84	5.82	6.42	24.94	19.90	21.56	21.81	25.29	16.32
Ce	21.19	16.19	19.58	108.23	78.02	90.41	84.60	104.25	69.36
Pr	3.33	2.98	3.30	6.10	4.94	5.34	5.34	6.26	3.99
Nd	14.70	14.48	14.16	21.56	18.04	18.97	19.37	23.00	14.61
Sm	2.69	2.08	2.44	3.75	3.16	3.25	3.43	4.05	2.57
Eu	0.68	0.55	0.64	0.67	0.57	0.57	0.59	0.71	0.43
Gd	1.60	1.66	1.65	1.39	1.90	1.93	2.05	2.41	1.51
Tb	0.25	0.21	0.23	0.27	0.23	0.23	0.23	0.28	0.17
Dy	1.69	1.39	1.50	1.42	1.21	1.17	1.24	1.46	0.85
Ho	0.34	0.27	0.29	0.23	0.19	0.18	0.19	0.23	0.13
Er	0.96	0.73	0.78	0.54	0.47	0.43	0.46	0.52	0.29
Tm	0.14	0.12	0.12	0.08	0.07	0.06	0.06	0.07	0.04
Yb	1.07	0.84	0.90	0.48	0.41	0.37	0.37	0.45	0.24
Lu	0.15	0.12	0.12	0.06	0.05	0.05	0.05	0.06	0.03
SUM	**57.16**	**49.36**	**53.50**	**174.16**	**133.01**	**148.16**	**143.65**	**173.54**	**113.06**
Lan/Ybn	1.18	1.18	1.18	1.18	1.18	1.18	1.18	1.18	1.18
Smn/Lan	1.68	1.68	1.68	1.68	1.68	1.68	1.68	1.68	1.68
Smn/Ybn	1.98	1.98	1.98	1.98	1.98	1.98	1.98	1.98	1.98
Y/Ho	**4.53**	**7.14**	**4.69**	**19.75**	**19.86**	**19.69**	**20.24**	**19.88**	**19.32**
Nd/Yb	**13.67**	**17.21**	**15.73**	**45.02**	**43.84**	**51.25**	**52.06**	**51.19**	**59.99**
La/Yb	**6.36**	**6.92**	**7.13**	**52.07**	**48.37**	**58.22**	**58.60**	**56.26**	**66.98**

Table 19 Internal recovery for the surface sediment samples from the Northwestern Pacific Ocean

Element	Concentration (μg/g)		Recovery (%)
	Sum	Total	
Cd	0.63	0.66	94.35
Pb	41.78	43.71	95.59
Mn	302.52	306.04	98.85
Fe	3713.38	3721.85	99.77
Co	10.18	10.51	96.83
Zn	29.39	29.80	98.62

Table 20 Location and some parameters of surface sediment of the Northwestern Pacific Ocean.

Station	Long (E)	Lat (N)	Salinity(PSU)	T(^{o}C)	pH	Al (%)	Carbonate (%)	SiO_2 (%)
1	141°01	36°00	34.2	8.4	7.6	10.3	7.3	2.0
2	141°27	37°20	34.0	9.5	7.8	4.4	7.1	3.0
3	141°31	37°35	34.0	9.3	7.8	14.2	5.3	2.7
4	143°54	37°49	34.7	1.8	7.6	5.1	15.3	2.1
5	150°00	40°50	34.7	1.5	7.7	3.0	21.9	1.7
6	155°00	44°00	34.7	1.6	7.6	2.7	27.9	3.6
7	160°05	47°00	34.7	1.6	7.6	4.1	15.5	10.8
8	165°00	47°10	34.7	1.7	7.6	4.4	18.5	4.1

Table 21 Concentration of trace metals by modified BCR sequential methods for surface sediment of the Northwestern Pacific Ocean

	Cd($\mu g.g^{-1}$)	Pb($\mu g.g^{-1}$)	Mn($\mu g.g^{-1}$)	Fe($\mu g.g^{-1}$)	Co($\mu g.g^{-1}$)	Zn($\mu g.g^{-1}$)
Station No.1						
Acid Soluble	0.02	0.12	14.5	293	0.24	6.27
Reducible	0.05	4.51	20.4	4641	1.55	24.5
Oxidable	n.d	1.80	12.8	1628	1.09	15.4
Residual	0.01	6.25	310	48421	4.36	48.1
Total	0.08	12.7	358	54983	7.24	94.3
Station No.2						
Acid Soluble	n.d	0.27	74.4	157	0.22	5.76
Reducible	n.d	6.15	25.9	1655	0.65	18.2
Oxidable	n.d	2.47	12.9	1488	0.87	16.2
Residual	n.d	12.8	339	55290	4.32	47.6
Total	n.d	21.7	452	58591	6.05	87.8
Station No.3						
Acid Soluble	n.d	0.12	13.0	247	0.19	3.37
Reducible	n.d	4.48	15.5	1448	0.45	12.8
Oxidable	n.d	1.61	8.58	1010	0.60	10.5
Residual	n.d	4.66	484	76133	6.38	50.3
Total	n.d	10.9	521	78838	7.61	77.0
Station No.4						
Acid Soluble	n.d	0.00	659	121	0.00	4.90
Reducible	n.d	4.90	4716	2272	4.01	14.9
Oxidable	n.d	2.30	547	2102	1.77	18.3
Residual	n.d	4.60	257	34362	3.71	35.5
Total	n.d	11.8	6179	38856	9.49	73.7

Station No.5						
Acid Soluble	0.07	n.d	466	126	n.d	16.7
Reducible	0.06	10.8	7301	3408	9.70	33.1
Oxidable	n.d	4.23	932	2078	2.30	20.1
Residual	n.d	5.32	252	29013	3.41	32.0
Total	0.13	20.3	8950	34627	15.4	102
Station No.6						
Acid Soluble	0.03	0.00	57.8	1078	0.48	10.7
Reducible	n.d	6.30	2104	7456	8.59	12.1
Oxidable	n.d	2.69	223	1670	1.55	12.4
Residual	n.d	4.20	251	29973	3.49	31.4
Total	n.d	13.2	2637	40178	14.1	66.8
Station No.7						
Acid Soluble	n.d	0.00	98.3	154	n.d	4.62
Reducible	n.d	4.40	2085	3681	6.59	14.1
Oxidable	n.d	2.52	176	775	1.22	10.4
Residual	n.d	5.25	319	19373	5.32	39.2
Total	n.d	12.1	2678	23984	13.1	68.4
Station No.8						
Acid Soluble	n.d	n.d	66.7	146	0.00	3.54
Reducible	n.d	6.61	2453	4399	13.7	12.3
Oxidable	n.d	3.46	200	742	1.59	9.36
Residual	n.d	5.23	432	24448	6.77	47.8
Total	n.d	15.3	3152	29733	22.1	73.1

n.d: no detected

Table 22 Pearson correlation coefficients between total concentration trace metals, aluminum, carbonates, and silicate in surface sediment of the Northwestern Pacific Ocean ($0.01 < P < 0.05$)

	Cd	Pb	Mn	Fe	Co	Zn	Aluminium	Carbonate	SiO2
Cd	1.00	0.38	0.52	-0.12	-0.53	0.79	-0.12	0.27	-0.40
Pb		1.00	0.26	-0.08	-0.30	0.61	-0.49	0.07	-0.26
Mn			1.00	-0.57	-0.45	0.25	-0.54	0.60	-0.17
Fe				1.00	0.18	0.23	0.81	-0.71	-0.49
Co					1.00	-0.35	0.46	-0.39	0.32
Zn						1.00	0.11	-0.27	-0.54

Table 23 Pearson correlation coefficients between concentration of trace metals in each fraction, aluminum, carbonates, and silicate in surface sediment of the Northwestern Pacific Ocean ($0.01 < P < 0.05$)

a. Carbonate Fraction

	Cd	Pb	Mn	Fe	Co	Zn	Carbonate	Aluminum	SiO2
Cd	1.00	-0.29	0.30	0.21	0.08	0.97	0.51	-0.30	-0.36
Pb		1.00	-0.40	0.21	0.31	-0.27	-0.74	0.36	-0.25
Mn			1.00	-0.32	-0.52	0.36	0.29	-0.36	-0.29
Fe				1.00	0.87	0.27	0.54	-0.17	-0.05
Co					1.00	0.12	0.54	0.13	-0.23
Zn						1.00	0.60	-0.47	-0.31

b. Oxides fraction

	Cd	Pb	Mn	Fe	Co	Zn	Carbonate	Aluminum	SiO2
Cd	1.00	0.59	0.43	0.10	0.07	0.95	0.06	0.02	-0.40
Pb		1.00	0.73	0.12	0.54	0.68	0.53	-0.52	-0.34
Mn			1.00	0.06	0.57	0.49	0.64	-0.57	-0.15
Fe				1.00	0.54	-0.09	0.72	-0.40	0.12
Co					1.00	-0.01	0.80	-0.64	0.19
Zn						1.00	0.01	-0.10	-0.40

c. Organic matter fraction

	Cd	Pb	Mn	Fe	Co	Zn	Carbonate	Aluminum	SiO2
Cd	1.00	-	-	-	-	-	-	-	-
Pb		1.00	0.74	0.18	0.82	0.29	0.68	-0.72	-0.04
Mn			1.00	0.62	0.91	0.66	0.57	-0.51	-0.24
Fe				1.00	0.54	0.92	0.24	-0.24	-0.65
Co					1.00	0.52	0.77	-0.69	-0.17
Zn						1.00	0.05	-0.26	-0.56

d. Residual fraction

	Cd	Pb	Mn	Fe	Co	Zn	Al	Carbonate	Aluminum	SiO2
Cd	1.00	0.03	-0.09	0.19	-0.11	0.34	0.43	-0.39	0.43	-0.24
Pb		1.00	0.05	0.32	-0.10	0.40	-0.11	-0.47	-0.11	-0.10
Mn			1.00	0.54	0.93	0.83	0.64	-0.55	0.64	0.06
Fe				1.00	0.23	0.63	0.82	-0.76	0.82	-0.46
Co					1.00	0.73	0.46	-0.39	0.46	0.32
Zn						1.00	0.68	-0.83	0.68	-0.05

Table 24 Total concentration of rare earth elements in surface sediment of the Northwestern Pacific Ocean

REEs	Concentration (μg/g)							
	St 1	St 2	St 3	St 4	St 5	St 6	St 7	St 8
Y	38.43	43.42	41.51	38.64	34.08	34.90	49.68	52.61
La	30.65	35.66	40.29	35.04	37.52	33.41	40.82	43.68
Ce	94.49	123.26	134.42	127.10	114.12	105.92	118.98	143.13
Pr	5.82	7.00	6.96	6.25	5.90	5.32	6.57	6.95
Nd	23.38	27.86	27.44	24.40	23.44	21.53	27.39	29.05
Sm	5.34	6.34	5.96	5.39	5.19	5.05	6.61	7.15
Eu	1.69	1.91	2.00	1.51	1.64	1.76	2.30	2.34
Gd	5.72	6.49	6.01	5.39	5.25	5.42	7.39	7.81
Tb	0.84	0.97	0.84	0.76	0.71	0.73	0.99	1.10
Dy	5.26	6.10	5.14	4.62	4.17	4.44	6.14	6.90
Ho	1.06	1.21	1.00	0.89	0.79	0.86	1.20	1.34
Er	3.06	3.50	2.81	2.52	2.18	2.43	3.44	3.80
Tm	0.45	0.50	0.40	0.36	0.31	0.36	0.49	0.55
Yb	2.95	3.36	2.66	2.42	2.09	2.40	3.29	3.64
Lu	0.34	0.39	0.30	0.28	0.24	0.28	0.38	0.42
SUM	**219.48**	**267.97**	**277.74**	**255.59**	**237.63**	**224.80**	**275.68**	**310.47**
Lan/Ybn	1.18	1.18	1.18	1.18	1.18	1.18	1.18	1.18
Smn/Lan	1.68	1.68	1.68	1.68	1.68	1.68	1.68	1.68
Smn/Ybn	1.98	1.98	1.98	1.98	1.98	1.98	1.98	1.98
Y/Ho	**36.30**	**35.77**	**41.39**	**43.19**	**43.18**	**40.50**	**41.34**	**39.26**
Nd/Yb	**7.93**	**8.29**	**10.32**	**10.07**	**11.21**	**8.96**	**8.33**	**7.99**
La/Yb	**10.40**	**10.61**	**15.15**	**14.46**	**17.94**	**13.91**	**12.41**	**12.01**

Table 25 The concentration of rare earth elements in carbonates fraction in surface sediment of the Northwestern Pacific Ocean

REEs	Concentration (μg/g)							
	St 1	St 2	St 3	St 4	St 5	St 6	St 7	St 8
Y	0.22	0.17	0.20	0.53	0.61	0.81	0.78	0.62
La	0.17	0.14	0.17	0.34	0.54	0.68	0.58	0.46
Ce	0.43	0.36	0.47	0.68	0.74	0.62	0.61	0.51
Pr	0.05	0.03	0.05	0.08	0.12	0.16	0.15	0.11
Nd	0.19	0.14	0.22	0.35	0.49	0.65	0.63	0.49
Sm	0.05	0.03	0.05	0.09	0.10	0.14	0.15	0.12
Eu	0.01	0.01	0.02	0.02	0.03	0.04	0.04	0.03
Gd	0.05	0.04	0.05	0.10	0.12	0.16	0.17	0.13
Tb	0.01	0.01	0.01	0.02	0.02	0.02	0.02	0.02
Dy	0.04	0.03	0.04	0.08	0.09	0.13	0.13	0.10
Ho	0.01	0.01	0.01	0.02	0.02	0.03	0.03	0.02
Er	0.02	0.01	0.02	0.04	0.04	0.06	0.06	0.05
Tm	0.00	0.00	0.00	0.00	0.00	0.01	0.01	0.01
Yb	0.02	0.01	0.02	0.03	0.04	0.05	0.06	0.04
Lu	0.00	0.00	0.00	0.00	0.00	0.00	0.01	0.00
SUM	**1.27**	**1.00**	**1.33**	**2.38**	**2.96**	**3.57**	**3.41**	**2.72**
Lan/Ybn	1.18	1.18	1.18	1.18	1.18	1.18	1.18	1.18
Smn/Lan	1.68	1.68	1.68	1.68	1.68	1.68	1.68	1.68
Smn/Ybn	1.98	1.98	1.98	1.98	1.98	1.98	1.98	1.98
Y/Ho	**25.78**	**25.86**	**24.23**	**32.52**	**31.54**	**31.16**	**29.65**	**29.84**
Nd/Yb	**10.45**	**10.31**	**12.48**	**10.28**	**12.61**	**13.51**	**11.39**	**11.95**
La/Yb	**9.19**	**10.30**	**9.46**	**9.91**	**14.02**	**14.14**	**10.44**	**11.31**

Table 26 The concentration of rare earth elements in oxides fraction in surface sediment of the Northwestern Pacific Ocean

REEs	Concentration (μg/g)							
	St 1	St 2	St 3	St 4	St 5	St 6	St 7	St 8
Y	13.77	14.90	19.37	19.93	20.30	18.87	27.83	28.71
La	11.90	12.71	19.36	15.74	20.92	19.89	25.01	27.32
Ce	33.79	37.55	56.45	52.41	72.93	74.37	81.75	103.04
Pr	0.87	0.91	1.47	1.13	1.41	1.58	1.97	2.14
Nd	3.47	3.67	6.01	4.54	5.55	6.43	8.16	8.90
Sm	0.75	0.79	1.33	0.98	1.15	1.47	1.86	2.06
Eu	0.16	0.17	0.26	0.24	0.29	0.35	0.45	0.49
Gd	0.81	0.86	1.36	1.12	1.30	1.50	1.99	2.18
Tb	0.12	0.12	0.18	0.16	0.19	0.21	0.28	0.32
Dy	0.63	0.68	0.99	0.94	1.06	1.21	1.61	1.83
Ho	0.12	0.13	0.18	0.18	0.20	0.22	0.30	0.33
Er	0.30	0.32	0.44	0.45	0.52	0.56	0.79	0.86
Tm	0.04	0.04	0.06	0.06	0.07	0.08	0.11	0.12
Yb	0.22	0.23	0.31	0.34	0.40	0.47	0.62	0.70
Lu	0.02	0.02	0.03	0.04	0.04	0.05	0.07	0.08
SUM	**66.95**	**73.11**	**107.81**	**98.25**	**126.33**	**127.24**	**152.79**	**179.06**
Lan/Ybn	1.18	1.18	1.18	1.18	1.18	1.18	1.18	1.18
Smn/Lan	1.68	1.68	1.68	1.68	1.68	1.68	1.68	1.68
Smn/Ybn	1.98	1.98	1.98	1.98	1.98	1.98	1.98	1.98
Y/Ho	**117.59**	**119.09**	**109.29**	**113.17**	**102.79**	**86.91**	**93.52**	**86.98**
Nd/Yb	**16.10**	**16.12**	**19.12**	**13.51**	**13.86**	**13.72**	**13.18**	**12.80**
La/Yb	**55.16**	**55.85**	**61.58**	**46.82**	**52.29**	**42.45**	**40.40**	**39.28**

Table 27 The concentration of rare earth elements in organic fraction in surface sediment of the Northwestern Pacific Ocean

REEs	Concentration (μg/g)							
	St 1	St 2	St 3	St 4	St 5	St 6	St 7	St 8
Y	2.79	3.47	3.30	3.96	4.38	2.50	3.60	3.47
La	2.74	3.25	3.77	2.63	3.35	1.99	2.44	2.81
Ce	6.74	8.69	9.70	8.96	12.92	6.98	7.86	10.18
Pr	0.80	0.98	1.11	0.99	1.30	0.75	0.96	1.07
Nd	3.28	4.21	4.67	4.45	5.81	3.33	4.35	4.80
Sm	0.76	1.02	1.06	1.22	1.61	0.96	1.26	1.40
Eu	0.18	0.23	0.25	0.36	0.47	0.41	0.46	0.50
Gd	0.75	0.98	0.97	1.19	1.51	0.92	1.20	1.36
Tb	0.11	0.14	0.14	0.18	0.22	0.13	0.17	0.20
Dy	0.62	0.81	0.73	1.03	1.28	0.75	1.03	1.16
Ho	0.12	0.15	0.13	0.19	0.23	0.14	0.19	0.21
Er	0.30	0.39	0.34	0.52	0.62	0.36	0.51	0.57
Tm	0.04	0.05	0.04	0.07	0.09	0.05	0.07	0.08
Yb	0.27	0.34	0.28	0.52	0.63	0.37	0.51	0.58
Lu	0.03	0.04	0.03	0.06	0.07	0.04	0.06	0.07
SUM	**19.52**	**24.74**	**26.53**	**26.34**	**34.51**	**19.69**	**24.69**	**28.46**
Lan/Ybn	1.18	1.18	1.18	1.18	1.18	1.18	1.18	1.18
Smn/Lan	1.68	1.68	1.68	1.68	1.68	1.68	1.68	1.68
Smn/Ybn	1.98	1.98	1.98	1.98	1.98	1.98	1.98	1.98
Y/Ho	**23.92**	**23.17**	**24.95**	**20.74**	**19.14**	**18.46**	**19.16**	**16.64**
Nd/Yb	**12.35**	**12.54**	**16.57**	**8.57**	**9.18**	**9.07**	**8.45**	**8.30**
La/Yb	**10.33**	**9.69**	**13.38**	**5.07**	**5.29**	**5.40**	**4.75**	**4.86**

Table 28 The concentration of rare earth elements in residual fraction in surface sediment of the Northwestern Pacific Ocean

REEs	Concentration (μg/g)							
	St 1	St 2	St 3	St 4	St 5	St 6	St 7	St 8
Y	21.65	24.88	18.64	14.21	8.79	12.71	17.47	19.81
La	15.85	19.56	16.99	16.34	12.71	10.86	12.80	13.09
Ce	53.53	76.66	67.80	65.05	27.54	23.95	28.76	29.40
Pr	4.12	5.08	4.33	4.05	3.07	2.83	3.50	3.62
Nd	16.43	19.84	16.53	15.07	11.59	11.12	14.25	14.86
Sm	3.78	4.49	3.52	3.11	2.33	2.47	3.34	3.58
Eu	1.34	1.50	1.47	0.89	0.85	0.96	1.36	1.32
Gd	4.11	4.61	3.62	2.97	2.31	2.84	4.02	4.14
Tb	0.60	0.69	0.51	0.40	0.28	0.36	0.51	0.57
Dy	3.97	4.59	3.37	2.57	1.74	2.36	3.37	3.80
Ho	0.82	0.93	0.68	0.51	0.34	0.48	0.69	0.78
Er	2.44	2.77	2.02	1.51	0.99	1.45	2.07	2.33
Tm	0.37	0.41	0.30	0.23	0.15	0.22	0.31	0.34
Yb	2.45	2.78	2.04	1.53	1.02	1.52	2.10	2.32
Lu	0.29	0.33	0.24	0.18	0.12	0.18	0.25	0.27
SUM	**131.74**	**169.13**	**142.07**	**128.62**	**73.82**	**74.31**	**94.79**	**100.23**
Lan/Ybn	1.18	1.18	1.18	1.18	1.18	1.18	1.18	1.18
Smn/Lan	1.68	1.68	1.68	1.68	1.68	1.68	1.68	1.68
Smn/Ybn	1.98	1.98	1.98	1.98	1.98	1.98	1.98	1.98
Y/Ho	**26.52**	**26.68**	**27.21**	**27.81**	**25.57**	**26.33**	**25.32**	**25.37**
Nd/Yb	**6.71**	**7.13**	**8.09**	**9.82**	**11.37**	**7.32**	**6.79**	**6.40**
La/Yb	**6.48**	**7.03**	**8.31**	**10.64**	**12.47**	**7.15**	**6.09**	**5.64**

Appendices